SAPIENZA
UNIVERSITÀ DI ROMA

XXIX CICLE

Ph.D PROGRAMME IN PHARMACOLOGY AND TOXICOLOGY

Ph.D course in Pharmacology

"Role of cortical TRPV1 in resting and chronic pain conditions"

Candidate:

Annunziato Morabito matr.1099466

Supervisors:

Dott.ssa Silvia Marinelli

Prof.Aldo Badiani

Academic year 2016/2017

INDEX

CHAPTER 1 :

GENERAL INTRODUCTION

1. TRPV1 channels

The transient receptor potential vanilloid type 1(TRPV1) , also known as vanilloid receptor , is a non-selective cationic channel. It belongs to the transient receptor potential channels (TRP) superfamily, which have been described for the first time in *Drosophila* phototrasduction[1]. Differently from other ion channels, TRP are grouped for their homology rather than their functions, as documented by their different roles in yeast ,protists and mammals. Mammalian TRP channels consist of six related protein subfamilies, with an homology lower than 20%: TRPC(classical),TRPV(vanilloid),TRPM(melastatin),TRPP(polycystin),TRPML(mucolipin),TRPA(ankyrin) **fig1**. All these channels comprise six trans-membrane domains that assemble as tetramers to form a cation-permeable pores [2].

TRPV1 was cloned first ,thus representing the lead of TRPV subfamily. TRPV1s are calcium-permeable, non selective cation channels. Current-voltage relationship experiments demonstrated that TRPV1 does not discriminate between monovalent cations and shows a particular preference for divalent cations(Ca^{2+}>Mg^{2+}>Na^{+}=K^{+}=Cs^{+}). Regarding calcium permeability these channels exhibit a very high related P_{CA}/P_{NA} ratio similar to the value reported for the glutamate receptor N-Methyl-D-aspartate (NMDA): TRPV1 P_{CA}/P_{NA}=9.60, NMDA P_{CA}/P_{NA}=10.6 [3,4].

Structurally, TRPV1 has six trans-membrane domains with an ankyrin like N-terminal and C-terminal domain located in the intracellular lumen of bi-layer cellular membranes. This channel assemblies as homomeric or heteromeric complexes formed by four subunits acted to create the pore of the channel. The cation selective pore loop is formed by the fifth and sixth trans-membrane domains(S5-pore loop-S6)[2].TRPV1as a polymodal receptor can be activated by

numerous activators : high temperatures(> 43^{o} C),low ph(<6.5) and voltage[3,5,6] . Endogenous agonists include anandamide, 2-arachidonoylglycerol, N-arachidonoyl dopamine, N-oleoyldopamine, ATP, lipoxygenase products and some active biolipids such as Lysophosphatidic-acid (LPA) and diacylglycerol (DAG)[7,8,]. Regarding its exogenous ligands, this channel is opened by capsaicin, the pungent ingredient of "hot" chili peppers, resiniferatoxin, a capsaicin analogue derived from the latex of Moroccan "Euphorbia Resinifera" and some venom toxin[3,9,10]. Given the broad spectrum of activators, TRPV1displays numerous binding sites modulating channel opening in the intra and extracellular region as well as different regulatory sites. Vanilloid binding site is allocated in the intracellular loop at S3(Tyr^{511}),a requisite for anandamide and capsaicin response[4]. Different substitution studies unveil that the replacement of Tyr^{511} aromatic residue with aliphatic or small aliphatic/polar residues decreases or abolishes TRPV1 current respectively, and low ph-evoked currents are even maintained [11]. These latter are attributed to a protonation of aminoacidic residuals present on the extracellular loop S5 and S6(Glu^{600}, Glu^{648}) of the channel [12] . On the other hand it has been reported that an allosteric modulation of C-terminus induce a conformational change of the protein during temperature increment[13].

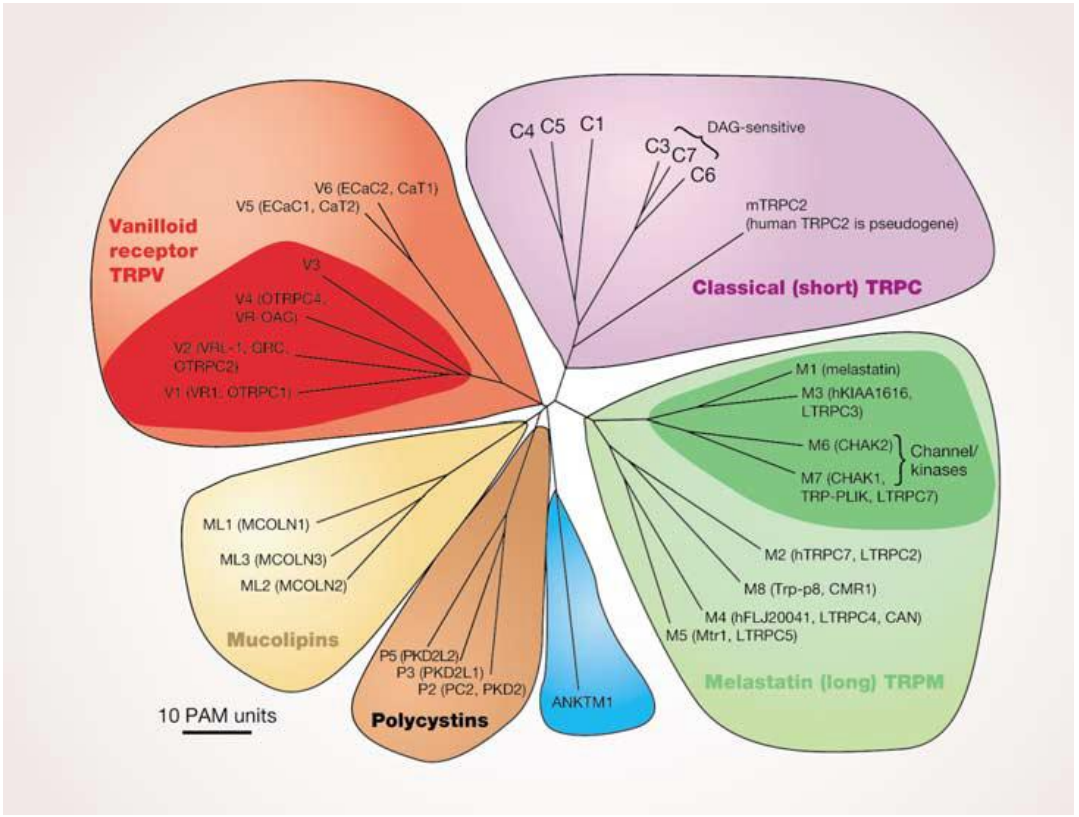

Figure 1: The TRP family tree (Clapman DE. "TRP channels as cellular sensors" Nature 2003)

1.1 Modulation of TRPV1 by cellular components

TRPV1 undergoes complex modulation that influences the channel opening or gating by extra and intracellular calcium or activation of tyrosine kinase or G-coupled receptors. These activators' participating to sensitization and desensitization of the channel, the most common feature for TRPV1, could influence the channel activation threshold [5,14, 15,16,17,18.]. Indeed , the channel being a noxious stimuli detector is modulated by different inflammatory mediators released upon physical and chemical damage which interact with their coupled receptors. In particular, bradykinin, prostaglandins, nerve growth factor, histamine, serotonine or ATP modulate this channel though protein kinase A or C (PKA,PKC) dependent phosphorylation on threonine or serine aminoacidic residual at different positions [20,21,14.]. PKA cascade activation can modulate both sensitization and desensitization of TRPV1 channel[16,22]. While the PKA sensitization of heat-evoked TRPV1 response is attributed to Thr^{144}, $Thr^{370}$and Ser^{502}phosphorylation,the PKA-mediated desensitization to anandamide or capsaicin occurs on Ser^{116} and Thr^{370} residuals[16,22,23]. PKC signaling represents another element involved in TRPV1 modulatory response, Ser^{502} and $Ser^{800}$are the principal targets of PKC activity[24,25,26]. Phosphorylation of these two sites is responsible of increasingTRPV1 response to its endogenous agonist NADA and strongly coupled to capsaicin and heat evoked response[27]. As sad below, intra and extracellular calcium could influence TRPV1 activity. Extracellular calcium dependent desensitization of TRPV1 in fact, represents another regulatory mechanism involved in the TRPV1 multimodal response[5]. This mechanism *per se* represents a well-integrated physiological control against calcium overload in the cell. TRPV1 desensitization, involving the channel in a refractory state, is fundamental for the setting of sensory neuron activation threshold and for

protecting from excessive receptor activation during continuous noxious stimuli exposure. Calcium regulation of TRPV1 implicates different players which act in different timing. Calcineurin, calcium calmodulin dependent kinase II (CAMKII) and calmodulin (CaM) has been described as "actors" involved in this mechanism [28,2930]. Several studies report that calcineurin seems to be coupled with CAMKII in the temporal regulation of TRPV1 during its opening/gating states. Probably initial calcium influx activates calcineurin first, which dephosphorylates and then desensitizes the channel, while CaMKII slowly re-activates and phosphorylating the channel[30]. On the other hand, the Ca^{2+}-binding protein CaM binds a 35-aa segment of the C terminus of TRPV1 and the disruption of this binding site prevents TRPV1 desensitization. However deletion experiments in the presence of mutated CaMs or CaMs inhibitors fail to achieve the same effect, suggesting that this mechanism might be CaM independent[29]. All binding and modulator sites are summarized in the **Figure 2**

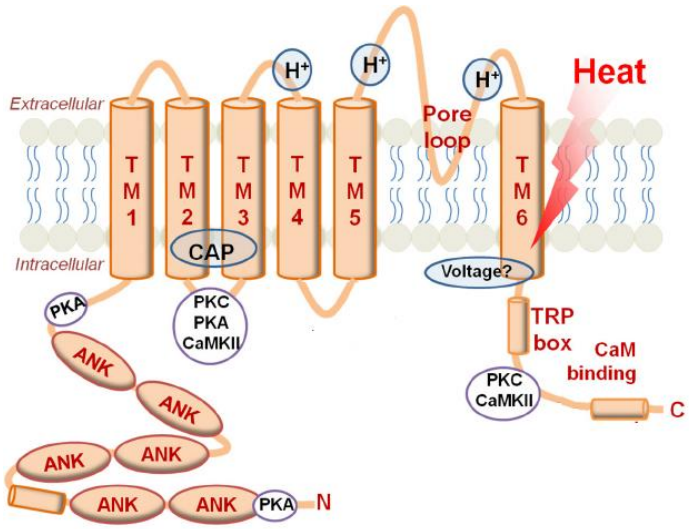

Figure 2: TRPV1 structure and principal sites of agonism/modulation

1.2 TRPV1 Splicing

TRPV1s are the results of TRPV1 gene located on chromosome 11 for mice on 17 for humans. Mouse gene accounts 16 codifying sections (exons) and different splice variants. The first published splice variant was identified in 5' in the rat mRNA (VR.5'sv)[31]. Compared with the full length sequence of the TRPV1, this variant is different for two peculiar variations: 1) the expression of a small portion of N-terminal part of the protein; 2) the loss of 60 amino acids at N-terminal region including a portion of the third N-terminal ankyrin domain. VR.5'sv has different genomic origin compared to the full length variant as it uses an additional transcriptional starting site at intron IV and encodes for TRPV1-like channel with truncated N-terminal domain[32]. Another splice variant was proposed in mice, identical to the full length TRPV1 but with the loss of polipeptide sequence encoded by exon 7. Afterwards this variant has been identified as TRPV1beta variant in mice (30 nucleotide loss in exon 7 codifying for 10 aa) and TRPV1b variant in humans (complete loss of exon 7)[33,34]. Both mRNA variants appear unstable and take particular care to their isolation. Regarding their pattern of expression, these variants have been found in peripheral and central nervous system. Finally, a cDNA encoding a TRPV1 variant defined as "TRPV1var" has been isolated from rat kidney papilla[35,36]. This variant had a larger mRNA respect to the native one but results in a dramatically truncated protein expressing only a part of N-ter region and the complete loss of the residual part of the protein. Functionally, the resultant proteins act as dominant negative subunit and block the activation of their TRPV1 full length "cousins" [37,38] **fig.3 .**

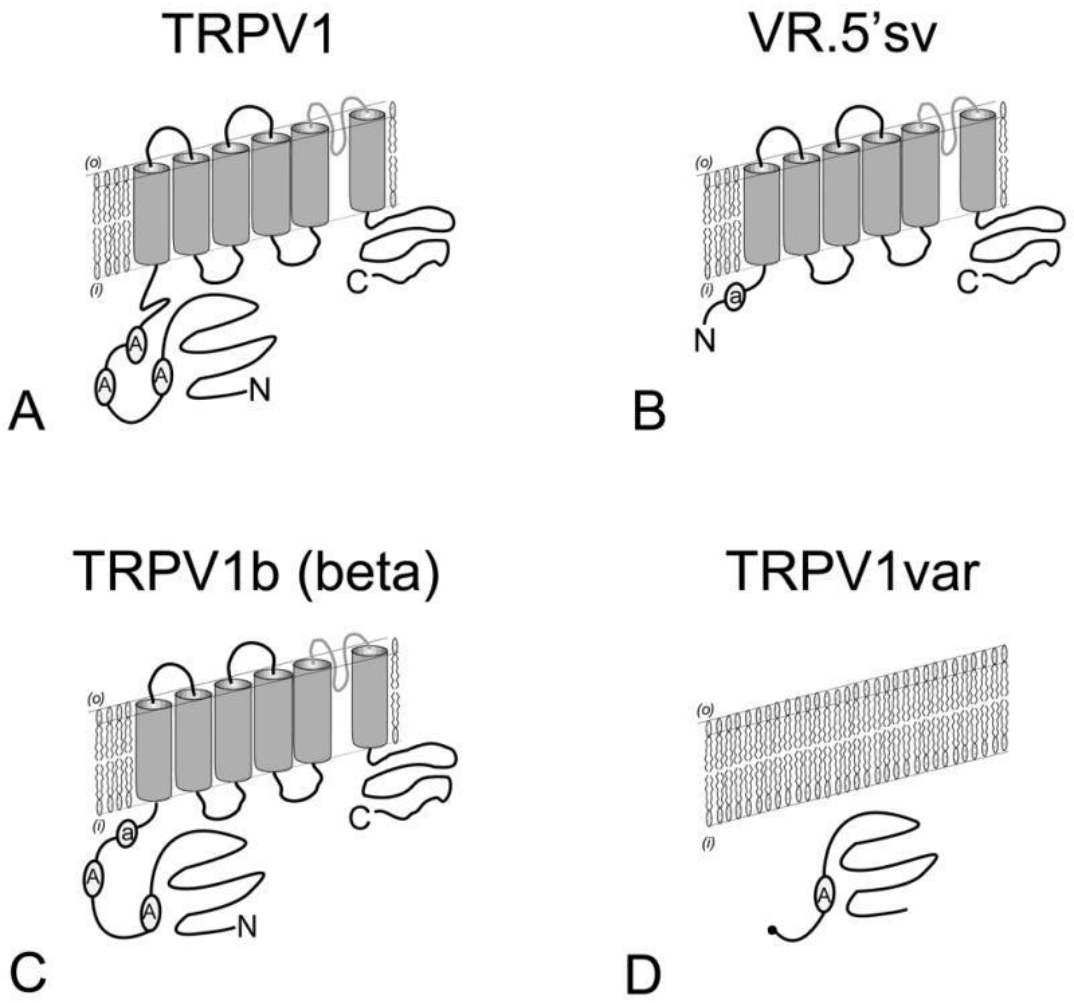

Figure 3:Different TRPV1 proteins resulted from mRNA post-transcriptional modification

A) Full length TRPV1; **B)** VR.5'sv; **C)** TRPV1-b(humans) or TRPV1-beta(mice); **D)** TRPV1var

2.TRPV1 localization and functions

Given the polymodal nature of activation of the nociceptor TRPV1, this receptors has been deeply characterized in primary sensory neurons. Different techniques have been used to investigate the TRPV1 expression pattern. First evidence was achieved by using in situ hybridization assay and allocated the TRPV1 as a specific nociceptor present exclusively in trigeminal (TG) and dorsal root sensory ganglia (DRG), in particular in a subset of neurons with small or medium size cell bodies [3]. Subsequent physiological studies defined these capsaicin-responsive cells as the unmyelinated C fibers and the small myelinated (A)nerve fibers [40,41] .

2.1 Peripheral structures

Based on their neurochemical phenotype, small DRG cells has been divided in nonpeptidergic isolectinB4(IB4) positive cells responsive to Glial Neurotrophic Factor(GDNF) peptidergic IB4 negative cells NGF responsive an positive for calcitonine gene-releated peptide (CGRP) and substance P(SP) and small myelinated (A)nerve fibers[42,43,44]. These classes are defined as capsaicin - sensitive and TRPV1-immunoreactive in the rat [5,45].

In the mouse TRPV1 seemed to be prominent expressed in peptidergic ones although electrophysiological evidence indicated that also nonpeptidergic cells respond to TRPV1 activation [46,47,48]. This discrepancy pointed to the need of novel genetic approaches to clarify the open question regarding TRPV1 distribution. Different "reporter mice" have been created with the purpose to follow TRPV1 distribution from embryo to adult in many areas [44,49] On the whole, both the

amount and expression pattern of TRPV1 positive DRG neurons was age–dependent. Compared to DRG, TRPV1 was less abundant in trigeminal ganglia and preferentially expressed in peptidergic neurons (73 % CGRP positive and 15% IB4 positive)[44] High number of TRPV1 positive cells have been stained in the Nodose Ganglia through in situ hybridization overlapping a profile of expression very similar to DRG in terms of density (81% of cells), data undetected by Caterina and colleagues in 1997 [41,44,50]. Tirosin kinase B receptor co-expression is assigned to these cells and TRPV1 mRNA signal was completely absent in neurofilament positive large cells confirming the more sparse expression of this receptor in myelinated cells even in this specific region [41]. Moving from DRG and sensory ganglia it is possible to find this receptor in various peripheral regions and organs such as: nerve terminals in the airways, in the cornea, glabrous and hairy skin of the mouse, urinary bladder, ureters and urethra, mucosa, mysenteric ganglia and muscular layers of the stomach, the small intestine, and the colon [44,51,52].

2.2 Central Nervous System

The functional expression of TRPV1 in peripheral structures, especially in primary sensory neurons, as well as in the spinal cord, is well established and accepted. On the other side, the localization and function of this channel in the brain is still a matter of debate.

2.2a Spinal cord

Anatomical evidence shows that TRPV1 is expressed in axons, somata and dendrites of spinal cord (SC)[54,55,56]. In the dorsal horn TRPV1 expression involved 70% GABAergic neurons while the occurrence of TRPV1 in non GABAergic

neurons is lower (25%). An excitatory/inhibitory balance was described as the key of TRPV1 integrative function of pathological states in the SC. In paticular, the functional role of TRPV1 in the SC is associated to the inhibitory control of spinal neurotransmission. In fact peripheral signals are integrated through inhibitory control principal excitatory neurons [56,57]. Other electrophysiological studies reveal that TRPV1 activation correlates with a decrease of evoked excitatory post-synaptic currents and an increase of spontaneous inhibitory currents[55],[58,59]. The TRPV1 seemed that modulating ascending and descending SC pathways induced sensitization or desensitization to somato-sensation and pain influencing excitatory and ihibitory neurotransmission at the occurence[56].

2.2 b TRPV1 in the Brain

Many studies shown that capsaicin induce a biological response in different brain areas but TRPV1 expression in the brain has been still debated. The use of TRPV1 genetic approach defined "reporter mice" restricted the presence of this receptor in very few areas of the brain with the highest level of expression primarily in the hypothalamus[60]. Different studies failed to detect the presence of TRPV1 mRNA by using in situ hybridization excluding the possibility of its functional localization in the brain[3,49]. However radiolabeled TRPV1 ligand, RNA expression and PCR, western blot and immunoprecipitation identified the TRPV1 in the brain of humans, rats and mice [61,62,63] . Specific expression has been achieved in major brain areas including cerebellum, cortex, hippocampus, dentate gyrus, amygdala, habenula, hypotalamus, suprachiasmatic nucleus, inferior olive, substantia nigra and others[61,64,54,65,66,67,68,69] These results have been further confirmed by variegated functional evidence. The capsaicin application on acute brain slices induce pre and post-synaptic response in different brain areas as well as change in temperature induce an TRPV1-mediated inward rectifying current

onto supraoptic hypotalamic vasopressine containing neurons [70]. The systemic capsaicin treatment lead the capability to bind silver salts(positive to neurotoxicity capsaicine-mediated) throughout the whole rat neuraxis [71].Different autoradiography studies with specific binding of [^{3}H]Resinferatoxin revealed positive results for the presence of this channel in widespread brain and capsaicin application induced the expression of immediate early gene C-fos in Amygdala[66,67]. In Mezey E. et al. 2000 is reported a positive immunoreactivity for trpv1 in rat and human different brain areas including all cortical areas, hippocampus ,amygdala and lower brainstem (cerebellum, locus coeruleus, nucleus of solitary tract, nucleus of trigeminal nerve, cochlear nuclei). Recent electron microscopy studies detected the presence on TRPV1 in molecular layer of dentate gyrus mostly localized in postsynaptic dendritic spines and in CA1cell body of pyramidal neurons in the stratum piramidale and into perisomatic gabaergic synapses[73,74]. However in Lee et al. 2015 the majority of gold particles representing the subcellular position of TRPV1 was found to be attached to intracellular membrane cisternae and have not plasma membrane localization . The subcellular compartment of the remaining gold particles are not described and all away from the plasma membrane. Regarding mRNA controversy there are several works that found TRPV1 -mRNA positive staining by using an antisense probe for in situ hybridization and real time-PCR in different brain regions including cortical and hippocampal regions [61,75]. The messenger RNA profile of TRPV1 expression appeared stable at different time point during the lifespan of mice excluding the possibility of a developmental decrease of expression as described in Cavanaugh et al.2011.

3. TRPV1 function in the brain

Most of the studies on brain TRPV1 showed that this channel acted as a modulator of neurotransmission. Exogenous TRPV1 activation by capsaicin mediated an enhancement of neurotransmitter release and for this reason was often principally reported as causative pre-synaptic protein. At excitatory synapses of substantia nigra capsaicin and/or N-Arachidonoyl dopamine (NADA) facilitated spontaneous excitatory post synaptic currents (EPSCs) frequency consistent with a presynaptic site of action and a TRPV1-mediated increase of glutamate release indirectly enhanced the firing rate of ventral tegmental area dopaminergic neurons[76,77,78]. The same presynaptic effect is reported in Locus Coeruleus adrenergic neurons[79]. The enhancement of synaptic transmission TRPV1-mediated has been attributed to Ca^{2+} increase in pre-synaptic terminals via activation of voltage-gated Ca^{2+} channels. Acute slice of medial preoptic nucleus the hypotalamus even revealed that capsaicin increases both excitatory and inhibitory post-synaptic currents frequency[80,81]. In the other hand, patch clamp experiments described TRPV1 as post-synaptic player. In TRPV1 is described as functional postsynaptic protein. An heat ramp (from 25 to 39 degrees) induces experimentally in hypothalamic vasopressin containing neurons a causative increase of the firing rate and an inward rectifying current, directly associated to TRPV1 activation [83].Both effects, in fact have been abolished in TRPV1 knockout mice. As post-synaptic "actor" the TRPV1 was also described as synaptic plasticity modulator. A separate paragraph discuss this activity below.

3.1 TRPV1-dependent synaptic plasticity

The TRPV1 is a high calcium permeable channel very similar to NMDA receptor in terms of calcium permeability. For this reasons was described as a great candidate for calcium-dependent synaptic plasticity. TRPV1modulation of synaptic plasticity was firstly reported in hippocampus, when the amount of LTP in TRPV1 -/- mouse was significantly reduced compared to WT mice [84] . Subsequent studies report TRPV1 receptor as mediator of synaptic plasticity in postsynaptic compartment. TRPV1modulated Long Term Depression (LTD) was reported in dentate gyrus by promoting calcineurin dependent α-amino-3-hydroxy-5-methyl-4-isoxazolepropionic acid (AMPA) receptor internalization increasing the calcium influx [85]. Other forms of synaptic plasticity has been described as post-synaptic effect of TRPV1. In the Nucleus Accumbens, anandamide , produced during high frequency post synaptic stimulation, induced a form of LTD modulated by both pre-synaptic CB1 and postsynaptic TRPV1. This cannabinoid-mediated LTD results in a reduction in neurotransmitter release Cannabinoid receptor 1-dependent and a in a TRPV1-mediated postsynaptic AMPA internalization[86]. Another form of TRPV1-dependent LTD has been reported in the bed nucleus of stria terminalis in which postsynaptic TRPV1 are activated by anandamide synthesized and released upon post-synaptic metabotropic glutamate receptor activation [87]. A peculiar pre-synaptic LTD is reported as TRPV1 dependent. In this mechanism the TRPV1-mediated reduction of glutamate release from pyramidal cell induces a LTD in perisomatic interneurons [82]. In conclusion TRPV1 in cooperation with other receptors has been reported in other forms of synaptic plasticity, underlining the importance of this channel in the synaptic strength shaping the functional organization of brain circuits [88].

4.Microglia

Microglia cells are defined as the immune-competent resident cells of CNS [89] . This group of cells was firstly described by Pio del Rio-Hortega during his visionary period of activity that represent the corner stone of current microglial studies **(fig4)**. He hypothesized that these cells are derived from circulating mononuclear cells with mesodermal origins that differentiate in the brain as mature branched microglia [89]. Actually, it is a common point of view that microglia originates from bone marrow. However two separated population of microglial precursors cells have been described : the first derived from progenitors with myeloyd/mesenchymal origin, the second depicts a transient and developmental form of fetal macrophage strictly related to amoeboid microglial population described in post-natal brain of mammals [90]. The main idea is that microglial cells exist as a stable population in the brain and have a very low turnover [91,92] .It is possible however that during pathological condition, circulating monocytes should invade the brain and a line of bone marrow-derived cells could replace until 50% of microglia in postnatal period [93,94]. Supporting this , it is reported that blood monocytes could differentiate in mature microglia in "astrocyte conditioned medium"[95].The morphological maturation in ramified microglia from immature blood monocytes should be due to different cytokines released by astrocytes. Neutralizing antibodies against transforming growth factor beta, macrophage colony-stimulating factor and granulocyte/macrophage colony stimulating factor added to "astrocyte conditioned medium" prevent this maturation process [96].

Generally microglia is classified according to its morphological phenotype: resting microglia, activated microglia and ameboid phagocyting microglia. In CNS however, is appreciable a "provincially adapted microglia" which is guided and shaped following the structural organization of the tissue and different

biochemical signals[97,98,99] .Physiologically, these immuno-competent cells of CNS are prepared to answer to different aversive signals(i.e. biochemical or infective stimuli) and their response is related to the perceived stimulus. In vivo two photon imaging shows that microglial processes and arborizations continuously monitored brain parenchyma every few hours carrying out a sub-form of homeostatic surveillance[100] .According to its condition, microglia should be found in three different phenotypes based on the environmental circumstance in which was involved . The resting/surveillant microglia, a polarized pro-inflammatory phenotype defined as $M_{1,}$ prominent during a cytotoxic response mediated by infective pathogens or during tissutal active phagocytosis and cell migration and a different phenotype, $M_{2,}$ assumed when microglia is involved in resolutive processes acting to protect the tissue from damage and promote differentiation of oligodendrocyte progenitor through the release of anti-inflammatory cytokines [101,102]. Experimentally, M_1 or M_2 phenotypes should be reproduced by inducing particular conditions in the extracellular milieu. The addition of the toll-like-receptor (TLR)-4 agonist (lipopolysaccharide; LPS), interferon (IFN)-γ, IL-17A, orTNF-α promotes the M_1 pro-inflammatory phenotype. Conversely , stimuli such as IL-4, IL-10, IL-13, transforming growth factor (TGF)-β and/or glucocorticoids induce a state of immunological regulation or alternatively, an activated phenotype (M2)[101,102] **(Fig5)** . The M_1/ M_2 paradigm has been increasingly studied in different pathologies in an attempt to uncover mechanisms of immune-pathogenesis. Understanding the molecular and functional states of microglia provides a framework to dissect out and interrogate both beneficial and harmful roles of these cells.

Figure 4:Images of ramified microglia discovered by Del Rio Ortega 1919 (Bol. de la Soc esp de biol 1919)

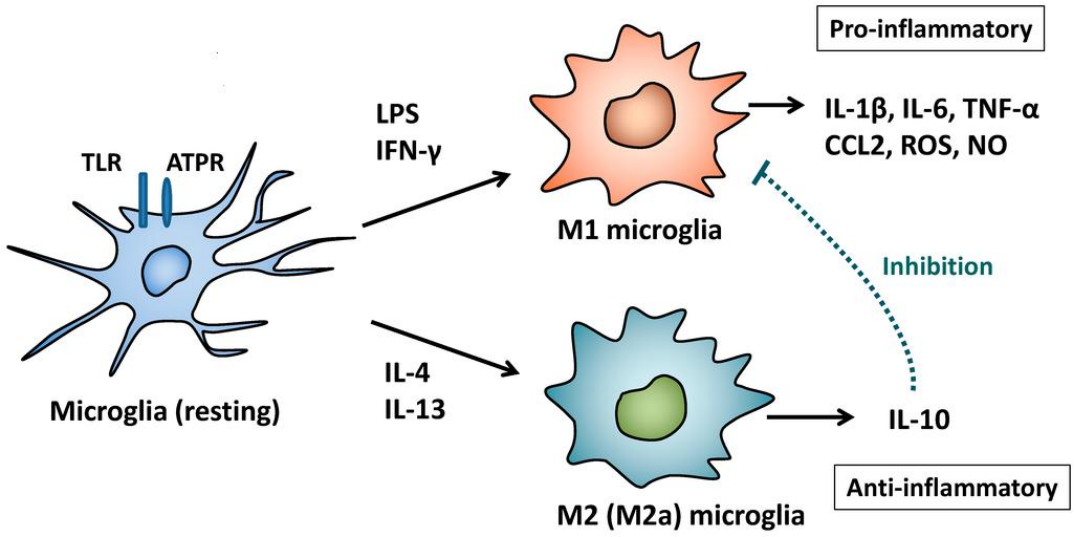

Figure 5 A schematic view of microglia activation.

Resting microglia in the presence of LPS or IFN-γ polarize in M_1 pro-inflammatory phenotype. In contrast "good signals" such as IL-4 or IL-13 induce M_2 protective phenotype. IL-10 production is an anti-inflammatory signal which down-regulates M_1 function (Adapted from Nakagawa Y. and Chiba K. Pharmaceuticals 2014) .

4.1 Microglia currents

Most of the functional studies on microglia cells have been performed *in vitro* and in *ex vivo* conditions in which microglial cells are already moderately activated. So far, there are not electrophysiological evidences of microglial cells basal properties (resting membrane potential, membrane currents or measurement of intracellular calcium homeostasis) in vivo. These cells are characterized by high input resistance and very low resting membrane potential ex vivo (mean -20mV) [103].The membrane conductance mainly consisted of delayed rectifying outward and inward currents ,accomplished by potassium channels, could be influenced by receptors already presents on microglia[104,105,106]. Recent evidence reports spontaneous microglia currents recorded from satellite cells (microglia that is in strictly contact to neuronal membrane) associated to the potassium and chloride reversal potential . These currents could be thus mediated by a cationic conductance, presumably sodium or calcium, or by a mixed cationic conductance[107].

4.2 Microglia "off-label" functions

4.2a Synaptic pruning

Excluding their principal function in the brain, as resident immuno-competent cells, microglia are highly motile cells in physiological and in pathological conditions[100]. During these movements is reported a very frequent and transient contact with the synapses [108,109] .These "contacts" have been described as crucial for brain development in early post natal period in rodents [110] .The key of this developmental mechanism was found in the selective increase of the chemokine fractalkine on the neuronal surface. This chemokine , whose receptor in the CNS

are a selective privilege of microglial cells, is reported as a "find-me" message during neuronal development in synapses in which occur phagocytosis[111,112,113]. The selective loss of neuron to microglia fractalkine signaling in early post natal period, as reported in the fractalkine receptor knock out mice model, increases excitatory dendritic spines as in an immature synapses[110] .These particular function of microglia is strategic for normal brain maturation and is reported as strictly important in development of a normal social behavior in mice [114] .

4.2b Microglia modulation of neurotransmission

Microglia communicate with neurons and astrocytes by direct physical contact as well as by releasing several soluble and insoluble mediators through classical or atypical secretory pathways [100,115]. In fact, imaging studies reveal that microglia dynamically interact with synapses responding to changes in neuronal activity and neurotransmitter release. Emerging studies indicate that activated microglia could influence both the synaptic neurotransmission and synaptic plasticity, laying the foundations for a quad-partite synapses. The acute stimulation of microglial cells by LPS modulates hippocampal excitatory synaptic neurotransmission through the activation of purinergic receptors on astrocytes [116]. Also in vitro model of combined both inflammation-hypoxia, describes a novel form of LTD in which microglia mediate AMPA receptor internalization in acute slices of hippocampus [117].Other studies underline an atypical microglia to neuron communication through the release of small signaling vesicles or exosomes defined " microvesicles" released upon microglia stimulation through i.e. purinergic or toll like 4 receptors [118]. Acute application of these exosomes on cultured neurons significantly increases GABA and glutamate release by influencing the sphingolipid metabolism and synaptic activity on pre-synaptic terminals [119,120,121] .Take

together these data underlie a growing evidence of microglia modulation of synaptic neurotransmission.

4.3 TRPV1channel on microglia

There are different direct or indirect evidences collected in vitro or in ex vivo experiments demonstrating the expression of several TRP channels on microglia. Primary rat cultured microglial cells express TRPV1 mRNA as demonstrated by RT-PCR and TRPV1 inhibition in cultured BV2-microglial cells seems to reduce oxigen species production and phagocytosis [122,123,124].In the other hand, in the rat retina, elevated hydrostatic pressure induces an increase of microglial IL-6 release and cytosolic TNF-alpha a phenomenon that is partially inhibited by 5-Iodoresiniferatoxin (5-IRTX) a specific antagonist of TRPV1[125]. Other ex in vivo experiments describe a strongTRPV1-dependent microglia damage in mice Substantia Nigra [122]. Altogether these data represent only indirect evidence on the functional expression of TRPV1 in microglia cells. Moreover, most of them have been obtained from cultured primary microglia or microglia-like cells in which the gene and consequently the protein expression can be altered.

5. Pain

The pain is an unpleasant sensorial and emotional experience which acts to preserve the organism against potential tissue damage. This protective mechanism should become chronic or debilitating when an eventual tissue damage persist or when in particular conditions the lesion has healed and the pain is continuously felt. Pain sensation is the result of the activation of peripheral nociceptive primary sensory neurons[126]. Nociceptors innervate the peripheral and deep tissues as well as the internal organs and detect a broad range of noxious

mechanical, thermal and chemical stimuli integrated in polimodal fashion. After a damage, the affected area undergoes a series of plastic changes resulting in a temporary sensitization of the afferent sensory fibers. In fact persistent pain associated with a peripheral injury results in an alteration of peripheral nerves properties and production of an inflammatory response, characterized by the release of cytokines, prostaglandins, neurotrophic factors, chemokines, lipids, peptides, ATP and glutamate. This inflammatory soup together with non neuronal cell infiltration and the persistent activation of inflammatory receptors characterizes the phenomenon called peripheral sensitization[127]. This hyperactivity give rise to phenomena defined allodynia (when normally innocuous stimulus is perceived as painful) and hyperalgesia (when normal pain stimulus elicit pain of great intensity). The pain experience initiated in the periphery should be maintained by both peripheral and in central loci. in fact, a deregulation of peripheral or central ways involved in pain can lead to physiologically and emotionally debilitating disease.

5.1 Anatomical overview

Peripheral sensory feelings are detected through nociceptors. The cell bodies of nociceptors are located in the DRG for the body and TG for the face. Nociceptors have a unique morphology in which central and peripheral terminals derive from a common axonal stalk and for this reason are called pseudo-unipolar neurons. Peripheral and central axonal branches innervate target organs and SC respectively. A single stimulus or a sum of stimuli that are recognized as noxious activate these neurons modifing the threshold of activation of these fibers underline the great capability of response that characterize the polymodal nociceptors[128]. There are two major classes of nociceptors: small-medium

diameter myelinated A-delta fibers and small diameter unmyelinated C fibers. The first fibers are involved in the the rapid/ acute pain and second in the integration of slow pain response (Meyer et al. 2008).The non-noxious sensory detection is leaved to A-beta larger diameter fast fibers. The A-delta class is subdivided in two principal classes: i) type I-high threshold nociceptors, responsive to mechanical and chemical noxious stimuli and characterized by high heat threshold (>50^{o}C) and ii) type II A-delta fibers, responsive to low threshold heat and for very high threshold mechanical stimuli. In the other side, the unmyelinated C fibers are very heterogeneous [129]. C fibers include a population which is susceptible to both heat and mechanical stimulus as well as a population heat-responsive but mechanically insensible (silent-nociceptors) activated only after an injury [130] .Primary afferent nociceptor fibers project to the dorsal horn of the SC. The SC is organized anatomically in distinct laminae (ten laminae). The dorsal horn involve the first five [131]. The A-delta fibers project to lamina I and to deeper lamina V; the A-beta fibers project in deep laminae III,IV and V. The C slow fibers terminate in lamina I and into the most dorsal and mid-region parts of the lamina II. Anatomical and electrophysiological studies have shown that SC neurons of lamina I and II are principally involved into noxious response, lamina III and IV are primary involved in innocuous stimuli detection and neurons in lamina V receive noxious and non-noxious inputs [128]. The major input of SC to the brain is constituted by lamina I and V projecting fibers[126]. Multiple afferent pathways , in particular the spino-thalamic and spino-reticulo-thalamic tracts, represent the pain ascending fibers to the thalamus and brainstem; both reach and integrate in cortical structures. In the supraspinal structures , there is not a single brain area essential for pain sensation, but a cooperative group of structures involved in sensory or emotional integration of pain defined the "pain matrix"[132,133].. Different

central areas are activated during noxious integration. In humans as well as in rodents, brain areas activated during pain experience are the somatosensory cortex 1, somatosensory cortex 2, anterior cingulate cortex (ACC), insula, prefrontal cortex, thalamus and cerebellum[134] . Other studies report also the amygdala and nucleus accumbens as nociceptive structures receiving input from the spinoparabrachial tract or spinoreticular-periacqueductal grey pathways [135,136,137,138]. The somatosensory cortices encode information in terms of sensory features, location and the duration of pain[139,140]. The ACC and Insula represent the most important areas encoding the emotional and motivational aspect of pain in humans and rodent [141,142,143] .The descending pain pathway represent the antinociceptive route or the "filter" controlling the pain felt. . The most frequently studied modulatory descending pathway involve the periacquedudctal brainstem nuclei, rostroventral medulla, locus coeruleus and the spinal cord . Stimulation of the descending pathway induces analgesia and involves endogenous opioids and catecholamines, namely noradrenaline and serotonin, which in turn control ascending projections and alter the pain perception[144] **(fig.6).**

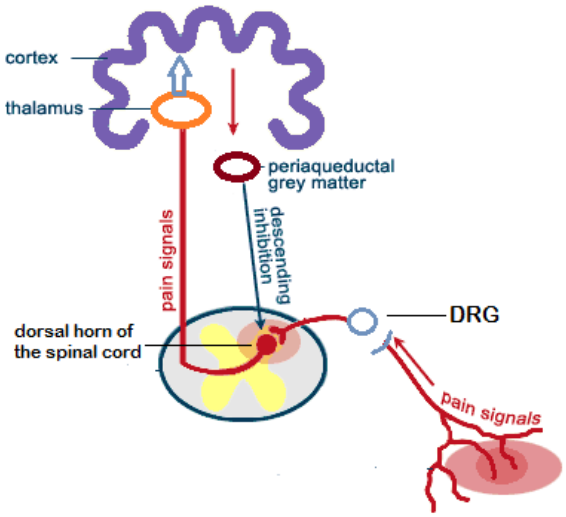

Figure 6:Semplified ascending and descending pain pathway

Pain signals arrive in the DRG which integrate in the dorsal horn of the spinal cord. Spino-thalamic and spinoreticular-thalamic afferents integrate in the thalamus. Sensory information arrive in the thalamus which in turn integrate in cortices (somatosensory cortex 1, somatosensory cortex 2, anterior cingulate cortex (ACC), insula, prefrontal cortex) and in limbic areas (not shown in the figure). Periaqueductal grey matter receives descending fibers from cortices and limbic areas. Descending pathway is involved in control of ascending pathway.

5.2 Neuropathic pain

Neuropathic pain (NP) is a form of chronic pain involving a broad spectrum of conditions associated with a lesion or disease of the peripheral or central somato-sensory system. Its prevalence in the general population may be as high as 7–8% and account 20-35 % of chronic pain [145,146]. The major cause of NP might be find in the lack of normal homeostatic reparative process of peripheral o central nervous system lesions. Conversely, the secondary forms, in terms of causal occurrence, are associated to a primary syndrome such as diabetes, primary oncological pain and secondary pain due to pharmacological treatment of tumors and genetics.

Central syndrome accont 8% of patients and occur after stroke, spinal cord injury and multiple sclerosis [147,148,149] .This NP syndrome acquires importance because of a very low rate of successful pharmacological treatments. The clinical symptoms are frequently characterized by continuous and evoked pain sensation, an allodynic and hyperalgesic syndrome in which normal non noxious sensory mechanical or thermal sensation triggers intense pain [150]. The emotional-cognitive sphere is usually strongly compromised and induce an aberrant behavioral response in terms of pain perception defined "central syndrome" (anxiety ,stress ,sleep deprivation etc.). This cognitive syndrome exacerbates, in the subject affected , the real perception of pain . So, we can define the "pain syndrome" a sum of these two part: an emotional-central somatization and a peripheral painful sensation[151,152,153,154].

5.3 Central supra-spinal sensitization

Persistent pain appears to be mediated by plastic changes and/or central sensitization, particularly in the pain matrix. The medial thalamus is the principal relay station of nociceptive input to the anterior cingulate and prefrontal cortices. The persistent stimulation of this pathway by pain during peripheral tissues injuries influence neurons excitability in the neocortex [155,156,157] . In particular the persistent pain is associated with long-term changes in the morphology, neurochemistry, and gene expression in the anterior cingulate cortex, which contribute to the maintenance and exacerbation of pain [158]. This brain region in fact, is deputed to the strict coupling between sensory and emotional component in humans as well as in mammals. The ACC, in fact is a key cortical region involved in pain integration [159,160,161] . The ACC is divided in different layers of pyramidal cells and local interneurons (**fig.7)**. Principal pyramidal cells are

located in layers II, III and V. Principal sensory input arises from the thalamus in the layer II-III. Output projections of the ACC, pyramidal cells are located in deep layer V which project to sensory related brain areas, including the motor cortex, amygdala, midbrain areas, brainstem and spinal cord **(Fig.8)**. Several plastic changes involve specific input and output regions during chronic pain condition in this area . The re-enforce and central sensitization during chronic pain occur as synaptic strengthening in ACC in pre- and in post-synaptic manner influencing the neurotransmitter release and increasing receptor balance in post-synaptic compartment exacerbating the "pain syndrome" [160,162].

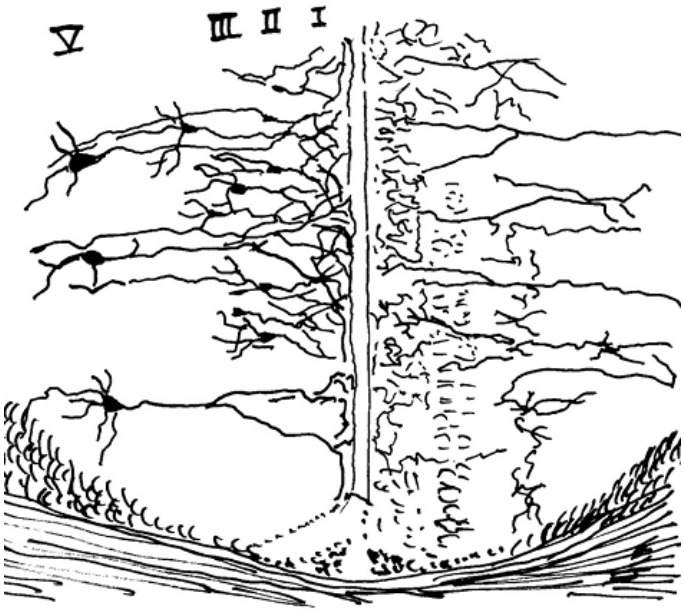

Figure 7: Anterior Cingulate cortex organization

A modified copy of Cajal's drawing of ACC. It is evident the typical layers subdivision of cortical areas. Layer II and III contain small soma pyramidal cells and interneurons. The dimensions of the soma is larger in pyramidal cells of the layer V. The branches of the pyramidal cells of the layer II-III and V extend to layer I.

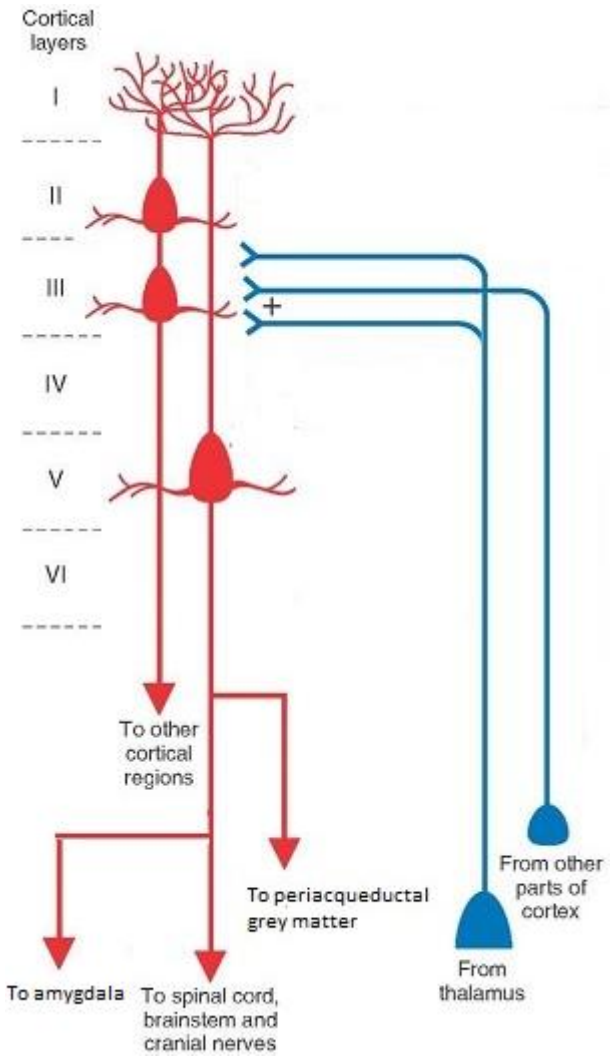

Figure 8: A schematic rapresentation of pain-related input and output in ACC

(red) Simpified circuitry of ACC.The thalamic and cortical (blue)excitatory input reaches the layer II and III of ACC. After the integrative process layer V of ACC communicate to output areas influencing descendig pathways of pain.The ACC projections to the amygdala are involved in emotional response to adversive events. Inter and intracellular cortical connections are frequently reported.

5.4 TRPV1 and pain

As reported above, TRPV1 is reported as the key in the peripheral sensory transmission but also a synaptic player whose activation modulates neurotransmitter release and synaptic plasticity. The TRPV1 role in pain perception and exacerbation assumes a predominant role when this receptor undergoes long-term modifications such as its sensitization. Robust hypersensitivity to heat is a clinical feature of chronic neuropathic pain and TRPV1 is a key component of thermal hyperalgesia mediated by inflammation[163,164].Indeed TRPV1 can be strongly activated by components of inflammatory soup in peripheral and in central nervous system such as bioactive lipids, extracellular protons ATP, NGF and bradykinin which influence the activation threshold of TRPV1. In CNS has been shown that activation of postsynaptic spinal TRPV1decreased functional AMPA receptor expression in interneurons of substantia gelatinosa and thus reduced excitation of these neurons. Moreover, GABAergicTRPV1 reduced inhibitory synaptic signaling to spino-thalamic neurons suggesting a mechanism of disinhibition of spinal cord projection neurons that are critical for the relay of nociceptive signals to higher brain centers[55]. At brain level the functional role of TRPV1 has been well characterized in the modulation of descending nociceptive pathway , in particular the periacqueductal-rostroventral-medulla circuit [165]. The activation of TRPV1s in the ventral lateral periacqueductalgrey (vlPAG) induces an anti-nociceptive effect by activating the glutamatergic cells in the rostral ventral medulla (RVM) and inducing a firing decrease in these pronociceptive cells[166].Conversly, capsaicin injection in the dorsolateral PAG induces pronociceptive effect[167]. Other works underline the importance of TRPV1 in the modulation of descending midbrain path. Mallet and collegues reported that acetaminophen metabolites N-(4-

hydroxyphenyl)-5Z,8Z,11Z,14Z -eicosatetraenamide as well as paracetamol metabolites (arvanil and olvanil) is capable to activate TRPV1 in the PAG inducing an antinociceptive effect in a formalin tail immersion model of pain. This effect is completely lost in Fatty amine idrolase(FAAH) an in TRPV1 knockout mice [168,169] Furthermore,the role of TRPV1 on pain matrix goes beyond the PAG-RVM circuits. The TRPV1 activity is reported in other areas that participate to pain integration such as the ACC, locus coeruleous and medial prefrontal cortex[79,170,171,172]. In these areas, TRPV1 activation induces an increase rather a decrease of glutamatergic neurotransmission and seems to contribute to persistent pain condition[171].Other studies performed in pre/intra limbic cortices suggest that TRPV1 activation is involved, as in ACC, in the processing of the affective pain component. Inhibition of TRPV1 in these areas reduced the pain behavioral response in a model of spinal nerve injury [172]. All these data underlining , as suggested in this study, a strong cortical TRPV1-dependent control on painful events.

Aim of the study

Since its discovery, the role of TRPV1 in the brain has not been clearly assessed. Moreover, compelling evidence indicate that TRPV1 has a highly restricted brain distribution. Conversely, numerous studies underlie that indeed TRPV1 is functional in different brain regions by acting both as postsynaptic mediator of different forms of synaptic plasticity and modulator of neurotransmitter release by a presynaptic mechanism. However, the immunohistochemical evidence does not support this latter effect. Considering the anatomical versus functional discrepancies on TRPV1, the objective of my thesis is to give more insights on the role of this channel in the brain in both physiological and pathological conditions i.e neuropathic pain. Among the painmatrix brain areas, this study focuses on the ACC to investigate the TRPV1 cellular mechanisms on the regulation of the emotional pain aspects.

CHAPTER 2 :METHODS

Animals

Both adult (P80-120) and young (P20-30), C57BL/6 (Charles River Laboratories, Como, Italy) and B6.129S4-*Trpv1*^{tm1Jul}/J mice (TRPV1$^{-/-}$; The Jackson Laboratory, Bar Harbor) were used in the present study. CX3CR1$^{+/GFP}$ male mice (P18-30) from D. Ragozzino (university of Sapienza, in Rome) were employed in this study.

Behaviour

Testing conditions and chronic constriction injury

All animals were housed in standard cages and kept under a 12-hour light-dark cycle in an air-conditioned facility. Following the procedure originally proposed by Bennett and Xie (1988), adapted for mice, chronic constriction injury of the sciatic nerve (CCI) was used as murine model of neuropathic pain. As previously described[68], CCI was obtained by three unilateral ligatures of sciatic nerve. In the following, injured and uninjured hindpaws are indicated as ipsilateral and contralateral hindpaws with respect to the sciatic nerve ligation. Anesthesia was performed intraperitoneally with zoletil (tiletamine and zolazepam, 100 mg/ml, 0.5 ml/kg) and rompun (xylazine, 20 mg/ml, 0.5 ml/kg).

All mice were examined for mechanical allodynia at days 3, 5, 7, 10, 12, 14, 17, 19, 21, 31 post-CCI. The behavioral analysis was conducted in the morning, and experimental procedure was in blind.

For ex vivo and in vitro experiments, mice were sacrificed at different time points after CCI and the assessment of allodynia development. For adults, we used the following time table: three days, one or four weeks after CCI, while young mice were sacrificed at three days, one or two weeks after CCI. In particular, for adults

the mechanical threshold (force-grams) was measured in naive and CCI at day 3 ($DF_{1,19}$; F 83,02; P<0,0001), 7 ($DF_{1,19}$; F 118,19; P<0,0001) and 21 ($DF_{1,19}$; F 28,05; P< 0,0001) after neuropathy induction.

As control, we used mice that underwent surgery without the sciatic nerve ligature (sham animals) and naïve animals, which did not undergo to any surgery. Both in vivo and in vitro data obtained from naïve and shams were pooled since no differences have been observed.

Mechanical allodynia

This parameter was assessed by measuring withdrawal threshold of both hindpaws to normally non-noxious punctuate mechanical stimuli by using an automatic von Frey apparatus (Dynamic Plantar Aesthesiometer, Ugo Basile, Comerio, Italy). After a 5 min of adaptation to the apparatus, the mechanical stimulus was applied to the midplantar surface of both hindpaws[68]. The mechanical threshold was measured as the maximal force (expressed in grams) at which mice withdrew its hindpaw. At each testing day, withdrawal threshold were taken as mean of three consecutive measurements with 10-s interval between each measurement.

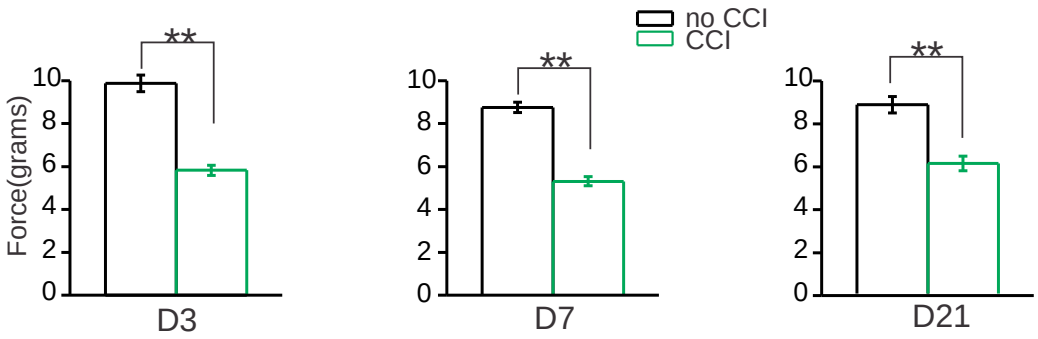

Development of allodynia after CCI .Mechanical threshold (force-grams) was measured in naive (no CCI, n=10) and CCI mice (n=11) at 3 (D3; $DF_{1,19}$; F 83,02; p<0.0001), 7 (D7; $DF_{1,19}$; F 118,19; p<0.0001) and 21 days (D21; $DF_{1,19}$; F 28,05; p< 0.0001) after neuropathy induction.

Electrophysiological recordings

From neurons

Both naïve/sham and CCI adult C57BL6 and TRPV1 KO mice were deeply anesthetized with isofluorane inhalation, decapitated, and brains removed and immersed in cold "cutting" solution (4°C) containing (in mM): 126 choline, 11 glucose, 26 $NaHCO_3$, 2.5 KCl, 1.25 NaH_2PO_4, 10 $MgSO_4$, 0.5 $CaCl_2$ equilibrate with 95% O_2 and 5% CO_2. Coronal slices (300 µm) were cut with a vibratome (Leica) and then incubated in oxygenated artificial cerebrospinal fluid (ACSF) containing (in mM): 126 NaCl, 26 $NaHCO_3$, 2.5 KCl, 1.25 NaH_2PO_4, 2 $MgSO_4$, 2 $CaCl_2$ and 10 glucose; pH 7.4, initially at 32°C for one hour, and subsequently at room temperature, before being transferred to the recording chamber and maintained at 32°C. Recordings were obtained from visually identified pyramidal neurons in layer 2/3, easily distinguished by the presence of an emerging apical dendrite. Experiments were performed in the whole-cell configuration of the patch-clamp technique. Electrodes (tip resistance = 3-4 MΩ) were filled with an intracellular solution containing (in mM): Kgluconate 135, KCl 4, NaCl 2, HEPES 10, EGTA 4, MgATP 4 NaGTP 2; pH adjusted to 7.3 with KOH; 290 mOsm. Whole-cell voltage-clamp recordings (-70 mV holding potential) were obtained using a Muticlamp 700B (Axon CNS, Molecular Device). Spontaneous EPSCs recorded in the presence of TTX 1□M (mEPSCs) were filtered at 1 kHz, digitized at 10 kHz, and recorded on computer using Digidata1440A and pClamp10 software (Molecular Device). Series resistances were not compensated to maintain the highest possible signal to noise and were monitored throughout the experiment. Recordings were discarded if Rs changed 25% of its initial value. Experiments in voltage-clamp recording were carried out in the presence of $GABA_A$ receptor antagonist picrotoxin (100□M) and TTX (1□M). Spontaneous events were detected and analyzed with Clampfit 10.4

using amplitude and area thresholds set as a multiple (3–4X) of the SD of the noise. Each event was also visually inspected to prevent noise disturbance of the analysis. The cumulative amplitude and interevent plots obtained for each cell in controls and after drug application were compared using the Kolmogorov–Smirnov (KS) test.

Each slice received only a single exposure to capsaicin or to other agonists. In experiments performed to investigate a postsynaptic TRPV1-mediated response, the ionotropic glutamate receptor blockers 6,7-dinitroquinoxaline-2,3,dione (DNQX, 10 µM) and DL-2-amino-5-posphonovaleric acid (DL-APV, 50 µM) and the $GABA_A$ receptor antagonist picrotoxin (100□M) were included in the bath solutions. For voltage-clamp experiments TTX were also added.

For current-clamp experiments membrane resistance was measured from responses to current injections (-60 pA, 250 ms, 0.2 Hz) and were performed in the presence of ionotropic glutamatergic and $GABA_A$ receptor antagonists.

From microglia cells

Acute slice of cingulate cortex (cG1 and cG2) was prepared from $CX3CR1^{+/GFP}$ male mice (P18-30). Animals were decapitated under halothane anesthesia, and whole brains were rapidly immersed for 10 min in chilled standard artificial cerebrospinal fluid (ACSF) containing (in mM): NaCl 125, KCl 2.3, $CaCl_2$ 2, $MgCl_2$ 1, $NaHPO_4$ 1, $NaHCO_3$ 26 and glucose 10 (Sigma Aldrich). The ACSF was continuously oxygenated with 95% O_2, 5% CO_2 to maintain physiological pH. Coronal 250 mm cingulate cortex slices were cut at 4 °C with a vibratome (DSK, Kyoto, Japan) and placed in a chamber containing oxygenated ACSF to recover for at least 1 hour at room temperature.

All recordings were performed on slices submerged in warmed ACSF (30-32 °C) and perfused (1 ml/min) with the same solution in the recording chamber under the microscope.

Visually identified GFP-expressing microglial cells were patched in whole-cell configuration in the cingulate cortex. Micropipettes (4–5 MΩ) were usually filled with solution containing the following composition (in mM): KCl 140, EGTA 0.5, MgCl2 2, HEPES 10, and Mg-ATP 2 (pH 7.3 adjusted with KOH, osmolarity 290 mOsm; Sigma Aldrich). Voltage-clamp recordings were performed using an Axopatch 200A amplifier (Molecular Devices). Currents were filtered at 2 kHz, digitized (10 kHz) and collected using Clampex 10 (Molecular Devices); the analysis was performed off-line using Clampfit 10 (Molecular Devices). Slicing procedure might activate microglial cells especially near the surface of the slice, whereby recordings were performed on deep cells. The current/voltage (I/V) relationship of each cell was determined applying ramp protocol from -120 to +50 mV in 500 msec every 10-30 seconds after whole-cell configuration was achieved (HP = -70 mV between steps). Resting membrane potential and membrane capacitance were measured at start of recording.

Capsaicin was first dissolved in DMSO and then in ACSF solution at a final concentration of 1 □M and applied in bath for 10 minutes.

Histology and immunofluorescence

From fixed sections of cortex, spinal cord and dorsal root ganglion

Both young (P21-24) and adult (P80-90) naïve and CCI C57BL6J/ *Trpv1-/-* mice were sacrificed with lethal dose of carbon dioxide and immediately underwent perfusion procedure. Blood was firstly transcardially washed out with cold phosphate buffer 0.9% saline solution (PBS), and tissues were fixed by cold 4%

paraphormaldehyde in 0.1 M pH 7.4 phosphate buffer (PB) with a peristaltic pump. Brains and spinal cords were dissected, postfixed for 18-22 hours at 4°C, washed from paraphormaldehyde with PB and cryoprotected in 30% sucrose/PB at 4°C.

Dry ice frozen brains were cut into 40 µm coronal sections with a cryostat microtome (Leica Microsystems) at -20°C, including anterior cingulated cortex (ACC, Fig 22- 28 of mouse brain atlas, Franklin e Paxinos, 2001). Frozen lumbar spinal cord (L4-L5) was cut into 40 µm sections. Dorsal root ganglia were dissected from not perfused animals, fixed by 4% paraphormaldehyde solution, cryoprotected in sucrose solution and cut in 30 µm sections.

Sections were rinsed for tree time in PB and incubated with a mix of primary antibodies in PB 0.3% Triton X-100 (Applichem, BioChemica, Darmstadt, Germany) overnight at room temperature. Primary antibody incubation step was followed by three 10-min rinses in PB at RT. Afterwards, sections were incubated for 2 h at RT in a mix of secondary antibodies, followed by three 10-min rinses in PB. DAPI was applied for 5 minutes in the second rinse, dissolved in PB solution.

To exclude non-specific signals of secondary antibodies, sections from each group of animals have also been stained with secondary antibody alone, following the same experimental procedure but omitting the primary antibodies.

From freshly acute cortical slices

Adult (P80-90) C57BL6 and B6.129S4-*Trpv1*^{tm1Jul}/J (TRPV1$^{-/-}$) mice were sacrificed after anesthesia with isoflurane and the brain was immediately dissected. 300 µm thickness coronal slices containing ACC were cut with a vibratome (Leica Microsystems) in oxygenated ACSF. Slices were then kept at 32°C in a submerged chamber containing ACSF equilibrated with a mixture of 5% CO2 and 95% O2. For

the pharmacological treatments, slices were transferred in a submerged chamber containing ACSF (control), ACSF plus DMSO (vehicle), capsaicin (1 □M) or LPS (500ng/ml) for 10 minutes (same time as used for electrophysiological recordings) and immediately after, fixed in 4% paraphormaldehyde ,0.1 M phosphate buffer (PB) for 2 h at room temperature. After the fixing, slices were cryoprotected in 30% sucrose/PB and resectioned into 40 µm coronal sections with a cryostat microtome, following the same procedure as for fixed slices.

Antibodies

The following primary antibodies were used: rabbit anti-TRPV1 (1:100, Immunological Sciences Rome, Italy), mouse anti-TRPV1 (1:100, Millipore Bioscience Research Reagents, USA), rabbit anti-TRPV1 (1:500, Neuromics, Edina, MN), rabbit or mouse anti-NeuN (1:1000, Millipore Bioscience Research Reagents, USA), rabbit anti-GFAP (1:500, DakoCytomation, Glostrup, Denmark), rabbit anti-Iba1 (1:500, Wako, Osaka, Japan), rat anti--CD11b (1:300, Serotec; Kidlington, UK), goat anti Glutamate Transporter (EAAC1, 1:100, Millipore Bioscience Research Reagents, USA). For nuclear staining, 4,6' diamidino2-phenylindole dihydrochloride (DAPI,1:2000, Life Technologies, Carlsbad, California) was used.
Secondary Cy3, DyLight488 and DyLight 649-conjugated antibodies were used (1:200, Jackson ImmunoResearch, West Grove, PA, USA).

Acquisition and analysis of images

Double-immunofluorescence and triple-fluorescence labeling was examined with a confocal laser scanning microscope (Leica SP5, Leica Microsystems, Wetzlar, Germany) equipped with four laser lines: violet diode emitting at 405 nm, argon emitting at 488 nm, and helium/neon emitting at 543 nm and 633. Confocal

images were acquired through the 40x/63x objective at the 1 zoom factor. In the case of magnifications, zoom factor was raised in order to focus only on the area of interest.

Points of colocalization were supposed when a merging area in the same cell was evident, showing a yellow resulting colour from the overlap of two green-red signals, and they were verified by magnifications and analysis on the z axes with 1-2 microns stacks.

Quantitative data from images were obtained keeping the following imagine acquisition criteria: 40x objective, 1024 x 1024 frame, 10 hz acquisition frequency, pinhole 1 airy unit, lasers at 50%.

For analysis of the area occupied by the signal, confocal acquisitions of ACC for each hemisphere were taken comprehending area covered by the 40x objective in both naïve and mice suffering from neuropathic pain (two for ipsilateral and two for contralateral ACC), in order to have an overview of the first cortical layers (layers 2-3), and a second acquisition including the more internal layers (layer five). Since there were no significant differences between medial and internal layers (measured for each couple of layers for any group, t Test $p > 0.05$), quantifications were cumulated so as to obtain an evaluation of the antibody expression in the whole ACC.

Each image has been analyzed with Image J free software (National Institutes of Health, US; http://imagej.nih.gov/) with the following procedure: for each single image the background was subtracted in a same proportion for each group, in a range between 10%-50% on respect to the specific antibody. Images were reduced at 8 bit from the original RGB acquisition and a threshold was established in order to obtain a digital image where neither original signal disappeared and nor new signal was created. These images were analyzed with the command

“analysis of particles”, setting a filter in order to the size of signal and measuring in micrometers. Data were expressed as Area Fraction, the percentage of the total image area covered by the measured object. To establish the percentage of neurons expressing TRPV1, or both TRPV1 and EAAC1 marker, images in double and triple staining were acquired. Cells immunopositive for NeuN, TRPV1 and EAAC1 were counted, in the merging images, by the use of non-automatic cell counting method (Leica Microsystems software). Data are presented as the percentage of means.

Colocalization was intended as two proteins that occupy the same volume of interest.

The amount of colocalization was evaluated by using the Pearson statistical index of correlation (r) between two variables. This analysis describes the effect size as the strength of the linear correlation between the two variables (Evans, 1996: 0-0.19 “very weak”, 0.20-0.39 “weak”, 0.40-0.59 “moderate”, 0.60-0.79 “strong”, 0. 80-1.0 “very strong”).

For colocalization analysis, a double fluorescence image (red and green dyes) was splitted in RedGreenBlu channels. Background was subtracted from the red and the green channels (8 bit each) and they were analyzed for correlation using the colocalization plugin with Pearson and Manders index. Pearson index was chosen for its consistency and lack of sensibility to the picture background.

For each colocalization analysis, 256×256 Red-green scatterplots were generated by the Image J program: the intensity of red pixels is used as the x-coordinate whereas the intensity of the green pixels as the y-coordinate.

Morphometric analyses

Morphometric analysis were performed on a high resolution imagine acquisition criteria: 40x objective, 2048 x 2048 frame, 200 hz acquisition frequency 3X average scan, pinhole 1 airy unit, lasers at 50%.

Although two 40x objective confocal acquisitions were acquired in order to obtain an overview of ACC (one for cortex layers 2/3 and one for layer five) only the first layers acquisition (L2/3) was chosen for morphometrical analysis.

Each image has been analyzed with plugin "Shape descriptor 1u" of Image J software (http://imagej.nih.gov/plugins) with the following procedure: images were reduced at 8 bit from the original RGB acquisition and a threshold was established in order to obtain a digital image where neither the original signal disappeared and nor new signal was created. The plugin setting was fixed at a minimum of 200 μm of size and analysis was performed automatically on cell silhouettes.

Transformation index (TI) was used as an index of microglia morphology [69,70] and calculated by the equation: [perimeter of cell (μm)]^2/4Π [cell area (μm²)]. Since TI is dependent on cell shape but independent of cell size, this latter crucial for the identification of the three different microglia activation states (bushy, ipertrophied and ameboid), we exploit this parameter in order to obtain an unbiased analyses and avoid negative falses. The area:TI ratio was calculated for each cell and a scale value was set to obtain 4 group of cells (Suppl Figures7A): RESTING cells (values of area:TI ranging from 1 to 25); HYPERTROPHIED cells (values of area/TI ranging from 25 to 35); BUSHY cells (values of area/TI ranging from 35 to 60); AMEBOID cells (values of area/TI up of 60). The percentage of cell ratio was calculated by dividing the number of a specific cell group (i.e. resting, bushy, hypertrophied and amoeboid) for the total cell number of each

experimental condition (control, vehicle, capsaicin/lps, in both wt and TRPV1 $^{-/-}$ tissue).The frequency of cells in each category was statistically quantified by the using of Fisher's exact test and performed on raw data.

Western Blotting

Western blotting was performed according to standard procedures. Briefly, isolated tissues (10 mg) and cells ($3x10^5$) were resuspended in lysis buffer (50 mM Tris-HCl, pH 7.4, 150 mM NaCl, 5 mM $MgCl_2$, 1 mM EGTA, 1% (v/v) Nonidet P-40, 10 µg/ml aprotinin, 10 µg/ml leupeptin, 1 mM PMSF), homogenized with a glass-Teflon homogenizer and/or sonicated prior to centrifugation. Proteins in the lysates were quantified by the Bradford assay kit (Bio-Rad, Hercules, CA), separated by SDS-PAGE (10%) and transferred to nitrocellulose membranes. Blots were then incubated with primary antibodies recognizing TRPV1 (diluted 1:1000), NeuN (diluted 1:500), Iba1 (1:500), or actin (diluted 1:100000). After incubation with the appropriate horseradish peroxidase-conjugated antibody, blots were developed using an enhanced chemiluminescence detection system (Luminata Crescendo Western HRP substrate, Merck Millipore, Darmstadt, Germany). Scanning densitometry on the developed film was conducted at 600 dpi using a CanoScan LiDE 210 (Canon, Tokyo, Japan) and analyzed using Image J 1.49v program (http://imagej.nih.gov/ij).

Isolation of Neuronal and Microglial cells and Flow cytometry analysis

Cerebral cortex from 12 C57Bl6J and 3 TRPV1$^{-/-}$ mice (60-70 days old) were dissociated to single-cell suspension by enzymatic degradation using neural tissue dissociation kit from MACS® Technology (Miltenyi Biotec) according to the manufacturer's protocol. Briefly, cortical tissues were weighed before mincing, a pre-warmed enzyme (Papain) mix added to the tissue pieces, and incubated under

slow, continuous rotation at 37 °C on a MACSMix Tube Rotator. The tissue was further mechanically dissociated by trituration and the suspension was applied to a 70-micron cell strainer. Myelin was removed using Myelin Removal Beads II kit on autoMACS Pro Separator. Cells were processed immediately for MACS MicroBead separations. In order to separate primary microglia, The CD11b-positive cells were magnetically labeled with CD11b (Microglia) MicroBeads and isolated on autoMACS Pro Separator. The negative fraction was further processed with Neuron Isolation kit by depletion of non-neuronal cells and neurons were obtained from the unlabeled cells running through autoMACS Pro Separator. Both cells populations were fixed with 4% paraformaldehyde (PFA) for 10 minutes and then stained first with mouse primary TRPV1 antibody and then with anti-mouse Alexa633 secondary antibody. Subsequently neuronal cells were stained with mouse primary antibody NeuN and then with anti-mouse Alexa488 secondary antibody, while microglial cells with PE-Cy7-conjugated CD11b. For microglial activation experiments, $2X10^5$ cells were left untreated or stimulated with Capsaicin (1 μM) for 10 minutes, washed and then left in complete medium in presence of Brefeldin A (10 μg/ml) in order to block cytokine exocytosis. At the end of the incubation, cells were stained at the cell surface with CD11b, fixed with 4% PFA for 10 minutes, and then stained intracellularly with APC-conjugated TNF-α and PE-conjugated IL-10 antibodies in 0.5% saponin for 20 minutes. Cells were acquired using FACSCyan ADP (Beckman Coulter) flow cytometer and analyzed using Flowjo software (TreeStar, Ashland, OR).

Microglia cell cultures

Primary cultures of cortical glial cells were obtained from 2-day-old C57BL6 mice and killed by decapitation according to Directive 2010/63/EU and as describe in Levi et al. 1984. Cells were plated at low density (3×10^6 cells per 90-mm dish)

and cultured in basal Eagle's medium (BME), supplemented with 10% heat-inactivated fetal calf serum (FCS) and 5 mM KCl for 20 days. Microglial cells were obtained by dish gentle shaking, collected by centrifugation and reseeded[71]. This protocol produced cultures with >90% microglial cells, as verified by immunofluorescence with monoclonal antibodies for the specific markers ED1 and iba1.

Quantification of EVs

Nanosight measurement. Microglia were exposed to serum free culture medium for 10 minutes, in order to quantify constitutive EV production. The medium was collected, the cells kept for about 5h in complete medium, and then re-exposed to serum free medium added with 300 nM capsaicin or 1mM ATP (positive control) for 10 min, to measure EV production upon TRPV1 stimulation. Conditioned media were pre-cleared from cells and debris at 300g for 10 min (twice) and the number and dimension of MVs and exosomes were analyzed with Nanosight LM10-HS system configured with a 405 nm laser and EMCDD camera (Hamamatsu Photonics). Videos were collected and analysed using the NTA-software (version 2.3), with the minimal expected particle size, minimum track length, and blur setting, all set to automatic. Camera shutter speed was fixed at 20.01 ms and camera gain was set to 350. Ambient temperature was ranging from 25 to 28° C. Five recordings of 30 seconds were performed for each sample. EV production under capsaicin exposure was normalized to constitutive EV release from the same Petri dishes, to minimize possible variability in the density of donor microglia.

Spectrophotometric quantification of shed MVs. Microglia were incubated with 5μM NBD-C6_HPC, washed with Kreb's Ringer solution, and stimulated with ATP

or capsaicin. Supernatants were collected, centrifuged 10 min 300*g* 4°C to remove cells and debris, and then total fluorescence was assayed at 463/536 nm with a Tecan Infinite500 spectrophotometric system (Tecan, Group Ltd, Switzerland). Constitutive or evoked MV shedding was quantified from at least three distinct Petri/condition in each experiment.

qRT-PCR.

Total RNA was extracted by previously isolated mouse neurons and microglial cellsas well as from spinal cord, using ReliaprepTM RNA Cell Miniprep System (Promega). cDNA reverse transcription was performed by means of Superscript VILO cDNA Synthesis Kit (ThermoFisher Scientific), according to manufacturer instructionsas reported (Chiurchiù et al., 2014 Atherosclerosis).The following program was used for the quantitative RT-PCR: 25 °C for 10 min, 42 °C for 50 min, 85 °C for 5 min, then after addition of 0.1 unit/ml of Escherichia coli RNase H, the product was incubated at 37 °C for 20 min. The target transcripts within the ECS were amplified by means of an ABI PRISM 7700 sequence detector system (Applied Biosystems, Foster City, CA), using the following specific primers forTRPV1 and β-actin: mouse TRPV1 F1 (5'-CATCCTCCTGCTCAACATGC-3') and R1 (5'-GCCTTCCTCATGCACTTCAG-3') and mouse β-actinF1 (5'-TGTTACCAACTGGGACGA-3') and R1 (5'-GTCTCAAACATGATCTGGGTC-3'). All assays were performed in duplicate, and for each well we used 10ng of sample template cDNA. Assays were run on Roche Lightcycler 480 Real-Time PCR System. 20 µl assays were prepared for each sample as it follows: 5 µl of cDNA product,10µl of SYBR Green master mix (Roche, cat # 04707516001), 2 µl of each primer (4 µM, Sigma) and 3 µl of PCR-grade water.The following PCR program was used: 5 min of pre-incubation at 95 °C, followed by 40 amplification cycles at 95 °C for 10 s, 61 °C

for 20 s, and 72 °C for 7 s.All data were obtained using automatic detection of TRPV1 gene Ct normalized with β-actin; for each sample, TRPV1relative expression was evaluated as fold increase of gene expression compared withβ-actin (2^ΔCt, with ΔCt= Ct (TPRV1) –Ct (β-actin)).The specificity of PCR reactions was evaluated at the end of each experiment by analyzing melting curves for each sample and, later, by running the assays in a 2% agarose gel.

Statistics

The sample number for electrophysiological experiments have been calculated on the basis of for previous experiment. All data were expressed as means ± S.E.M. For immunofluorescence experiments, significance was tested using one-way ANOVA followed by a Tuckey post hoc test for internal significance or student T test in the case of two groups comparisons. For electrophysiological data, Shapiro-Wilk test was exploited to verify a normally distributed data population. We then applied parametric or non-parametric tests. For the former, we used ANOVA and Student t Test. For non-parametric data we used Wilcoxon Signed Rank test (paired samples) and Mann-Whitney test and Kolmogorov Smirnov test (unpaired samples).Statistical differences were considered as significant at $p<0.05$. Statistical analysis was performed by using Origin 8.1 software (OriginLab Corporation).

CHAPTER 3 :

RESULTS AND DISCUSSION

TRPV1 is expressed in microglia of ACC and other supraspinal pain areas

Our immunohistochemical evidence achieved by using a TRPV1-monoclonal antibody shows that this antibody stain fibers in ACC sections of adult mice (n=16 from 9 mice; **Fig. 9a,b**). The antibody specificity was tested in tissue samples from TRPV1$^{-/-}$ mice (n=8 from 6 mice).The polyclonal antibodies, in this experimental conditions, continue to stain cytoplasm of cells in tissues of TRPV1$^{-/-}$ mice, this nonspecific stain is completely absent by using the anti-TRPV1 monoclonal antibody (**Fig.10**). Double immunofluorescence for TRPV1 and the neuronal marker NeuN showed that the TRPV1 positive fiber principally surrounded neuronal bodies (**Fig. 9a**, n=5 from 4 adult mice). Sparse overlapping between the two antibodies was evident in confocal maximum projection (**Fig. 9a**, TRPV1/NeuN panel). However single 1-2 μm z-stacks showed that merged signal is not the result of a neuronal staining but could be attributed to the slight overlap of TRPV1 fibres surrounding neurons. The amount of colocalization between TRPV1 and NeuN was “very weak” as indicated by the Pearson coefficient of correlation (PCC; r=0.125 ±0.012, n=5 from 4 mice; **Fig. 9** . Double immunostaining with the anti-TRPV1 MAb and the microglial marker Iba1 revealed that TRPV1 was mostly expressed in microglia (**Fig. 9b**) as confirmed by the high grade of colocalization of TRPV1 and Iba1 signals (r=0.720 ±0.010, n= 5 from 5 mice, **Fig. 9 d**).This microglial TRPV1 expression pattern was also evident in other “painmatrix” areas i.e somatosensory cortex, dentate gyrus, thalamus and periaqueductal gray (PAG) (**Figure 11**). In order to confirm this pattern of expression and our hypothesis, analyses on highly purified neurons and microglial cells from cortical adult tissues were performed. Protein analysis evaluated by flow cytometry revealed low mean fluorescence intensity levels of surface TRPV1 expression in NeuN positive neurons (MFI=48.2±7.4, n= 3 from 3 mice pools), whereas CD11b positive

microglial cells showed intense levels (MFI=124.8±15.2, n= 3 from 3 mice pools) (**Fig. 12 a-b**). These findings were further confirmed through western blot analysis on protein extracts of ACC and postnatal cortical microglia cultures. TRPV1 was immunodetected as a band of 100 kD in the ACC extracts from wild-type but not from TRPV1 $^{-/-}$ mice (**fig.12 c**). We also detected a second band of 75 kDa that was still present in TRPV1 $^{-/-}$ tissues and was absent in cultured microglia cells (non specific band) **(Fig. 12 d**).

This evidence can also be observed when comparing TRPV1 expression in the ACC *vs* cortical microglia cultures, whereby this receptor was 6-fold higher in the latter cells (**fig12 e**). Finally, in order to verify that such highly expressed TRPV1 on microglial cells was also fully functional, we performed patch-clamp recordings of CX3CR1-GFP expressing microglial cells from ACC slices upon application of capsaicin. As expected and consistent with the typical properties of TRPV1 channels, we observed the activation of a capsaicin-evoked outward rectifying current (**Fig. 12.g**), suggesting that functional TRPV1 is present in the microglia of mouse cortex. The differences in TRPV1 protein expression is independent from TRPV1 mRNA synthesis. Acute isolated cortical neurons and microglial cells express similar amount of TRPV1 protein(**fig. 12f**)

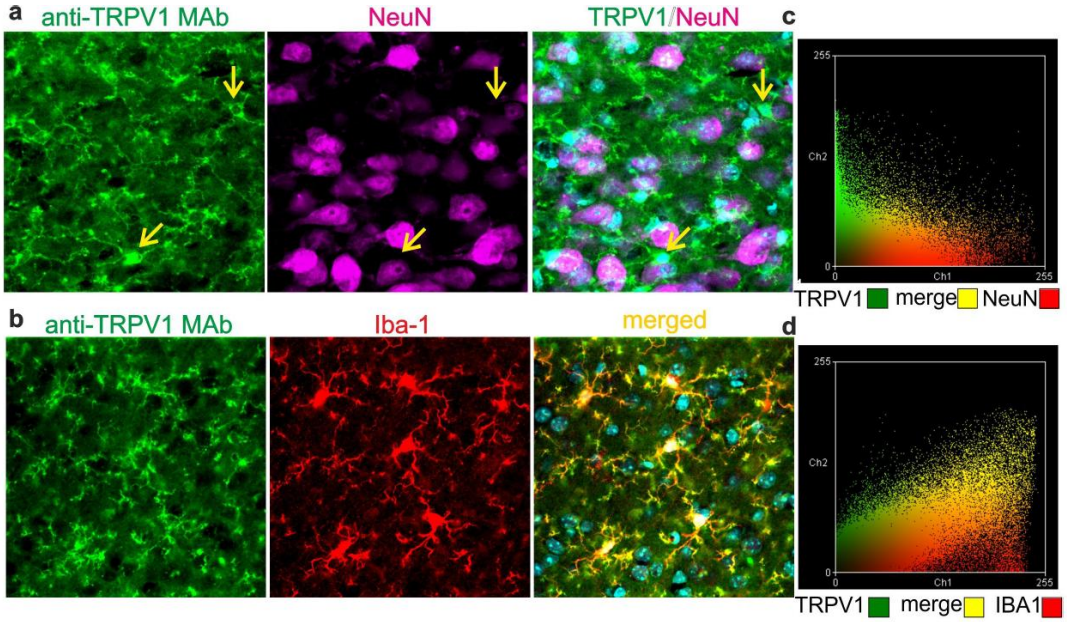

Figure 9 . TRPV1 protein expression in microglial and neuronal cells of the ACC of adult and young naïve mice. (**a**) Photomicrograph of double immunofluorescence for anti-TRPV1 MAb (green) and NeuN (magenta). The anti-TRPV1 MAb labels mainly fibers surround neurons (NeuN positive cells) and different type of cells (yellow arrows) .(**b**) Anti-TRPV1 positive processes highly overlap with the microglial marker iba1 (in red) in the layer 2/3 of ACC. (**a,b**) DAPI, nuclear marker (in blue) . (**c,d**) Graphic representation (scatter plot) of the correlation coefficient of Pearson (PCC) for quantifying the colocalization between the anti-TRPV1 and NeuN (in yellow, PCC=0.13) and anti-TRPV1 and Iba-1 (PCC=0.77). Note that higher PCC values correspond to a strong colocalization (Evans, J. M. Straightforward Statistics for the Behavioral Sciences. (1996).

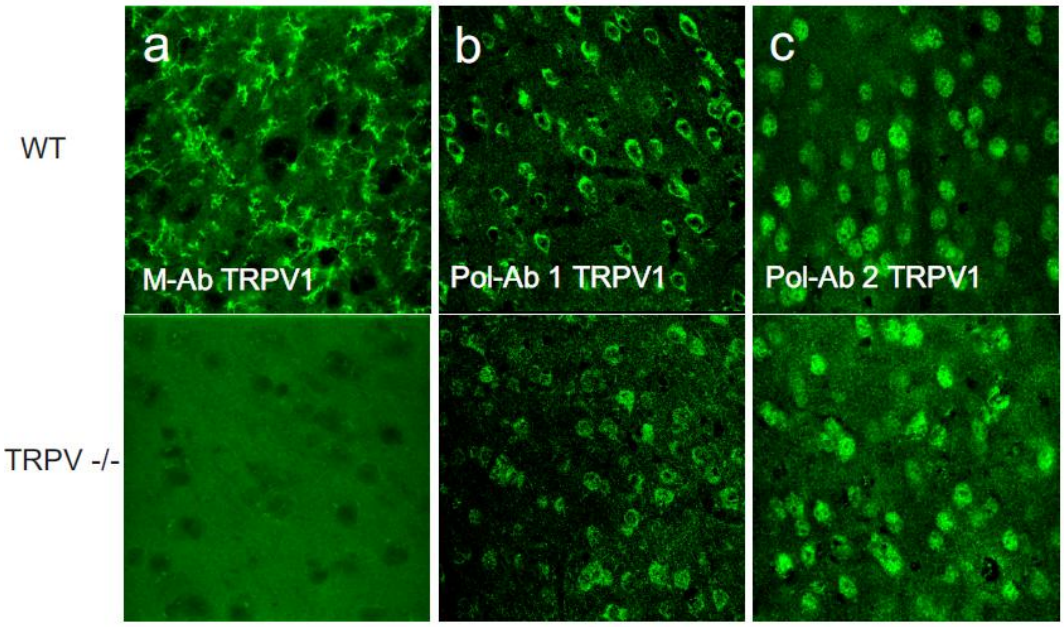

Figure10:TRPV1-MAb antibody validation. High resolution confocal laser scanning photomicrographs of ACC sections **wt and TRPV1-/- mice ,** showing the staining pattern of three different anti-TRPV1 antibodies (Abs). **(a)** Anti-TRPV1 MAb labeling of fibers (Millipore Chemicon, 1:100). Same protocol of immunostaining on TRPV1-/- mice tissues shows no stain from both primary or secondary antibody **(b-c)** The cell cytoplasm or whole-cell body labelling of two anti-TRPV1 pAbs is similar in cortical tissues from wt and -/- mice.

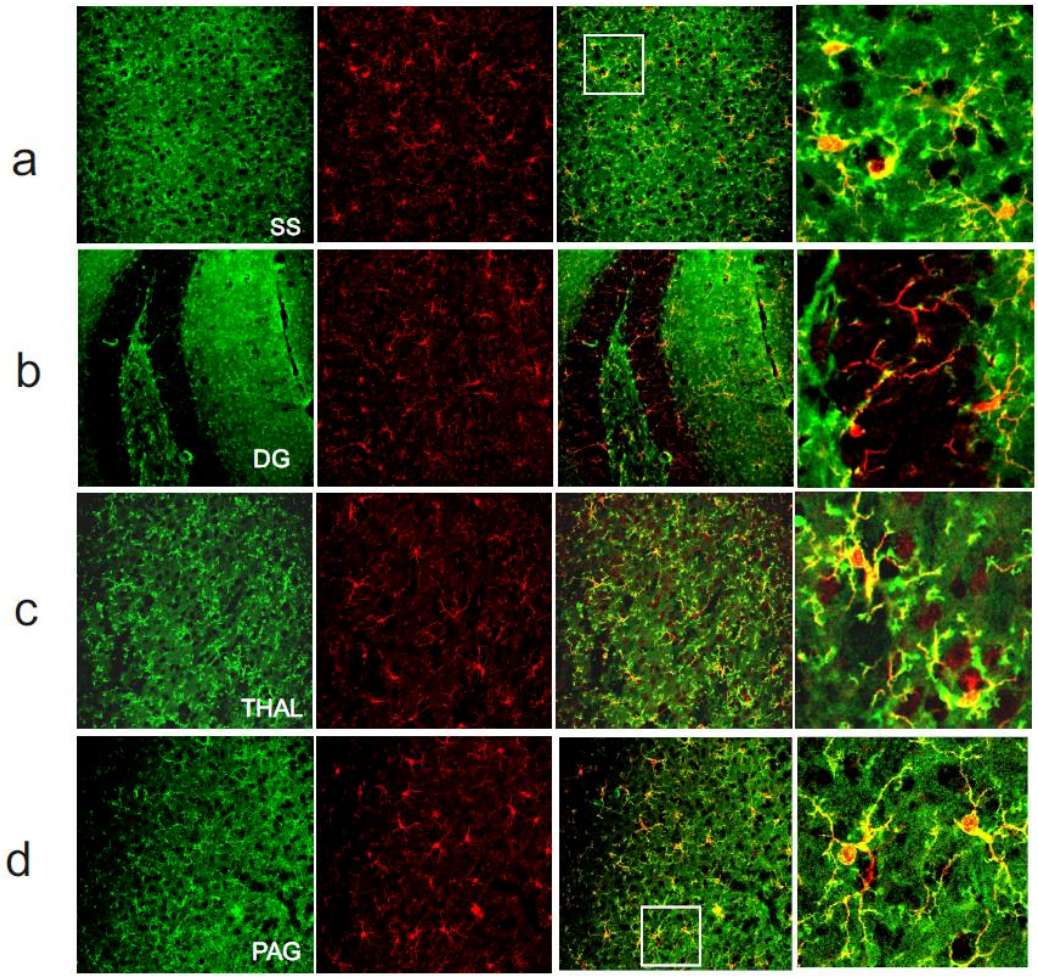

Figure 11:(**a-d**) Confocal laser scanning photomicrographs of somatosensory cortex (SS n=17/9),dentate gyrus (DG n=17/9), thalamus (THAL n=17/9) and periaqueductal gray (PAGn=11/6) showing labeling for anti-TRPV1, Iba-1 and their merged. Like the ACC, also in these brain regions the TRPV1 is mainly expressed in the microglia.

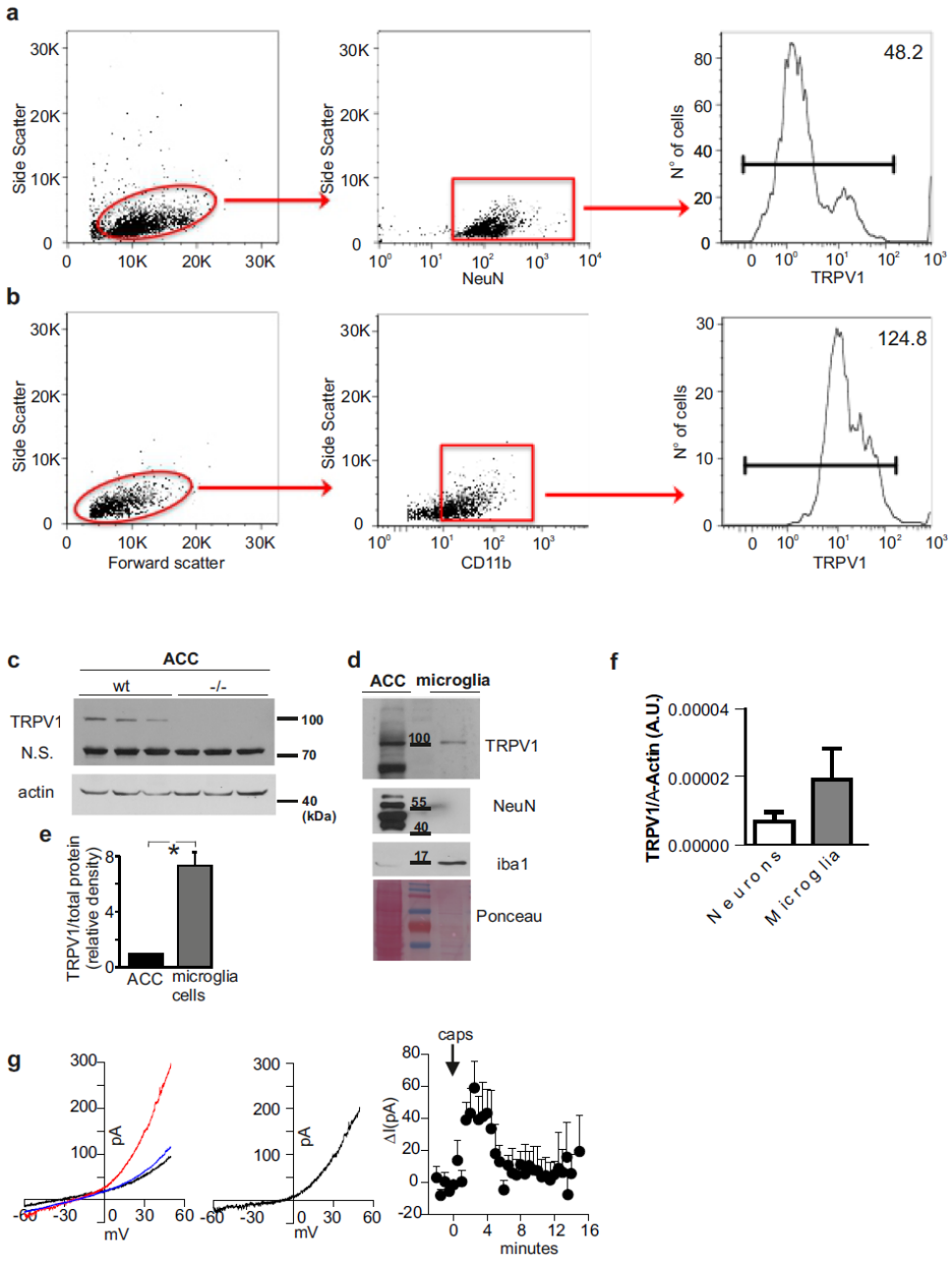
a
Side Scatter
NeuN
N° of cells
48.2
TRPV1
b
Forward scatter
CD11b
124.8
c
ACC
wt
-/-
TRPV1
N.S.
actin
100
70
40
(kDa)
d
ACC microglia
TRPV1
NeuN
iba1
Ponceau
e
TRPV1/total protein (relative density)
ACC
microglia cells
f
TRPV1/A-Actin (A.U.)
Neurons
Microglia
g
pA
mV
caps
ΔI(pA)
minutes

Figure 12

Figure 12 TRPV1 protein is mainly expressed on microglial cell and is functional active

Neuronal and microglial cells were isolated from cortical tissue using specific magnetically labeled kits. According to physical parameters, obtained cells were gated on NeuN and CD11b for identification of neurons **(a)** and microglial cells **(b)** respectively. Surface expression of TRPV1 was analyzed by means of flow cytometry. Data are representative of a single experiment and show the mean fluorescence intensity (MFI) of 3 independent pools of at least 3 mice. **(c)** Representative immunoblot of TRPV1 expression in ACC fromwild-type (wt) and TRPV1-/- (-/-) mice. Protein lysate of each tissue was subjected to immunoblotting following SDS-10% PAGE against the anti-TRPV1 monoclonal antibody. The bottom portion of the nitrocellulose membranes was probed with the anti–actin antibody, as loading control. N.S.: non specific band. Note that this band is still present in tissue from TRPV1-/- mice. **(d)** Representative immunoblots comparing the TRPV1 content in ACC (50 µg) and microglial cells (6 µg). Microglial cells isolated from mice were lysed and subjected to immunoblotting against the anti-TRPV1 antibody. Note that N.S. band is absent in microglia cell cultures. Due to a strong difference in relative abundance of actin in the protein extracts of ACC tissues and isolated microglial cells, the enrichment in TRPV1 expression was assessed by normalizing optical density values for the Ponceau staining of total proteins. Particularly, optical density values were internally normalized by Ponceau staining of total protein content and further corrected for the value of ACC considered equal to 1.. ìThe purity of microglial cultures was assessed by assessing specific markers for neurons (NeuN) and microglia cells (Iba1). (**e**)Histograms of TRPV1 expression od normalized TRPV1 in ACC against microglial cultures *p<0.05 **f**) RT-PCR of TRPV1 gene expression cortical neurons (white bar) and microglial cells (dark gray bar) isolated from C57BL6J mice: for each sample, TRPV1 threshold cycle was normalized to that of β-actin. Data are expressed as mean±SD and are representative of two independent pools of mouse cortices (4 mice/pool) p=0.27 Student t-test). (**g**) *Left*, Current-voltage relationship of the capsaicin-induced current by application of capsaicin 1µM in a microglial cell from acute cortical slice of CX3CR1+/GFP mouse before (black curve), during (red curve) and after (blue curve) capsaicin application; *Middle*, capsaicin induces an outward rectifying current with reversal potential at about 0 mV (results obtained by subtracting the current before and after the capsaicin application). *Righ*t, time plot of the mean current amplitude at +50 mV (n=9). The arrow indicate 3-9 minutes of capsaicin application.

TRPV1 is expressed on astrocytes processes of ACC and hippocampus

The anti-TRPV1 MAb also labeled astrocytes of the ACC (n=3 from 3 mice, **Figure 13a)**, although its expression was significantly lower than in microglial cells (r=0.720 ±0.010 and r =0.291 ±0.011, for microglia and astrocytes, respectively, p<0.01; Two Sample t-Test). Since GFAP positive cells in the ACC were very scarce, the hippocampus has been chosen as comparison area to avoid an underestimation of TRPV1 in astrocytes (**Figure 13b)**. Despite the wider population of GFAP positive cells, a low degree of TRPV1-GFAP colocalization was also detected in hippocampus (r=0.344 ±0.016 n=3 from 3 mice; **(Figure 13c,d**).

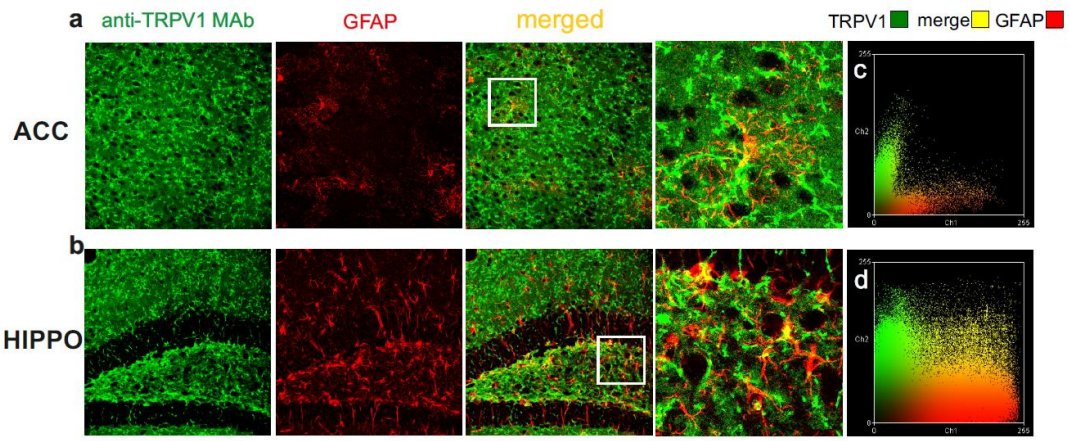

Figure 13: TRPV1 expression on GFAP+ cells : a comparison between ACC and Hip

(**a,c**) Representative photographs of anti-TRPV1 staining in GFAP positive astrocytes of ACC (left panels) and hippocampus (HIPPO; right panels). GFAP staining in the hippocampus is higher than in cortex. (**b,d**) Correlative color scatter plots of TRPV1(green) and GFAP (red) from the experiments reported in a and c respectively. In yellow, the colocalization (merged) of the two antibodies (ACC r= 0.30, Hippor=0.36).

TRPV1 m-Ab stains principally GCRP peptidergic neurons in DRG

To test the effective quality of TRPV1-mAb we decided to assess the TRPV1 staining in DRG, a region in which TRPV1 profile of expression has been broadly described. The TRPV1 positive(TRPV1+) cells in this area (n=8 observations n=7 mice) was 67,11% of NeuN positive cells, TRPV1 signal was completely absent in DRG of TRPV1 ko mice (**fig.14b**) We tested a subset of neuronal markers to identify the nature of TRPV1+ cells. The markers used were the following: CGRP(for peptidergic cells), IB4(for not peptidergic cells) and NF200 (for myelinated A-b cells). As already reported in other studies most of the TRPV1+ cells are CGRP positive (34,62%) (**fig.15a**). The remaining TRPV1+ cells are identified as immunopositive for IB4 (13.57%) and NF200(12.92%) corroborating already reported literature regarding the principal expression of TRPV1 on peptidergic fibers [46,47,48] (**fig.15b-c**).

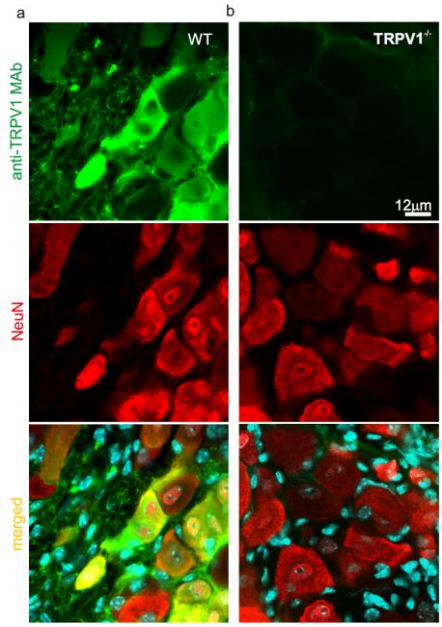

Figure 14: TRPV1- MAb stain DRG NeuN positive cells in WT mice (a)TRPV1 MAb signal is present NeuN positive cells in DRG of WT mice. **(b)** TRPV1 MAb signal is absent in the TRPV1 -/- DRG confirming the specificity of the antibody.

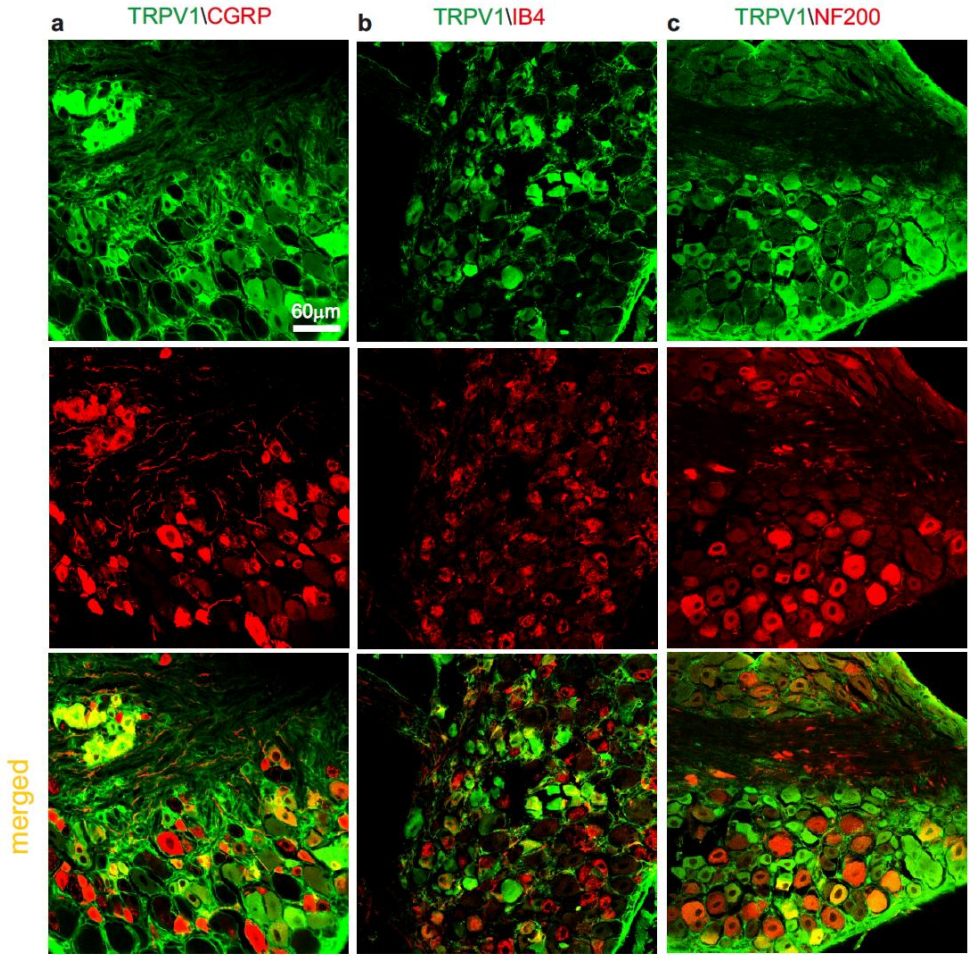

Figure 15: TRPV1 is mainly expressed in CGRP positive DRG neurons (a)TRPV1-MAb co-localizes abundantly with CGRP positive cells. **(b-c)** TRPV1 is partially expressed in IB4 positive (non peptidergic) and NF200 positive (myelinated) cells

TRPV1 channels are expressed in cortical neurons of mice suffering from neuropathic pain

Our new evidence on TRPV1 localization in brain microglia. However is supposed that neuronal expression of this channel is induced by exacerbated pathological

conditions as chronic pain. This common idea suggest us to assess the expression pattern of this channel in the ACC of adult mice suffering from neuropathic pain at different time points from the ligature of the sciatic nerve (chronic constriction injury, CCI). Three days after the nerve constriction, TRPV1 was still expressed in cortical microglia similarly to sham- mice (n=7 from 3 mice; **Fig. 16**). One week after CCI, anti-TRPV1 MAb started to stain also the cytoplasm and the apical dendrite of Iba1-negative cells, whose morphology resembled neurons (n=7 experiments, 5 mice; **Fig. 16 a-h**), and this immuno-reactivity pattern was limited to layer 2/3 of both hemispheres and was less marked in the ispilateral than the contralateral hemisphere. At 4 weeks after CCI, the cytoplasmic expression of TRPV1 in Iba1-negative cells was broadly distributed throughout all layers of the contralateral hemisphere (**Fig. 16p**; n=19, 7 mice). In line with these observations, TRPV1 microglial expression decreased in the contralateral ACC of 1 week and 4 week CCI mice. Indeed, the Pearson correlation coefficient for anti-TRPV1/Iba1 signal colocalization was weaker in the contralateral ACC of 1 week and 4 week CCI mice compared to ispilateral cortices (**Fig. 16 q-t**). This evidence was corroborated by a double immunofluorescence staining with NeuN and anti-TRPV1 that revealed TRPV1 expression in both cytoplasm and branches of NeuN-positive neurons (n=7 from 3 mice; **Fig. 17 a**), thus suggesting that TRPV1 was also expressed in cortical neurons upon induction of neuropathic pain. In particular, by adding to the immunostaining EAAC1, the neuronal glutamate transporter marker, we also showed that TRPV1 was mostly expressed in pyramidal neurons. Indeed, whereas almost all EAAC1 immunopositive neurons expressed TRPV1 (**Fig. 17b)**, only a small fraction of EAAC1 negative neurons were immunoreactive for TRPV1 (n=3 from 3 mice**).** The neuronal expression pattern was prominent in ACC,

although other areas such as the thalamus, somatosensory (ss) cortex, PAG and hippocampus sporadically displayed TRPV1 expression in neurons .

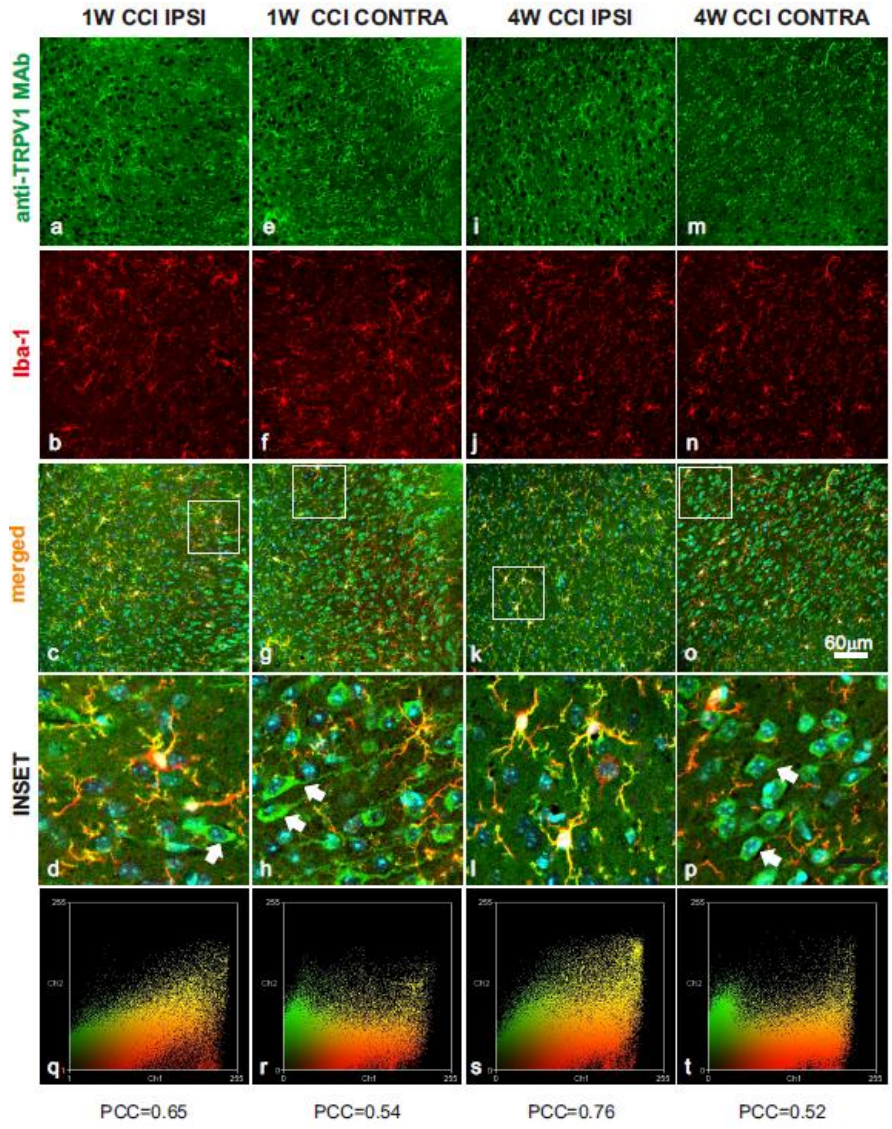

Figure 16: TRPV1 distribution pattern in the ACC of CCI adult mice. Beyond microglia cells (iba-1 positive, in red), the anti-TRPV1 MAb stains both the cytoplasm and apical processes of some iba1

immunonegative cells (white arrows in the INSET). This expression pattern was minor in the superficial cortical layers of the ipsilateral (IPSI; **a-d**) than contralateral (CONTRA, **e-h**) hemisphere of mice that underwent surgery from 1 week (1W CCI mice). In 4-week CCI mice (**i-l**, **m-p**), when the chronicization of pain becomes established, the anti-TRPV1 MAb labels both cytoplasm and apical processes of iba1 negative cells (green) of the CONTRA hemisphere (**o,p**). Note that this staining pattern is also present in the deeper layers of the ACC (**o**) while is absent in the IPSI hemisphere of 4W CCI mice (**k**,**l**). (INSET) High-power views of cells from the box areas in all merged panels. (**q**-**t**) Color scatter plots representing the amount of colocalization (yellow) between the anti-TRPV1 (green) and iba-1 (red) in each condition. Smaller PCC values denote a higher expression of TRPV1 in the cytoplasm of iba1-immunonegative cells.

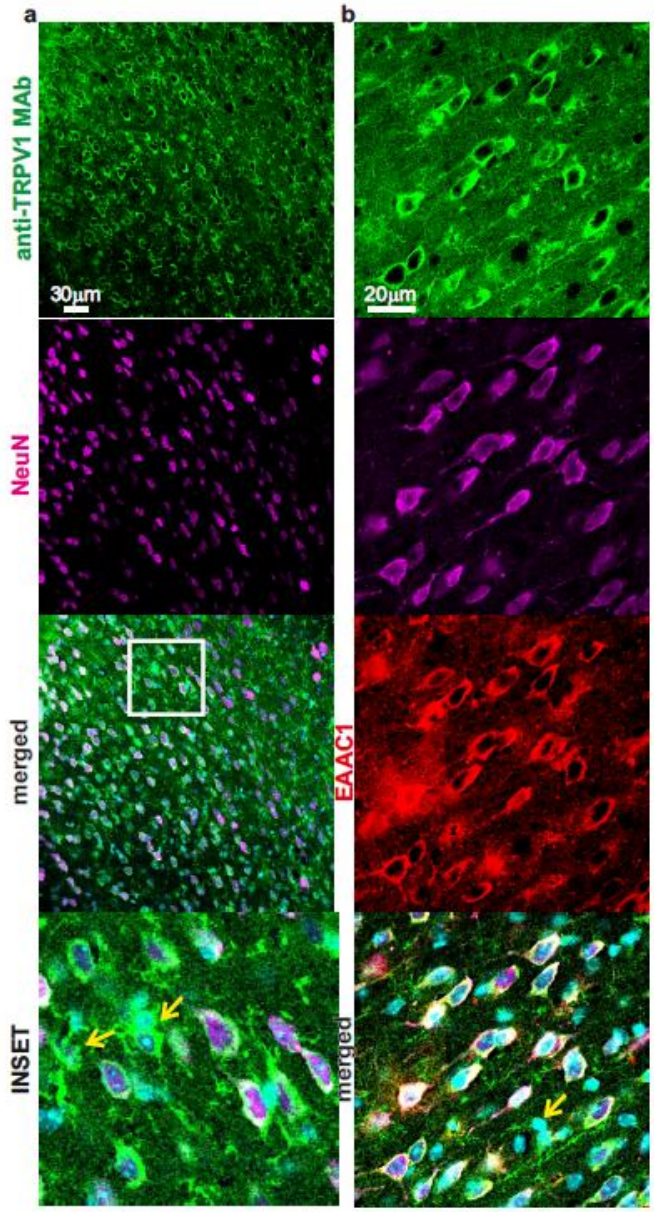

Figure 17 :TRPV1 is also expressed in principal neurons of the ACC from CCI adult mice Contralateral ACC photomicrographs of 4 weeks CCI mice, from two independent experiments (**a,b**). (**a**) Anti-TRPV1 MAb labels both the cytoplasm and the apical dendrite of NeuN positive cells. The remnant TRPV1 positive fibers and cytoplasms probably belong to glial cells (yellow arrows). (**b**) Anti-TRPV1 MAb labels EAAC1 positive neurons and NeuN negative cells (yellow arrow)

Microglial TRPV1 stimulation tunes cortical glutamatergic neurotransmission

Growing evidence shows that activation of brain microglia modulates excitatory neurotransmission and increases synaptic strength[116,117,173]. Given our data on TRPV1 expression in brain microglia, we hypothesized that the well-characterized presynaptic modulation of neurotransmission by TRPV1 is achieved by direct stimulation of TRPV1 on microglia.

To address this possibility we first explored the action of TRPV1 stimulation in the ACC. As reported for other brain areas, capsaicin ($1\mu M$) selectively increases the frequency of miniature excitatory postsynaptic currents (mEPSCs) onto PNs of ACC without affecting their amplitude (**Fig. 18 a**) suggesting a pre-synaptic mechanism of action. Both pharmacological blockade through the non-competitive antagonist IRTX and genetic deletion of TRPV1 inhibited the enhancement of mEPSC frequency by capsaicin (**Fig. 18 b**). The TRPV1 effect on neurotransmission is mediated downstream by AMPA receptors on post-synaptic compartment. In fact bath application of the non NMDA receptors antagonist, 6,7-dinitroquinoxaline-2,3-dione (DNQX, 20 μM) completely abolished both frequency and amplitude of mEPSCs and in this experimental conditions capsaicin increased neither frequency nor amplitude of mEPSCs (**Fig. 19**). Assessed this , in order to demonstrate that such TRPV1-induced modulation of pre-synaptic neurotransmission was mediated by microglial cells, we activated TRPV1 in the presence of the microglial inhibitor minocycline. The application of minocycline *per se* (100nM) did not affect basal mEPSCs (from 2.34±0.59 to 2.28±0.66 Hz, p=0.85 and from 19.54±1.49 to 19.29±1.62 pA, p=0.82; n=9), and strongly counteract the capsaicin-induced increase of mEPSC rate (**Fig. 20 a-c**) suggesting that the enhancement of glutamatergic neurotransmission by capsaicin is due to the activation of TRPV1 expressed by microglia cells. We found, while in a low amount, a partial

expression of TRPV1 on GFAP positive cells. To exclude a possible role of astrocytes in such microglia-neuron communication upon TRPV1 activation, patch-clamp recordings were performed also incubating the slice with the astroglial-specific toxin fluoroacetate (FAc 1 mM) [116] .As expected, capsaicin still enhanced mEPSCs rate (**Fig 20 d,e**), suggesting that at least in this experimental conditions astrocytes are irrelevant for the TRPV1-mediated microglia-to-neuron communication.

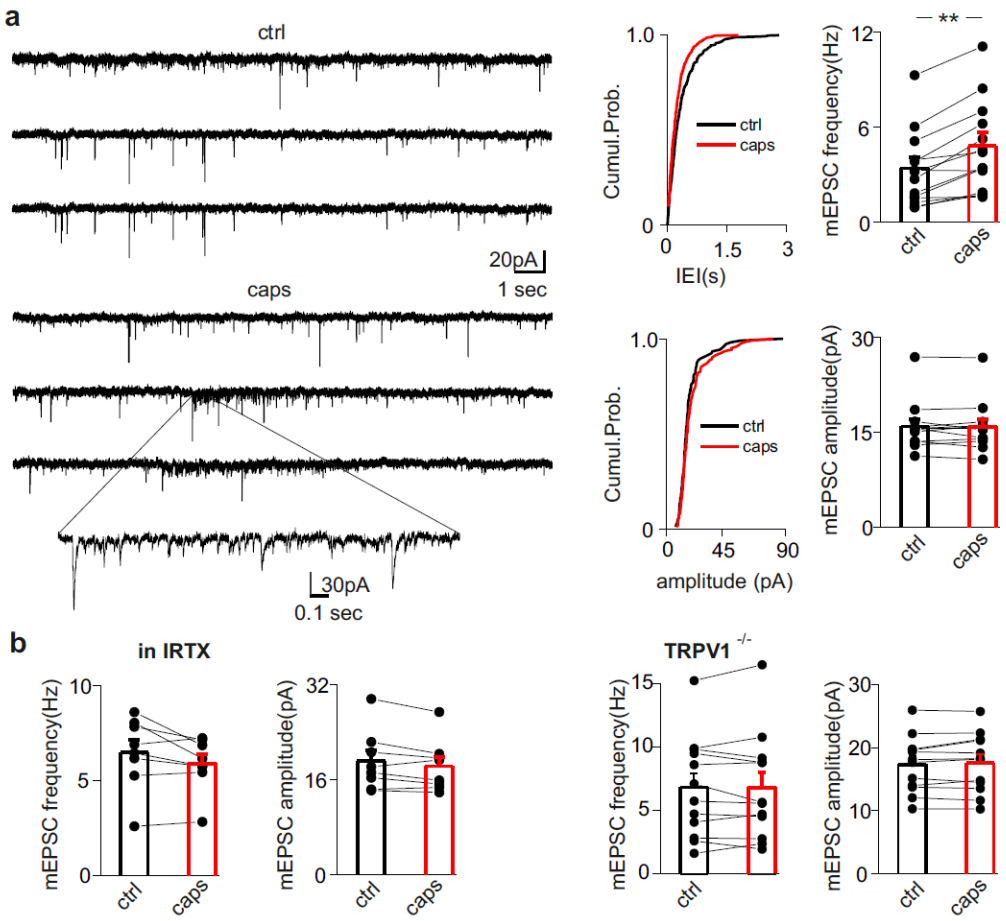

Figure 18: TRPV1 activation increases mEPSCs frequency onto pyramidal neurons of the ACC. (a) Left, example traces of AMPAR mEPSCs recorded from a PN at -70 mV, in control and after 1 μM capsaicin (caps), in the presence of picrotoxin (100μM). Below trace shows expanded trace

recording during caps. Middle, cumulative distributions of mEPSC interevent interval (IEI) and amplitude from cell shown on the left (p<0.02 and p=0.32 respectively). Right, summary histograms and line series plots of mEPSC frequency and amplitude showing that capsaicin significantly increases the frequency but not the amplitude of mEPSCs (from 3.40±0.71 to 4.83±0.84 Hz, n=12, p < 0.001; from 15.97±1.13 to 15.90±1.60 pA, n=12, p=0.83). Data are values from single cells (black filled circle) and mean ± SEM. (**b**) Group data of mEPSC frequency and amplitude showing the lack of effect of capsaicin in the presence of the TRPV1 antagonist IRTX (left; from 6.46±0.68 to 5.88±0.50 Hz, n=8, p=0.11) or in cortical tissue from TRPV1-/- mice (right; 6.84±1.15 to 6.81±1.20 Hz, n=12, p=0.9).

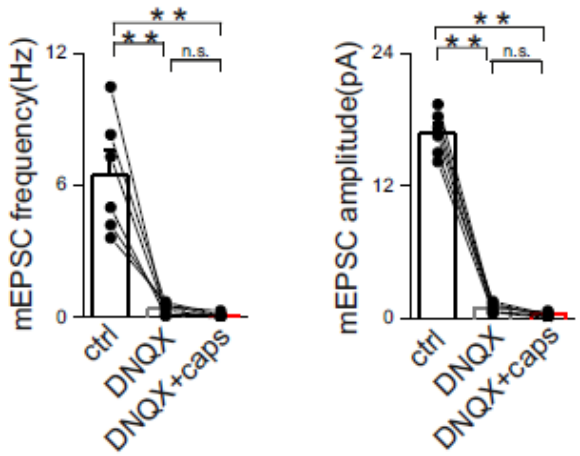

Figure 19: Bath application of the non NMDA receptors antagonist, 6,7-dinitroquinoxaline-2,3-dione (DNQX, 20 µM) completely abolished both frequency and amplitude of mEPSCs (from 6.45+/-1.09 Hz to 0.38 +/- 0.11 Hz, n= 6,paired T-test p= <0.001; from 16.79+/-0.80 pA to 0.88+/-0.18 pA, n=6, paired t test p= <0.001). In these conditions, capsaicin increased neither frequency nor amplitude of mEPSCs, suggesting that downstream TRPV1 signalling is AMPA receptor mediated. The NMDA component was excluded in this type of experiments.

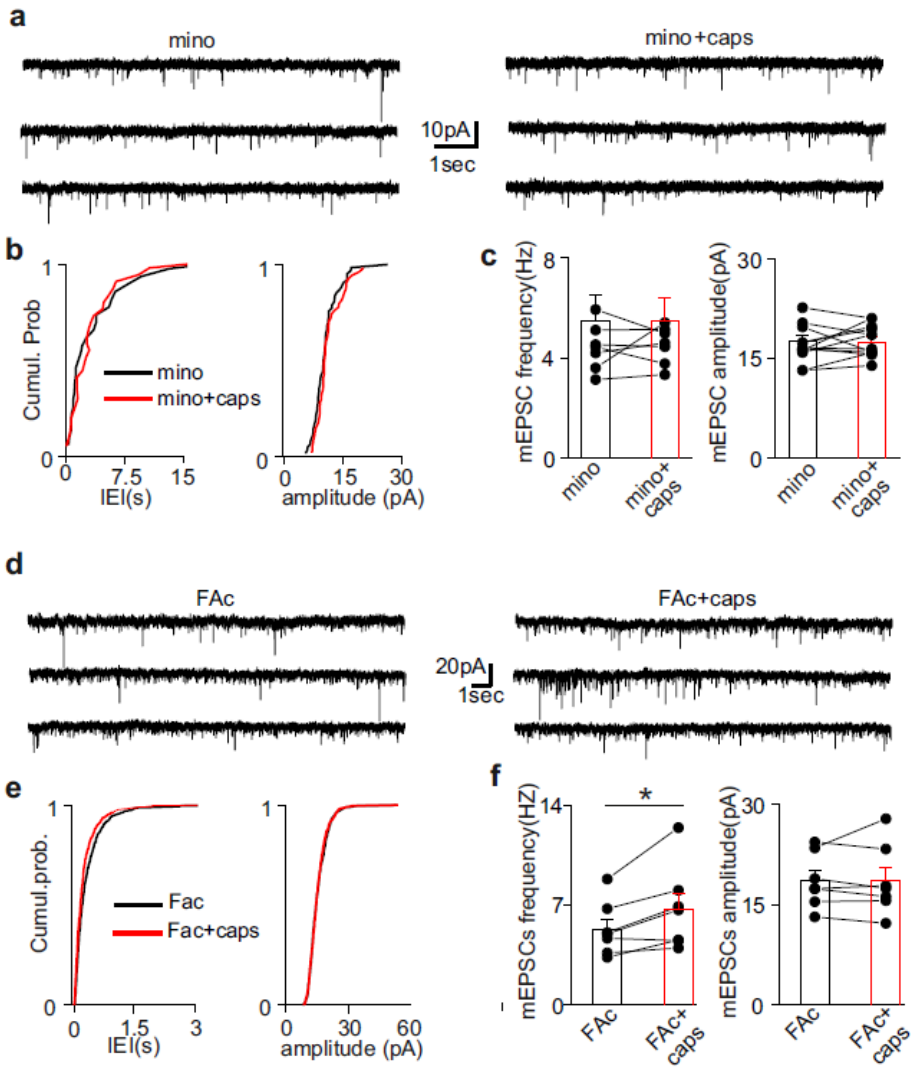

Figure 20: Microglial TRPV1 modulates synaptic neurotransmission **(a)** Example recording of mEPSCs before (left) and during (right) capsaicin in the presence of 100 nM minocycline and 10 □M picrotoxin. **(b)** Cumulative probability plots comparing minocycline (black line) and minocycline plus capsaicin (red line) on mEPSC interevent interval (IEI) and amplitude of the recording showed above (p=0.25 and p=0.31, KS test). (**c**) Bar histograms of group data showing the lack of capsaicin-mediated increase of mEPSC rate when microglia activation is blocked by minocycline (from 3.98±0.35 to 4.13±0.33 Hz, n=9, p=0.53; from 17.54±0.94 to 17.34±0.79 pA, n=9, p=0.70, Paired Sample t-Test). Group data are presented as single value and mean±S.E.M. (**d**) Example recording of mEPSCs before (left) and during (right) capsaicin in the presence of 1mM fluoroacetate (FAc)

and 10 μM picrotoxin. **(e)** Cumulative probability plots comparing FAc (black line) and minocycline plus capsaicin (red line) on mEPSC interevent interval (IEI) and amplitude of the recording showed above ($p<0.01$ and $p=0.28$, KS test). **(f)** Summary data of both mEPSC frequency and amplitude recorded in the presence of FAc before and during capsaicin application (FAc 5.30±0.72 Hz, FAc+caps 6.70±1.10 Hz, *$p<0.05$ Paired t-test; FAc 18.58±1.55 pA, FAc+caps 18.63±1.98 pA, n=7, $p=0.89$ Paired Sample t-Test).

Glutamate metabotropic receptors are not involved in microglia to neuron communication on pre-synaptic terminal

Different studies reported that glial cells induce an increase of neurotransmitter release activating metabotropic receptors of glutamate on pre-synaptic terminals receptors[116,174] .To investigate a possible involvement of these receptors in the presynaptic modulation of glutamatergic transmission upon TRPV1 activation, capsaicin was applied with the mGluR5 antagonist MPEP (50μM) or with the non-selective group I mGluR antagonist MCPG suggesting that mGluR are not involved in the upstream TRPV1 signalling.Both MEP and MCPG did not induce changes in basal synaptic properties (**Fig21 a-b**)

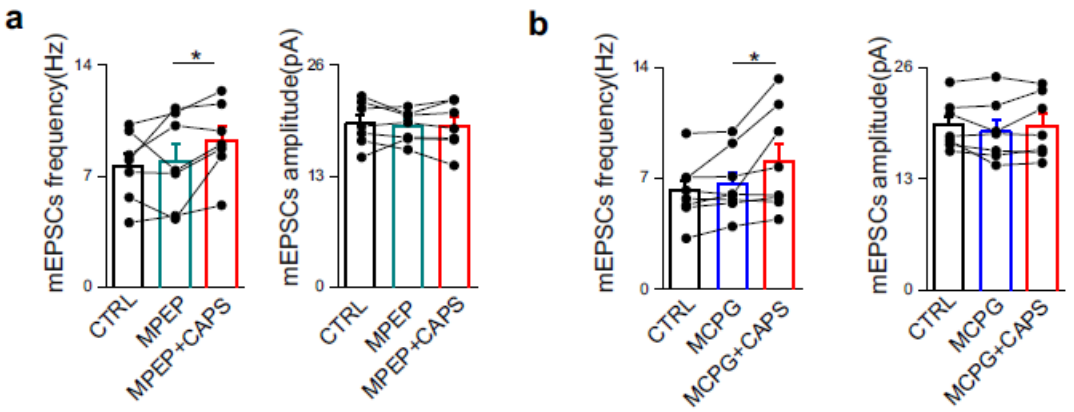

Figure 21: Cortical pre-synaptic metabotropic receptors are not invonved in microglia capsaicin-mediated pre-synaptic effect on excitatory neurotransmission .Capsaicin was applied with the mGluR5 antagonist MPEP (50μM) or with the non-selective group I mGluR antagonist MCPG

(100 M) (a-b). In both assays capsaicin significantly increased mEPSC frequency (from 7.96+/-1.11 to 9.27 +/-0.89,n=7, p= 0.040 paired sample T-test; from 6.67 +/- 0.71 to 8.039+/-1.14385, n=8, p=0.042 paired sample T-test), suggesting that mGluR are not involved in the upstream TRPV1 signalling.Both MPEP and MCPG did not induce changes in basal synaptic properties. (Ctrl7.62203 +/- 0.83 Hz, MPEP 7.95877+/- 1.10 Hz; Ctrl 19.16708 +/- 0.98 pAMPEP 18.83072 +/- 0.69 pA, n=7,p=0.61 and p=0.62 respectively, Paired sample T-test; Ctrl 6.19 +/-0.67606 MCPG 6.66+/-0.71Hz; Ctrl 19.46 +/-0.97 MCPG18.66 +/-1.18,n=8, p=0.10 and p=0.13, Paired sample T-test.)

TRPV1 activation stimulates the release of microglia-derived microvesicles

The molecular mechanism underlying the increase of mEPSC frequency driven by microglial TRPV1 activation remain the unresolved point. Several factors, drive microglia-to-neuron communication, through EVs shed from the plasma membrane of microglia, called microvesicles (MVs) or ectosomes[119,120,121].Has been reported that the production of MVs increases in reactive microglia[175], and is strongly enhanced by ATP through activation of $P2X_7$ receptors[119]. Assessed this idea, we hypothesized that TRPV1 stimulation on microglia should promote MV shedding as in $P2X_7$ activation. To verify this hypothesis, cultured murine microglia were incubated with capsaicin (300 nM) for 10 min and EVs, both shed MVs and smaller vesicles, were quantified and sized by nanoparticle tracking analysis (NTA). NTA showed a multimodal size distribution of quite large vesicles, presumably MVs (mean diameter control= 298.2±21.2 nm; capsaicin= 305.0±16.32 nm; n=3), with a major peak consisting of vesicles about 200 nm in size and few smaller peaks of larger MVs (**Fig. 22a**). EV concentration increased by 1.5 fold under TRPV1 or ATP stimulation (**Fig. 22b**, n=3). Selective quantification of MVs shed from microglia that have incorporated fluorescent phosphocholine (NBD-C6_HPC) in the plasma membrane, confirmed that both ATP and capsaicin enhance MV production to the same extent (**Fig. 22c**, n=3; $p<0.05$). These data strongly suggest

that TRPV1 activation on microglia may increase mEPSC rate on neurons by triggering release of MVs.

To substantiate this, we employed a newly synthesized inhibitor of acid ceramidase(Bach A. et al. 2015), the ARN14988 , in order to prevent neuronal sphingosine production, which is essential for MV-induced stimulation of synaptic activity[31]. Furthermore, in slices pre-treated with ARN14988, capsaicin did not affect either frequency or amplitude of mEPSCs (**Fig. 22d**). To exclude possible inhibitory effects of ARN14988 on MV production or activity, microglia cultures were treated with the ceramidase inhibitor before exposure to capsaicin. quantification showed that ARN14988 did not inhibit capsaicin-induced MV release (**Fig. 22 f**). Furthermore, patch-clamp recordings revealed that MVs from ARN14988-treated cells maintained the capability to increase mEPSC frequency in cultured neurons (**Fig. 22 g**). To strongly demonstrate that MV released by microglia act on synaptic terminals of pyramidal cells and induce increasing in neurotransmitter release we tried to block MV mechanism of release upstream, blocking microglia MV release. Is reported that p38 MAPK is activated downstream by P2X7 ATP receptor and is essential for MV shedding [176] Given that p38 MAPK is activated even by TRPV1 receptors[177] , we hypothesized that inhibition of p38 MAPK could block capsaicin-induced MV shedding in the same manner. Demonstrated that capsaicin-induced MV shedding from cultured microglia treated was significantly reduced in the presence of p38 MAPK inhibitor SB203580 (**fig.22 h**) we performed a similar experiment on acute slice. Capsaicin failed to affect the frequency and amplitude of mEPSCs in slices incubated with SB203580 (**Fig. 22 e)** indicating that capsaicin might increase spontaneous glutamatergic synaptic activity by promoting shedding of microglial MVs, which in

turn stimulate sphingosine metabolism in neurons and enhances presynaptic release probability as reported in Antonucci et al. 2011.

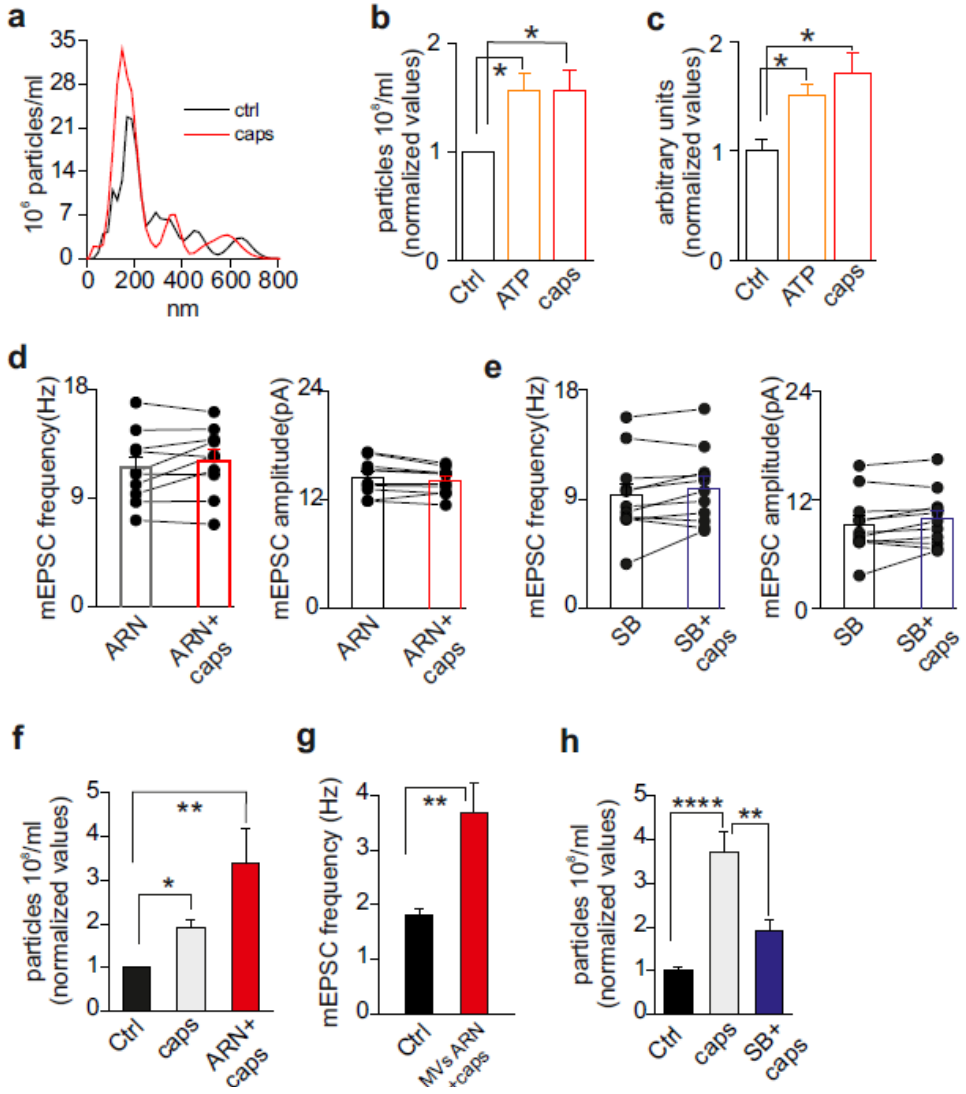

Figure 22: TRPV1 modulates synaptic transmission by microvesicles shedding (**a**) Representative size profile of EVs released constitutively (black line) or upon capsaicin challenge (red line) from 5X10^5 murine microglia in 500µl of serum free medium during a period of 10 minutes. (**b**) Histogram showing the fold increase of total EV concentration detected by Nanosight upon stimulation with ATP or capsaicin (Kruskal-Wallis test, p=0,035). (**c**) Histogram showing the fold

increase of MVs shed selectively from the plasma membrane and measured by a spectrophotometric assay under the same stimuli (Holm-Sidak's, p<0,05). (**d**) Group data showing that addition of ARN14988 significantly counteracts capsaicin-mediated increase of mEPSC frequency in cortical slices (from 11.51±0.92 to 12.12±0.88 Hz, p=0.15; from 14.52±0.61 to 14.10±0.46 pA, p=0.06, Paired Sample t-Test, n=10). (**e**) Summary graph of mEPSC frequency (left) and amplitude (right) in the presence of 2 M SB203580 before (black bar) and after capsaicin (blue bar) (from 9.30±1.00 to 9.93±0.90 Hz, p=0.08; from 10.67±0.47 to 10.75±0.49 pA, n=11, and p=0.89, Paired Sample t-Test and Wilcoxon Signed Rank Test, respectively).Data are values from single cells and/or mean±SEM. *p<0.05. **(f)** Microglia cell cultures were challenged with vehicle, capsaicin or ARN+capsaicin and MVs shedding were measured. Histogram shows the fold increase of total EV concentration detected by Nanosight upon stimulation of microglia cultures with vehicle (ctrl, black bar), capsaicin (light gray bar) or ARN+capsaicin (dark grey bar; One way Anova *p<0.05,**p<0.01 Dunn's Method for multiple comparison test). **(g)** Changes of mEPSCs evoked by MVs previously treated with ARN+caps (ctrl n=10, caps n=8, p<0.01 Mann-Whitney Rank Sum Test). (**h**) Microglia cell cultures were challenged with vehicle, capsaicin or 400nM SB203580+capsaicin and MVs shedding were measured. (violet bar; One way Anova ****p<0.0001 followed by Tukey's multiple comparison test)

Lysophosphatidic acid(LPA) activates TRPV1 receptor

Lysophosphatidic acid (LPA), a bioactive and proinflammatory signalling lipid is highly produced during inflammation[189] and that activates microglial cells which in turn self-sustained LPA synthesis. Similarly to capsaicin, LPA was recently described as TRPV1 possible agonist despite this lipid have its own receptors. We demonstrate that as capsaicin, LPA significantly enhanced the frequency of mEPSCs (**Fig.23a**) and did not affect mEPSC amplitude (p<0.9). The enhancement of mEPSC rate by LPA was significantly dampened in slices incubated with IRTX (**Fig. 23b-c**). Accordingly LPA triggers excitatory neurotransmission even when its own when metabotropic receptors were blocked(**Fig.23d)** this effect was

completely abolished when both TRPV1 and LPA receptors were counteracted (**Fig.23e**), suggesting that LPA may behave as a potential endogenous activator of TRPV1 in the brain during pathological inflammation.

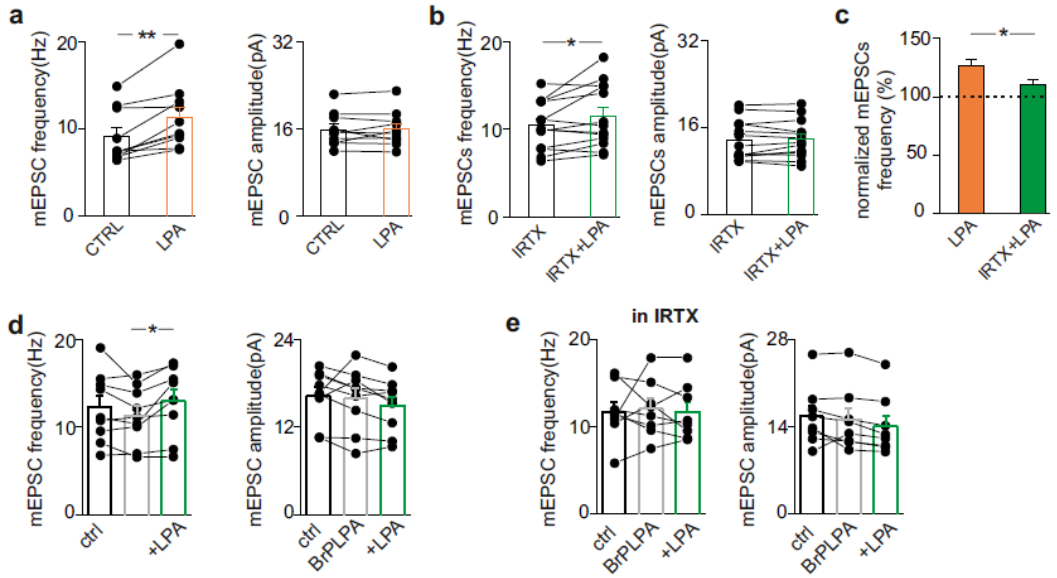

Figure 23: LPA is the potential TRPV1 agonist during acute inflammation (a) Summary graph of mEPSC frequency and amplitude before (black bar; 9.10±0.96 Hz and 15.43±0.95 pA, n=10) and during 5 μM LPA (orange bar; 11.32±1.1 Hz and 15.38±1.07 pA, n=10). LPA significantly boost mEPSC frequency ($p<0.002$; Wilcoxon Signed Ranks Test). (**b**) Same as in previous graphs but in the presence of IRTX (IRTX 10.41±0.76.14, IRTX+LPA 11.54±1 Hz, n=13; $p<0.05$ Paired Sample T Test; IRTX 12.92±0.93,IRTX+LPA 13.01±0.93 pA, n=13).. (**c**) Note that LPA is significantly less effective when TRPV1 is inhibited ($p<0.05$, Two-sample T test) (*$p<0.05$, **$p<0.001$). (**d-e**) In the presence of LPA1-4 metabotropic receptors antagonist BrP-LPA, LPA increases glutamatergic transmission by TRPV1 activation. (**d**) Left, summary graphs of mEPSC frequency and amplitude before (black bar; 12.21±1.32 Hz and 16.31±1.9 pA, n=9), during BrP-LPA (5 μM; grey bar; 11.32±1.1 Hz and 15.95±1.4 pA, n=9) and with LPA (green bar; 12.94±1.3 Hz and 15.00±1.2 pA, n=9). (**e**), same as in **f** but with the addition of IRTX (ctrl 11.71±1.14 Hz, BrLPA 12.03±1.15 Hz, BrLPA+LPA 11.67±1.16 Hz, n=8; ctrl 15.70±1.70 pA, BrLPA 15.16±1.80 pA, BrLPA+LPA 14.31±1.60 pA, n=8). (*$p<0.05$, Paired Sample t-Test).

TRPV1 controls cortical microglia activation and is involved in acute inflammatory response

Resident microglia in physiological conditions continuously check the brain microenvironment and maintain its correct homeostasis. Upon an insult these cells activate immune response shifting to an activated state characterized by dramatic changes in the cellular shape, in functional behavior and through the release of different proinflammatory and immunoregulatory factors. Capsaicin is reported to be capable of inducing microglial chemotaxis, and our collected data suggesting that could also regulate microglial activation in vitro. So we answered whether TRPV1 stimulation could directly induce functional changes (morphology, citokines release) on ex vivo microglial cells. Morphometric analyses (ImageJ plugin, **Fig. 24**) was performed on microglial cells from acute ACC slices. In control conditions (ACSF) iba1 positive cells presented a small cell body with thin and elongated processes (**Fig. 25a,g**).In capsaicin treated slices (10 minutes,capsaicin 1 mM), iba1 positive cells displayed a gain of hypertrophied branches and a larger cell bodies. (**Fig.25 c,g**). Capsaicin-induced morphological changes were absent in sections from TRPV1$^{-/-}$ mice (**Fig. 25f,h**), whereby microglia appeared already in an activated state in baseline conditions (**Fig.25d-f,h**). Subsequent flow cytometry experiments revealed that acute isolated cortical WT microglia treated with capsaicin produced significantly higher levels of proinflammatory citokine TNF-alpha accompained by a decrease in protective citokine IL-10 (**Fig25i,l**), on the other side TRPV1$^{-/-}$ microglia expressed equal amounts of TNF-alpha after capsaicin exposure and compared to WT microglia produce a significantly greater amounts of IL-10 in basal condition, capsaicin treatment did not alter this balance neither the TNF-alpha production(**Fig.25i,l**). The eventual role of interleukine 1-beta(IL-1beta), another major pro-inflammatory chemokine released by

stimulated microglia, was excluded in both the groups. In fact in patch-clamp experiments the presence of IL1-beta receptor antagonist primarily incubated on acute cortical slices was not sufficient to prevent capsaicin-mediated effect on mEPSCs (**Fig.26**).

Confirmed the direct role of TRPV1 in controlling inflammatory microglia response, we next asked whether TRPV1 might be endogenously active under inflammatory conditions as in acute inflammatory environment induced experimentally by stimulating slices with Lipopolysaccharide (LPS), the most abundant component within the cell wall of Gram-negative bacteria.In electrophysiology experiments, 500ng/ml LPS increased per se the mEPSC frequency without affecting their amplitude (35% of mEPSC frequency enhancement, (**Fig.27a,b**).Furthermore, the overall LPS-induced increase of glutamatergic neurotransmission was significantly reduced by IRTX ($n=14$, $p<0.05$; **Fig. 27c** right panel). Accordingly, the enhancement of mEPSCs and morphological changes induced by LPS were absent in TRPV1$^{-/-}$ mice (**Fig. 28a-b)** However, the application of capsaicin following LPS failed in inducing any further potentiation of mEPSCs(**Fig.2 9a-b**). Altogether, these results suggest that the TRPV1 activation might be responsible for microglia activation in inflammatory conditions.

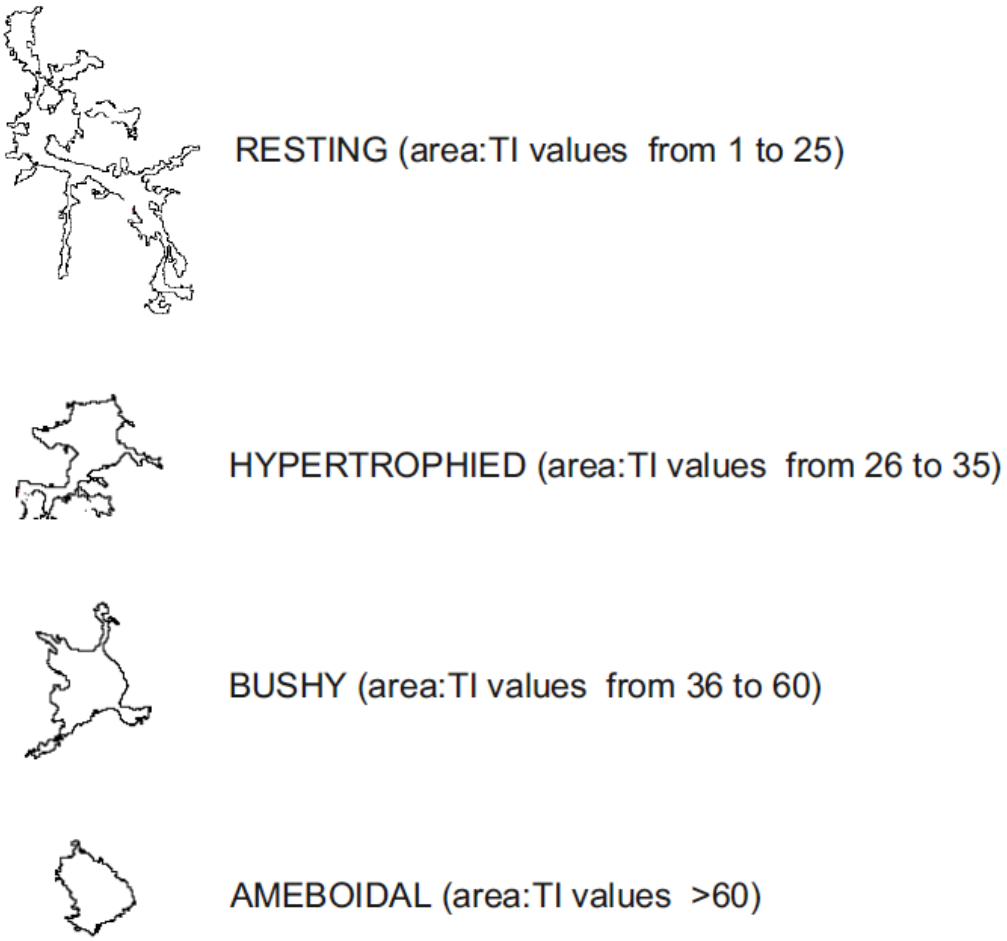

Figure 24: Example of binary (digital) silhouettes of microglia cells from cortical slices acquired by transforming the tiff files of Iba1-immunoreactive cells to binary files by means of the ImageJ software. The cell area values and the TI were calculated for each silhouette and the obtained area:TI ratio value was used to classify each cell in a specific category (resting, ipertrophied, bushy and amoeboid).

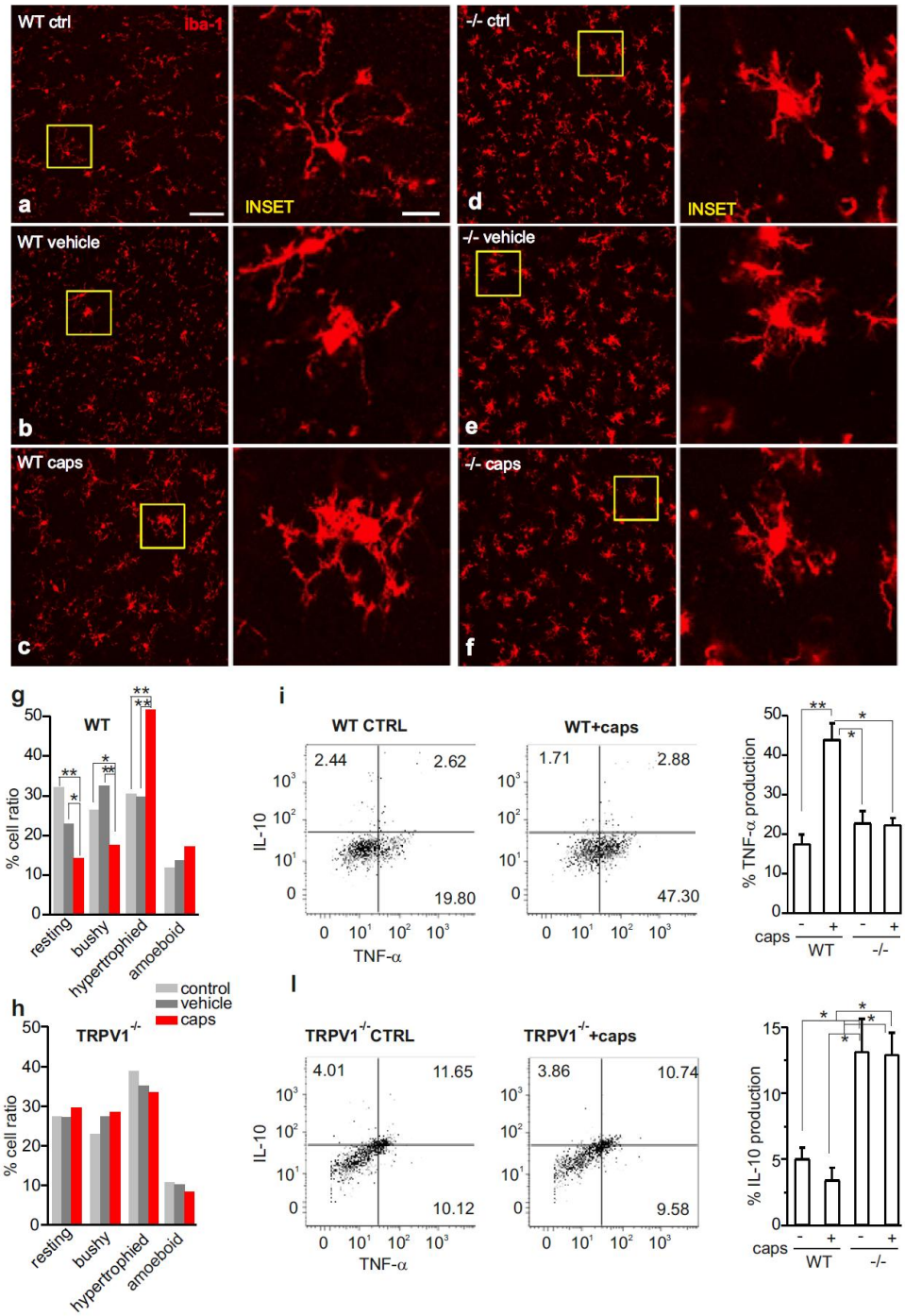

Figure 25: The presence or absence of TRPV1 influences microglia phenotype. (**a-f**) Sections of cortical tissue from WT and TRPV1$^{-/-}$ mice, fixed after exposure to aCSF (**a,d**), aCSF plus vehicle (DMSO; **b**,**e**) and aCSF plus 1 M capsaicin (**c,f**) and immune-processed for iba-1 to stain microglia

cells (in red). INSETs are zoom images taken from an area delimited by the yellow square for each condition. (**g**), Bar graph of percentage of cortical microglia cell phenotype (resting, ameboid, bushy and hypertrophied), in control (grey bars), vehicle- (dark grey bars) and capsaicin- treated (red bars) cortical sections from WT mice. Capsaicin treatment causes a significant shift from resting and bushy to hypertrophied state. (**h**), Same as in "g" but in cortical sections from TRPV1$^{-/-}$ mice. In these tissues capsaicin fails to induce morphological changes of microglia cells. Note that microglia cells in -/- tissues are already hypertrophied in control conditions (**d**,**e**,**f and h**). *p<0.05, **p<0.01 Fisher exact test. Acutely isolated CD11b+ microglial cells from WT (**i**) and TRPV1$^{-/-}$ mice (**l**) were cultured in the absence (-) or presence (+) of capsaicin (1µM) for 10 minutes, washed and then incubated with Brefeldin A for 6 hours to allow cytokine accumulation in vesicles. Intracellular production of TNF-α and IL-10 was analyzed by means of flow cytometry. Data represent percentage of cytokine production ± SEM of 3 independent pools of at least 3 mice. *p<0.05, **p<0.01 (Bonferroni's multiple comparison test following parametric one-way Anova).

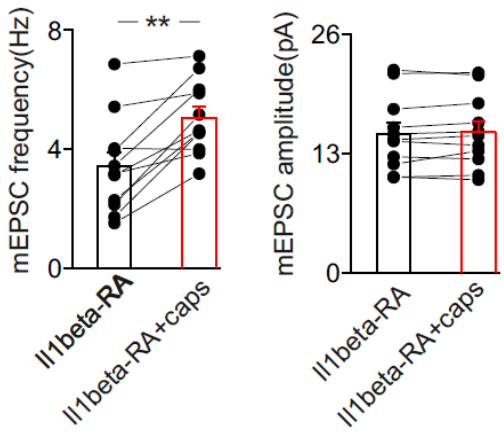

Figure 26: IL1beta is not involved in microglia TRPV1-dependent modulation of excitatory neurotransmission. Summary graph of mEPSCs frequency and amplitude in the presence of IL1beta receptor antagonist and after plus the application of capsaicin (mEPSCs frequency from 3.41 +/-0.48 to 5.04 +/-0.37 Hz ,n=11, p= 0.00048 paired sample T-test; amplitude from 15.15 +/-1.21 to 15.34 +/-1.18 pA ,n=11;p= 0.20 paired sample T-test).

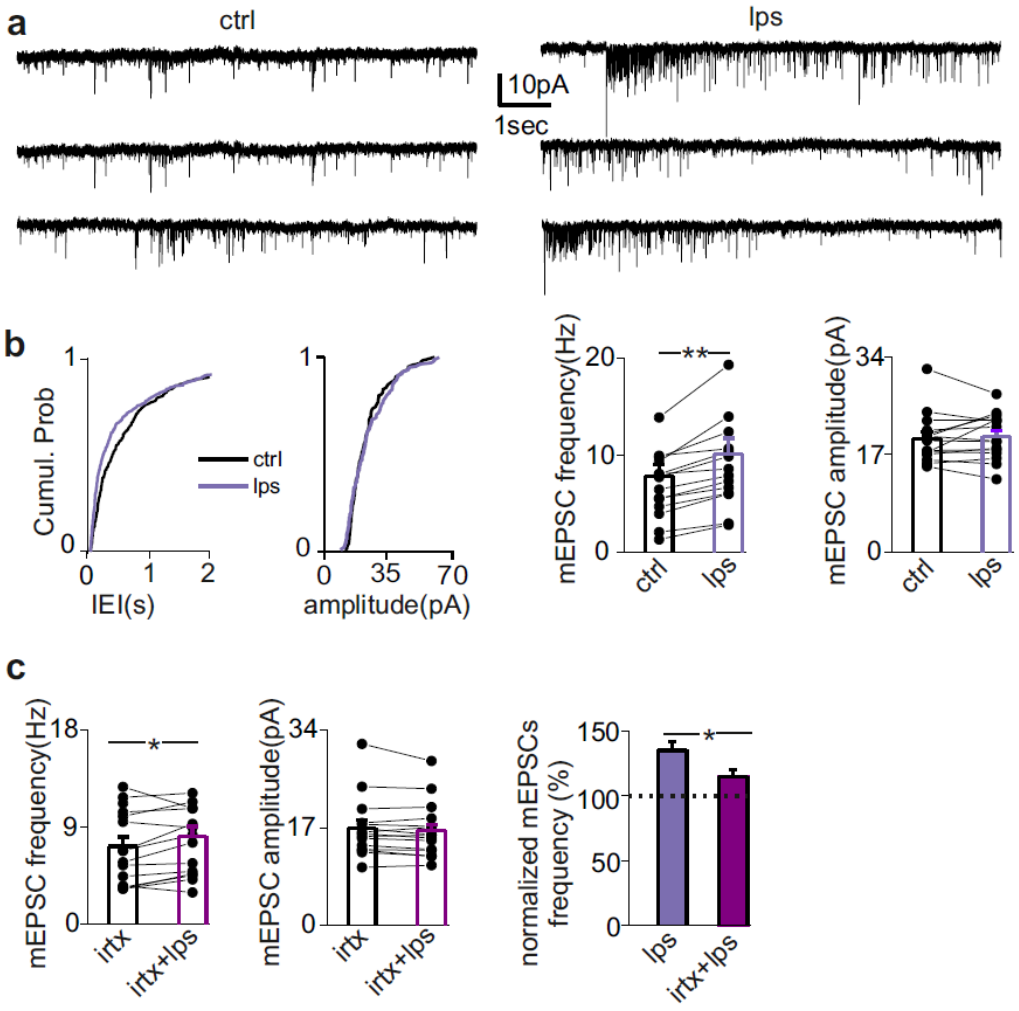

27: TRPV1 tonically controls LPS-mediated effects. (a) Example recording of mEPSCs in control (ctrl) and during LPS exposure (500ng/ml). Below the cumulative probability plot of mEPSC interevent interval and amplitude ($p<0.01$ and $p=0.24$, respectively, KS test). **(b)** Population plot of mEPSC frequency before (black bar and filled circle) and during LPS (violet bar and filled circle), showing that LPS, similarly to capsaicin, increases selectively the mEPSC frequency (from 7.67±1.32 to 10.09±1.73 Hz, n=14, $p<0.001$ Paired Sample Wilcoxon Signed Rank test) without a significant effect on the amplitude (from 20.05±1.30 to 19.76±1.32 pA, $p=0.5$ Paired Sample t-Test). (**c**) As in b, but in the presence of 300 nM IRTX (from 6.8±1.06 to 7.78±1.19 Hz, n=14, $p<0.01$ Paired Sample Wilcoxon Signed Rank test; from 17.47±1.17 to 17.11±1.23 pA, $p=0.09$ Paired Sample Wilcoxon Signed Rank test). Right, the percentage increase of mEPSC frequency by LPS in the presence of

the TRPV1 antagonist IRTX, is significantly reduced compared with the rate enhancement induced by LPS applied alone (p=0.01 Mann-Whitney test).

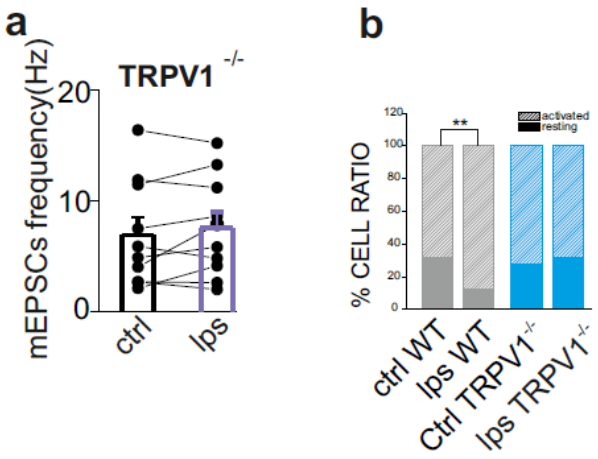

Figure 28 TRPV1 controls microglia inflammatory response a) Population data of mEPSC frequency in control and during LPS obtained from PNs of TRPV1-/- mice (from 7.36±1.90 to 7.69±1.81 Hz, n=9, p=0.52 Two Samples t-Test). **(b)** Stack column graph showing a greater percentage of activated cells (striped bar) related to resting microglia (filled bar) in WT slices (grey bars) treated for 10 minutes with LPS (500ng/ml). The same treatment carried out on slices from TRPV1-/- mice (blue bars) produced no changes in the number of activated cells. (*p<0.05, **p<0.01 Fisher's exact test).

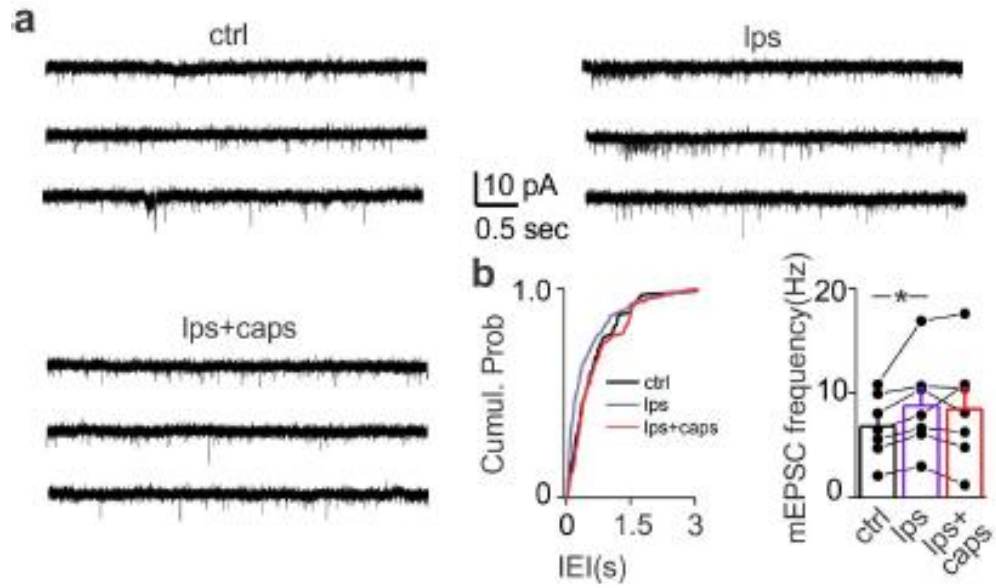

Fig:29 LPS pretreatment occludes TRPV1 mediated effect (a) Trace records from a PN in control condition (ctrl), in LPS and LPS plus capsaicin. Following LPS perfusion, capsaicin is no longer able to further facilitate glutamatergic neurotransmission. (**b**) Right below, cumulative distribution probability of the interevent intervals from the same neuron (ctrl vs LPS $p>0.0001$, LPS vs caps $p<0.0001$, ctrl vs caps $p=0.54$).Left below a summary graph of mEPSC frequency before (black bar), during LPS (violet bar) and LPS+caps (red bar) (ctrl 6.69±1.15 LPS 8.78±1.68 Hz, LPS+caps 8.45±1.97 Hz, n=7,ctrl vs LPS$p<0.05$, LPS vs LPS+caps $p=0.68$, ctrl vs LPS+caps $p=0.15$ Paired Sample t-Test;. Data are values from single cells and/or mean ± SEM. *$p<0.05$, **$p<0.001$.

TRPV1 neuronal distribution directly affects intrinsic membrane properties and synaptic strength of cortical principal neurons

As reported TRPV1 receptor was expressed in time dependent manner on neuronal cells 2 weeks after the CCI of sciatic nerve. In order to confirm its functional role electrophysiology experiments were performed.

In first we assessed that, in baseline conditions, neither Input resistance (shams 137.37±9.9 MΩ n=24, CCI 147.12±10.6 MΩ n=23, p=0.5, Two Samples t-Test) nor

resting membrane potential (shams -70.96± 1.52 mV n=24, CCI -67.93±2.65 mV n=23,p=0.32, Two Samples t-Test) of PNs neurons from sham and CCI mice are unchanged suggesting that passive properties of membranes are not affected by TRPV1 expression on principal cells. In parallel, mEPSC frequency was enhanced in CCI mice compared to control animals (**Fig.30a)**, whereas the amplitude of mEPSCs was strongly reduced (**Fig.30b)**. The amplitude drop of spontaneous glutamatergic currents could be attributed to AMPA receptor trafficking as neuronal homeostatic mechanism subsequent to the persistent increase of synaptic activity [178]. Instead, TRPV1 expression in the soma and dendrites of cortical pyramidal neurons (PNs) of CCI mice directly affect neuronal excitability. The number of action potentials evoked by current injections of increasing amplitude was significantly higher in CCI than shams(**Fig.30d**-left and right input-output curves, respectively)**.** The increase of firing can at least partly be ascribed to TRPV1 expression in CCI mice neurons, since IRTX caused a rightward shift in the input current to action potential rate curves (**Fig.30e).**

Furthermore, as expected, application of capsaicin, besides frequency (as in control mice, see **Fig. 30 f-g**) significantly scaled up both amplitude and charge transfer of mEPSCs in CCI mice (12% and 16% increase, respectively; **Fig. 30f**). To dissect out microglial vs. neuronal TRPV1 contribution in such capsaicin-induced increase of synaptic strength, PNs from CCI mice were recorded also in the presence of minocycline. We found that, in these conditions capsaicin significantly enhanced the mEPSC amplitude and the charge transfer in a subset of cells**(fig.31 b),** that could be TRPV1 positive, but not the frequency in the total of cells investigated suggesting that only neuronal TRPV1 account for capsaicin effect on miniature synaptic events amplitude, the increase in frequency is still dependent from microglial TRPV1**(fig.31 a)**

Beside its effects on the glutamatergic transmission, capsaicin also induced a slight but consistent membrane depolarization associated with a significant reduction of the input resistance in PNs of CCI mice (**Fig. 32a-b-c**). This effect was independent from postsynaptic glutamatergic or GABAergic ionotropic receptors stimulation, as it was obtained in the presence of DNQX, APV and picrotoxin. Conversely, in neurons from shams we found no change in the same intrinsic membrane parameters (**Fig.32b**). Additionally, in voltage clamp experiments, capsaicin elicited rectifying inward currents associated with a significant enhancement of membrane conductance in CCI PNs, but not in shams (**Fig. 32d-e**), - effect that was significantly reverted by IRTX (**Fig.32f-g**).

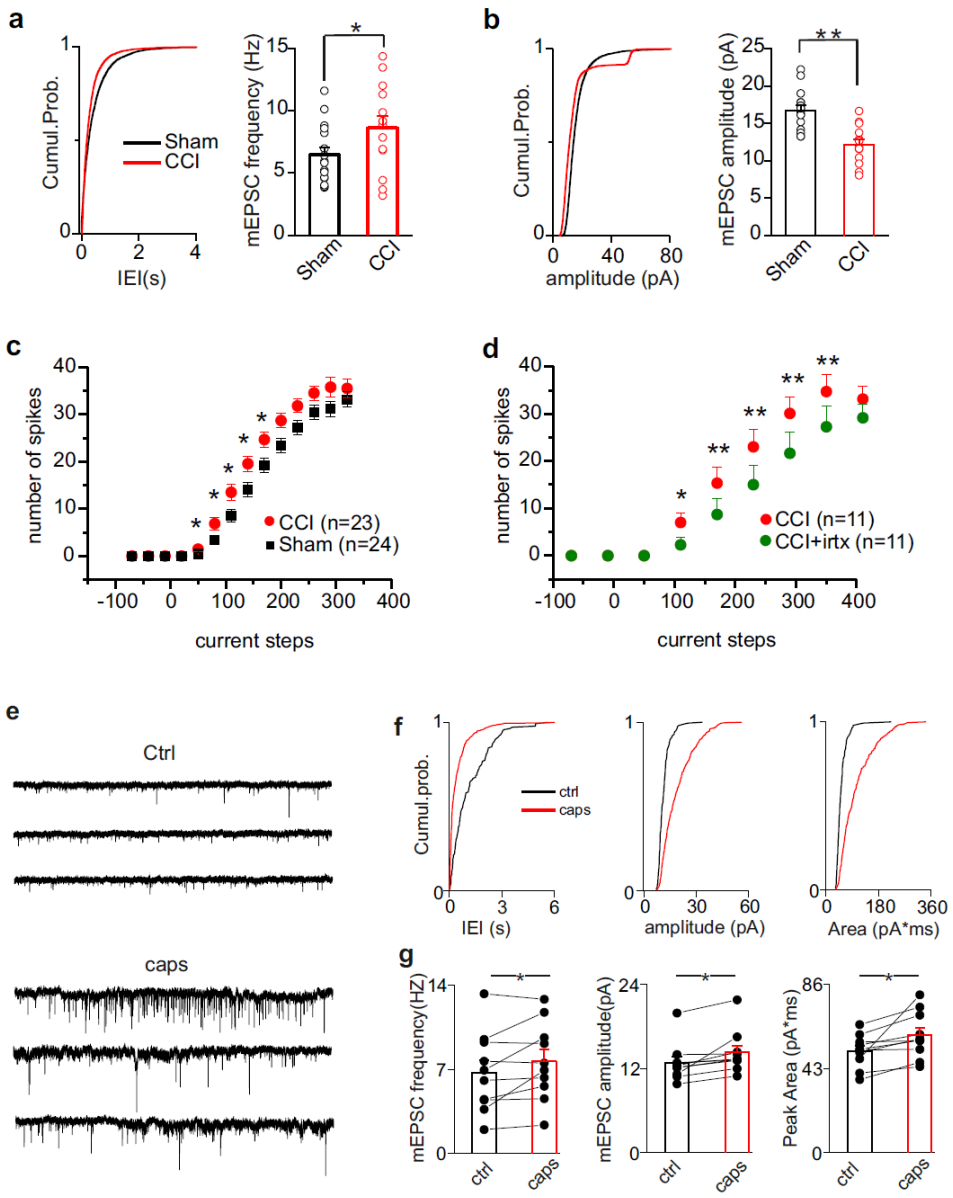

Figure 30: Chronic ligature of sciatic nerve modifies basal synaptic excitability trough TRPV1 expression (**a**) On the left, cumulative probability curves of mEPSC interevent intervals for the total recorded neurons from sham (n=16, black line) and CCI mice (n=14, red line) ($p<0.001$ Kolmogorov-Smirnov test). Right, summary histograms and line series plots of mEPSC from PNs of shams and CCI mice (6.47±0.58 and 8.63±0.92 Hz shams[n=16] and CCI mice [n=14], respectively $p<0.05$ Two sample T-test). (**b**) Left, cumulative probability distributions of mEPSC amplitudes of

total recorded PNs from shams (in black) and CCI (in red), p<0.001 KS test. Right, summary histograms and line series plots of mEPSC amplitudes from PNs of sham and CCI mice (16.76±0.65 and 12.2±0.67 pA, respectively, p<0.01 Two sample T-test. (**c**) Comparison between average input-out (input current/number of spikes) curvesfor the two conditions, shams (black dots) and CCI (red dots). The sciatic nerve ligation caused a leftward shift of the input current to action potential curves, with a significant increase of firing rate over a range of current injections. P<0.05 Mann-Whitney test. (**d**) Average input current/number of spike curves for control (red) and after IRTX (green) from CCI PN recordings. The inhibition of TRPV1s significantly reverted the leftward shift of the input-output curve induced by the surgery of the sciatic nerve (*p<0.05, **p<0.005, Paired Sample Wilcoxon Signed Rank test). (**e**), Example recording of mEPSCs before (upper traces) and during capsaicin (below traces) from a CCI pyramidal neuron. Note that capsaicin increases both the frequency and amplitude of mEPSCs. (**f**), Cumulative probability plots comparing the interevent interval (IEI) (left panel), amplitude (middle panel) and area (right panel) of control mEPSCs with those recorded in capsaicin, (KS-test p<0.001). (**g**) Summary graph of mEPSC frequency (left), amplitude (middle) and peak area (right) before (black bar, solid circle) and during capsaicin (red bar, solid circles) (frequency from 6.73±1.05 to 7.66±1.02 Hz, p=0.05 Paired Sample t-Test; amplitude from 12.90±0.84 to 14.26±0.95 pA, p<0.01 Paired Sample Wilcoxon Signed Rank test; Area from 52.03±2.67 to 60.20±3.74 pA*ms, p<0.05 Paired Sample t- test; n=10). Data are values from single cells and mean ± SEM. *p≤0.05.

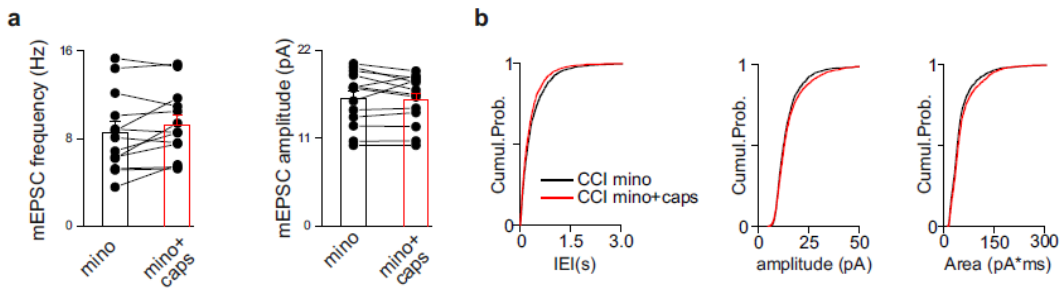

Figure 31: Microglial TRPV1 is not involved in the increase of neuronal synaptic strenght (a) Summary graph of mEPSC frequency , amplitude of experiments performend in CCI mice in the presence of minocycline and in the presence of minociclyne plus capsaicine(mino 8.55±1.00 mino+caps 9.27 ± 0.87 Hz, n=13 13 p=0.70 Paired Sample t-Test; mino 16.00 ±0.96 mino+caps

15.78 ± 0.86 pA, n=13 , p=0.64 Paired Sample t-Test);. Data are values from single cells and/or mean ± SEM) (**b**) Cumulative probability distributions of interevent intervals (left) amplitude (center) and area (left) of mEPSCs recorded from 4 cells of CCI mice in the presence of minocycline ($p<0.01$, KS test).

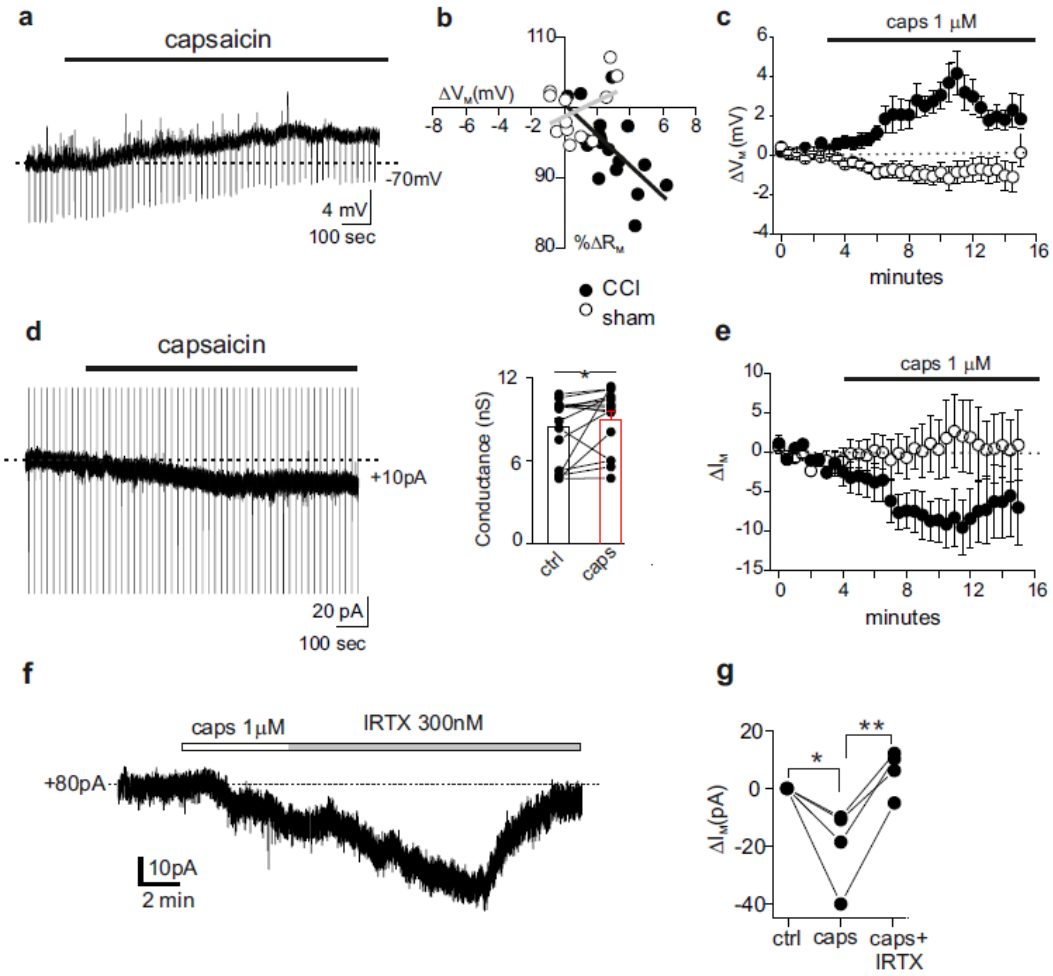

Figure 32: Neuronal TRPV1 stimulation directly modulates layer 2/3 pyramidal neuron synaptic strength in CCI mice. (**a**) Current-clamp recording of a pyramidal neuron responding to capsaicin with depolarization and reduced R_M in the presence of 6,7-dinitroquinoxaline-2,3-dione (10μM), D(−)-2-amino-5-phosphonovaleric acid (50μM) and picrotoxin (100μM). Negative deflections are membrane potential responses to negative current injections (60pA).**(b)** Plot of $\%\Delta R_M$ (normalized

to pre- capsaicin values) versus ΔV_M (membrane potential values in capsaicin subtracted from baseline ones) in all tested neurons from CCI and sham mice (n=18 and n=12, filled and white symbols, respectively). These data were analyzed by performing a linear fit to evaluate the strength of association between the two variables, through the coefficient of determination r^2. In sham, ΔR_M values do not correlate with variations in ΔV_M (r^2=0.07) while in PNs from CCI mice, capsaicin-induced changes of V_M correlate with a R_M with a value of r^2=0.36. **(c)** Summary time plot of subtracted membrane potential (ΔV_M) of CCI and sham PNs in response to capsaicin (p<0.001, Two Sample t-Test). (**d**) Left, example of voltage-clamp recording (at -70mV) of a CCI PN responding to capsaicin with an inward shift of the holding current, in the presence of tetrodotoxin (0.5µM), 6,7-dinitroquinoxaline-2,3-dione (10µM), D(−)-2-amino-5-phosphonovaleric acid (50µM) and picrotoxin (100µM). Vertical deflections (truncated in the figure) are membrane current responses to voltage steps to test passive properties (i.e. membrane conductance) and recording stability. Right, population graph of membrane conductance in control (black bar) and during capsaicin perfusion (red bar; n=12; *p<0.05 Paired Sample Wilcoxon Signed Rank test). (**e**), Summary plot of ΔI_M (membrane current values during capsaicin subtracted to baseline values) versus time for PNs from sham and CCI mice (n=12 and n=14, respectively; p<0.001, Mann-Whitney test). (**f**) Voltage-clamp recording of layer 2/3 PN from a 4 week CCI mice in the presence of picrotoxin, APV, TTX, and DNQX. Application of capsaicin induced an inward current that was reverted by IRTX. (**g**) Summary plot of changes in IM after application of capsaicin and subsequent application of IRTX (n=4, *p<0.05 **p<0.01).

Discussion

The present study shows that TRPV1 is abundantly expressed and functional in the microglia, rather than in neurons, of the anterior cingulate cortex of healthy mice. Notably, TRPV1 activation directly affects microglia function, which in turn modulates synaptic neurotransmission. This evidence is supported by: a) high levels of TRPV1 protein expression in cortical microglia cells as indicated by western blotting, flow cytometry and immunofluorescence assays in cortical tissues; b) the outward rectifying current induced by capsaicin in microglia cells from cortical slices; c) the shedding of microvesicles from microglial surface upon capsaicin application; and d) morphological and phenotypic changes of microglial cells upon TRPV1 activation. Importantly, TRPV1-mediated increase of cortical spontaneous glutamatergic neurotransmission is absent when microglia is switched off by minocycline and is occluded by the inflammatory agent LPS. Conversely, we found that in the cortex of mice suffering from neuropathic pain, TRPV1 is expressed also in neurons, affecting their intrinsic electrical properties and synaptic strength. This different TRPV1 expression pattern under chronic pain conditions places microglial TRPV1 at the center of a new important mechanism, providing a link between physiological and pathological states.

TRPV1 is functional in microglia[122,123,124] and growing evidence indicates a modulatory role of excitatory neurotransmission by microglia cells[116,117]. In addition, our study demonstrates that, under resting conditions, acute activation of TRPV1 expressed in microglia, rather than in neurons, accounts for its presynaptic modulation of neurotransmission widely observed in several rodent brain areas [76,77,78].

The results from our study may also add new insights on the controversy with regards to the postsynaptic localization of TRPV1 and its role in modulating

presynaptic neurotransmitter release at several central synapses[85,86]. The use of a specific monoclonal antibody allowed us to reveal microglial TRPV1 expression, that was not detectable with the polyclonal antibodies commercially available used in previous investigations to indicate a pure neuronal TRPV1 localization[53]. Moreover, a microglial expression explains the apparent paradox of a postsynaptic TRPV1 localization inducing pre-synaptic effect on glutamate release.

In contrast to the high levels of TRPV1 in microglia, we found a very low amount of this protein in cortical acutely isolated neurons, and both immunofluorescence and electrophysiological experiments in cortical slices showed that TRPV1s are not detectable and do not alter neuronal intrinsic properties. Evidence using TRPV1 reporter transgenic mice, based on IRES polycistronic mRNA transcribed from the TRPV1 genomic locus, suggested that this channel is restricted to both low level expression and few brain areas[60]. It is well known, though, that the expression downstream of IRES sequences is variable, and orders of magnitude lower than that from the cap-dependent translation of the primary mRNA. Thus, the ensuing expression pattern of the reporter genes might not precisely mimic the real expression of TRPV1, but reflect a limitation of the seemingly precise and sensitive method used[60]. In addition, the identity of the TRPV1-positive cells stained in the brain by lacZ reporter was not investigated and their neuronal identity not formally demonstrated[60]. Hence, those results from TRPV1 reporter mice are entirely consistent with ours, that demonstrate in a direct way the expression of TRPV1 in cortical microglia, with a well-validated anti TRPV1 monoclonal antibody, that does not react with TRPV1 knock-out sections.

Remarkably, the present data clarify the TRPV1 role in the brain with respect to that held by the same receptors in the peripheral somatosensory system. Indeed,

TRPV1s expressed in the main immune cells of the brain may similarly function as detectors of nociceptive and inflammatory stimuli/agents.

Accordingly, we found that capsaicin shifted microglia to a hypertrophic and pro-inflammatory state by increasing the production and release of cytokines i.e. TNα. showed increase production of IL6 and ROS formation following TRPV1 activation in microglial cells [101,102,124]. Notably, during inflammation or upon more generic environmental cellular insults, potential endovanilloids such as n-acyl amides, monoacylglycerols and bioactive lipids markedly increase [179,180]. Among these candidates, LPA seems to be a suitable endogenous agonist since, similarly to capsaicin, it activates potassium outward currents in microglia cells and induces microglial microvesicles shedding [181]. Our present data unveil a TRPV1-mediated enhancement of excitatory neurotransmission by LPA. Certainly, other candidates cannot be excluded

Remarkably, the present study shows that TRPV1 is expressed and functional in the microglia, rather than in neurons, of the anterior cingulate cortex of healthy mice. Notably, TRPV1 activation directly affects microglia function, which in turn modulates synaptic neurotransmission. This evidence arises from: a) mRNA TRPV1 expression in cortical microglia, validated by the lack of expression in cells from knock out tissue as negative control; b) high levels of TRPV1 protein expression in cortical microglia cells as indicated by western blotting, flow cytometry and immunofluorescence assays in cortical tissue; b) the outward rectifying current induced by capsaicin in microglia cells from cortical slices; c) the shedding of microvesicles from microglial surface upon capsaicin application; and d) morphological and phenotypic changes of microglial cells upon TRPV1 activation. Importantly, TRPV1-mediated increase of cortical spontaneous glutamatergic neurotransmission is absent when microglia is switched off by minocycline and is

occluded by the inflammatory agent LPS. Conversely, we found that in the cortex of mice suffering from neuropathic pain, TRPV1 is expressed also in neurons, affecting their intrinsic electrical properties and synaptic strength. This different TRPV1 expression pattern under chronic pain conditions places microglial TRPV1 at the center of a new important mechanism, providing a link between physiological and pathological states.

TRPV1 is functional in microglia and growing evidence indicates a modulatory role of excitatory neurotransmission by microglia cells. Accordingly, our study demonstrates that, in resting conditions, acute activation of TRPV1 expressed in microglia accounts for the well-known presynaptic modulation of glutamatergic neurotransmission by this channel observed in several rodent brain areas, and adds new insights on the apparent paradox of a postsynaptic TRPV1 localization inducing presynaptic effect on glutamate release[15,61]. In addition to the glutamatergic hypothesis, microglia affects neuronal excitability also by disinhibition mechanisms[62], thus likely explaining the TRPV1 regulation of inhibitory neurotransmission at dentate gyrus synapses[63]. Differently, in "activated" conditions, our evidence on TRPV1 functional expression in neurons may argue for the postsynaptic TRPV1 modulation of some forms of long term depression[21–24].

Hence, the use of a specific monoclonal antibody allowed us to reveal microglial TRPV1 expression, that was not detectable with the commercially available polyclonal antibodies used in previous investigations which rather provided a pure neuronal and sparse astrocytic TRPV1 localization[19,64]. This conclusion is complemented by the evidence at the mRNA level, exploiting probes covering the exon sequence lacking in the TRPV1 mutant mice: TRPV1 mRNA is copiously

expressed in cortical microglial cells, as well as in neurons, while no significant amount is detected in TRPV1$^{-/-}$ tissue and cells.

Our data do not exclude the existence of a functional TRPV1 postsynaptically expressed. Neurons may express a different splice variant of the protein from that expressed by microglia cells, that may not be detected by the anti-TRPV1 MAb employed in IF in fixed tissue (although the anti-TRPV1 MAb recognized the native neuronal receptor in the cytofluometry assay on living neurons). In addition, this putative different form of the channel could be activated upon specific stimuli, thus not showing up under our experimental conditions of the immunofluorescence and electrophysiological analysis. Indeed, only models of long term synaptic plasticity unveil a TRPV1-mediated postsynaptic effect.

Evidence using TRPV1 reporter transgenic mice, based on IRES polycistronic mRNA transcribed from the TRPV1 genomic locus, previously suggested that this channel is restricted to both low level expression and few brain areas[16]. It is well known, though, that the protein expression downstream of IRES sequences is variable, and can be orders of magnitude lower than that from the cap-dependent translation of the primary mRNA[65,66]. Also, it is well known that the precise genomic context around a reporter gene can significantly affect the chromatin organization of that locus and thus the expression pattern of the reporter gene. Finally, the RNA metabolism and regulation of the IRES containing mRNA in the TRPV1 reporter mouse might be different from that of the endogenous TRPV1 mRNA. Thus, the ensuing expression pattern of the reporter genes might not precisely mimic the real expression of TRPV1, but reflect a limitation of the seemingly precise and sensitive method used[16]. In addition, the identity of the TRPV1-positive cells stained in the brain by lacZ reporter was not investigated and their neuronal identity was not formally demonstrated[16]. Intriguingly, these cells

could also very well include non neuronal cells such as the glial cells immunopositive for the TRPV1 monoclonal antibody recognized/identified in the present study.

Remarkably, the present data clarify the TRPV1 role in the brain with respect to that held by the same receptors in the peripheral somatosensory system. Indeed, TRPV1s expressed in the main immune cells of the brain may similarly function as detectors of nociceptive and inflammatory stimuli/agents.

Conclusions and final remarks

The TRPV1 localization in microglia, detected in this study by using a monoclonal antibody, resolves the anatomical vs functional discrepancies mentioned above, offering a mechanism of vanilloid-mediated presynaptic modulation of neurotransmitter release by microglia. On the other hand, our data do not exclude the existence of a functional TRPV1 postsynaptically expressed. Neurons may express a different splice variant of the protein from that expressed by microglia cells, that may not be detected by the anti-TRPV1 MAb employed in IF in fixed tissue (although the anti-TRPV1 MAb recognized the native neuronal receptor in the cytofluometry assay on living neurons). In addition, this putative different form of the channel could be activated upon specific stimuli, thus not showing up under our experimental conditions of the immunofluorescence and electrophysiological analysis. Indeed, only models of long term synaptic plasticity unveil a TRPV1-mediated postsynaptic effect.

Our study reveals a novel function and expression of TRPV1s in control conditions: they directly and indirectly control microglial functions and neurotransmission, respectively, thus providing a link between neuroinflammation and synaptic transmission alterations. This is an emerging issue that sees microglia as the fourth element of the quadripartite synapse.

Our study confirms also evidence on the "on demand" TRPV1 neuronal expression during pathological conditions although we are conscious that these data will fuel the already present controversy and debate regarding TRPV1s in the brain.

Overall, we describe that, in an healthy brain, TRPV1 can function as a detector of inflammatory stimuli and plays a key role in the communication between immuno-competent cells and neurons. Upon injury, this channel receptor can behave as a brain biomarker of inflammation.

The experiments reported in this study reveal a strategic distribution of TRPV1, which is modulated by pain induction with significantly different outcomes. Finally, our data clarify and resolve its role in the mouse brain, which appears similar to that fulfilled in the peripheral nervous system. In particular, given the role of microglia cells as immune component of the central nervous system, TRPV1 may represent a sentinel of the brain environment by participating to the continuous scanning of harmful stimuli.

Author contribution statement:

This work include data that are collected in collaboration with different researchers and research groups. The candidate Annunziato Morabito performed collected and analyzed all electrophysiological experiments presented in this work and participated to the preparation of biological samples used for morphological and molecular biology studies.

References

1- Neuron. 1989 Apr;2(4):1313-23. Montell C, Rubin GM. Molecular characterization of the Drosophila trp locus: a putative integral membrane protein required for phototransduction.

2-Nature. 2003 Dec 4;426(6966):517-24. Clapham DE.TRP channels as cellular sensors.

3-Nature. 1997 Oct 23;389(6653):816-24. Caterina MJ, Schumacher MA, Tominaga M, Rosen TA, Levine JD, Julius D. The capsaicin receptor: a heat-activated ion channel in the pain pathway.

4- Cell 108,421–430 (2002). Jordt, S. E. & Julius, D. Molecular basis for species-specific sensitivity to “hot” chili peppers.

5- Neuron. 1998 Sep; 21(3):531-43. . Tominaga M, Caterina MJ, Malmberg AB, Rosen TA, Gilbert H, Skinner K, Raumann BE, Basbaum AI, Julius D. The cloned capsaicin receptor integrates multiple pain-producing stimuli

6-J Neurosci. 2003 Feb 15;23(4):1340-50. Vlachová V, Teisinger J, Susánková K, Lyfenko A, Ettrich R, Vyklický L. Functional role of C-terminal cytoplasmic tail of rat vanilloid receptor 1.

7-Nat Neurosci. 2014 Feb;17(2):164-74.10.1038/nn.3612. Piomelli D, Sasso O.Peripheral gating of pain signals by endogenous lipid mediators.

8-Nature. 1999 Jul 29;400(6743):452-7. Zygmunt PM, Petersson J, Andersson DA, Chuang H, Sørgård M, Di Marzo V, Julius D, Högestätt ED. Vanilloid receptors on sensory nerves mediate the vasodilator action of anandamide.

9-Nature. 2006 Nov 9; 444(7116):208-12. Siemens J, Zhou S, Piskorowski R, Nikai T, Lumpkin EA, Basbaum AI, King D, Julius D. Spider toxins activate the capsaicin receptor to produce inflammatory pain.

10-Toxicon. 2012 Sep 1; 60(3): 254–264. Christopher J. Bohlen and David Julius. Receptor-targeting mechanisms of pain-causing toxins: How now?

11-J Biol Chem. 2016 Jun 24;291(26):13855-63.10.1074/jbc.M116.726372. Kumar R, Hazan A, Basu A, Zalcman N, Matzner H, Priel A. Tyrosine Residue in the TRPV1 Vanilloid Binding Pocket Regulates Deactivation Kinetics.

12-J Neurosci. 2009 Jan 7;29(1):153-8.10.1523/JNEUROSCI.4901-08.2009. TRPV1 is activated by both acidic and basic pH. Dhaka A, Uzzell V, Dubin AE, Mathur J, Petrus M, Bandell M, Patapoutian A.

13-J Neurosci. 2006 May 3;26(18):4835-40. Brauchi S, Orta G, Salazar M, Rosenmann E, Latorre R.

A hot-sensing cold receptor: C-terminal domain determines thermosensation in transient receptor potential channels.

14-J Physiol. 2001 Aug 1;534(Pt 3):813-25. Vellani V, Mapplebeck S, Moriondo A, Davis JB, McNaughton PA. Protein kinase C activation potentiates gating of the vanilloid receptor VR1 by capsaicin, protons, heat and anandamide.

15-Channels (Austin). 2015;9(2):73-81. 10.1080/19336950.2015.1025186. Zhang X. Molecular sensors and modulators of thermoreception.

16-Neuron. 2002;35:721–731. Bhave G, Zhu W, Wang H, Brasier DJ, Oxford GS, Gereau RWT. cAMP-dependent protein kinase regulates desensitization of the capsaicin receptor (VR1) by direct phosphorylation.

17-Cell Calcium. 2004;35:471–478. Mandadi S, Numazaki M, Tominaga M, Bhat MB, Armati PJ, Roufogalis BD. Activation of protein kinase C reverses capsaicin-induced calcium-dependent desensitization of TRPV1 ion channels.

18-Europ J Neurosci. 1999;11:3143–3150. Guenther S, Reeh PW, Kress M. Rises in $[Ca^{2+}]_i$ mediate capsaicin- and proton-induced heat sensitization of rat primary nociceptive neurons.

19-Proc Natl Acad Sci USA. 2001;98:6951–6956. Tominaga M, Wada M, Masu M. Potentiation of capsaicin receptor activity by metabotropic ATP receptors as a possible mechanism for ATP-evoked pain and hyperalgesia.

20 Neuron. 1999;23:617–624. Cesare P, Dekker LV, Sardini A, Parker PJ, McNaughton PA. Specific involvement of PKC-epsilon in sensitization of the neuronal response to painful heat.

21-Nature. 2000;408:985–990. Premkumar LS, Ahern GP. Induction of vanilloid receptor channel activity by protein kinase C.

22-J Biol Chem. 2003;278:50080–50090. Mohapatra DP, Nau C. Desensitization of capsaicin-activated currents in the vanilloid receptor TRPV1 is decreased by the cyclic AMP-dependent protein kinase pathway.

23-J Neurosci. 2002;22:4740–4745. Rathee PK, Distler C, Obreja O, Neuhuber W, Wang GK, Wang SY, Nau C, Kress M. PKA/AKAP/VR-1 module: A common link of Gs-mediated signaling to thermal hyperalgesia.

24-J Biol Chem. 2002;277:13375–13378. Numazaki M, Tominaga T, Toyooka H, Tominaga M. Direct phosphorylation of capsaicin receptor VR1 by protein kinase C epsilon and identification of two target serine residues

25- Proc Natl Acad Sci USA. 2003;100:12480–12485. Bhave G, Hu HJ, Glauner KS, Zhu W, Wang H, Brasier DJ, Oxford GS, Gereau RWT. Protein kinase C phosphorylation sensitizes but does not activate the capsaicin receptor transient receptor potential vanilloid 1 (TRPV1)

26- Curr Drug Targets CNS Neurol Disord. 2004;3:479–485. Numazaki M, Tominaga M. Nociception and TRP channels.

27-J Neurophysiol. 2004;91:1442–1449. Premkumar LS, Qi ZH, Van Buren J, Raisinghani M. Enhancement of potency and efficacy of NADA by PKC-mediated phosphorylation of vanilloid receptor.

28-J Gen Physiol. 2004;123:53–62. Rosenbaum T, Gordon-Shaag A, Munari M, Gordon SE. Ca^{2+}/calmodulin modulates TRPV1 activation by capsaicin.

29-Proc Natl Acad Sci USA. 2003;100:8002–8006. Numazaki M, Tominaga T, Takeuchi K, Murayama N, Toyooka H, Tominaga M. Structural determinant of TRPV1 desensitization interacts with calmodulin.

30-J Biol Chem. 2004;279:7048–7054. Jung J, Shin JS, Lee SY, Hwang SW, Koo J, Cho H, Oh U. Phosphorylation of vanilloid receptor 1 by Ca^{2+}/calmodulin-dependent kinase II regulates its vanilloid binding.

31- J Biol Chem. 2000 Jan 28; 275(4):2756-62. Schumacher MA, Moff I, Sudanagunta SP, Levine JD Molecular cloning of an N-terminal splice variant of the capsaicin receptor. Loss of N-terminal domain suggests functional divergence among capsaicin receptor subtypes.

32-Genomics. 2001 Aug; 76(1-3):14-20. Xue Q, Yu Y, Trilk SL, Jong BE, Schumacher MA. The genomic organization of the gene encoding the vanilloid receptor: evidence for multiple splice variants.

33-J Biol Chem. 2004 Sep 3; 279(36):37423-30. Wang C, Hu HZ, Colton CK, Wood JD, Zhu MX. An alternative splicing product of the murine trpv1 gene dominant negatively modulates the activity of TRPV1 channels.

34-Mol Pharmacol. 2005 Apr; 67(4):1119-27. Lu G, Henderson D, Liu L, Reinhart PH, Simon SA TRPV1b, a functional human vanilloid receptor splice variant.

35-Am J Physiol Renal Physiol. 2006 Jan; 290(1):F117-26. Tian W, Fu Y, Wang DH, Cohen DM. Regulation of TRPV1 by a novel renally expressed rat TRPV1 splice variant.

36 Am J Physiol Renal Physiol. 2008 Feb; 294(2):F316-25. Feng NH, Lee HH, Shiang JC, Ma MC . Transient receptor potential vanilloid type 1 channels act as mechanoreceptors and cause substance P release and sensory activation in rat kidneys.

37-Neuroreport. 2007 Jul 2; 18(10):969-73. Eilers H, Lee SY, Hau CW, Logvinova A, Schumacher MA. The rat vanilloid receptor splice variant VR.5'sv blocks TRPV1 activation.

38-PLoS One. 2008; 3(10):e3419. Pecze L, Szabó K, Széll M, Jósvay K, Kaszás K, Kúsz E, Letoha T, Prorok J, Koncz I, Tóth A, Kemény L, Vizler C, Oláh Z. Human keratinocytes are vanilloid resistant.

40-Pharmacol Rev. 1991 Jun;43(2):143-201. Holzer P. Capsaicin: cellular targets, mechanisms of action, and selectivity for thin sensory neurons.

41-J Neurosci. 1999 Mar 1;19(5):1844-54. Michael GJ, Priestley JV.Differential expression of the mRNA for the vanilloid receptor subtype 1 in cells of the adult rat dorsal root and nodose ganglia and its downregulation by axotomy.

42-J Neurosci. 1998 Apr 15;18(8):3059-72. Bennett DL, Michael GJ, Ramachandran N, Munson JB, Averill S, Yan Q, McMahon SB, Priestley JV.A distinct subgroup of small DRG cells express GDNF receptor components and GDNF is protective for these neurons after nerve injury.

43-Neuron. 1998 Apr;20(4):629-32. Snider WD, McMahon SB. Tackling pain at the source: new ideas about nociceptors.

44-J Neurosci. 2011 Jul 13;31(28):10119-27. doi: 10.1523/JNEUROSCI.1299-11.2011. Cavanaugh DJ, Chesler AT, Bráz JM, Shah NM, Julius D, Basbaum AI. Restriction of transient receptor potential vanilloid-1 to the peptidergic subset of primary afferent neurons follows its developmental downregulation in nonpeptidergic neurons.

45-Exp Physiol. 1992 May;77(3):405-31. Jancsó G. Pathobiological reactions of C-fibre primary sensory neurones to peripheral nerve injury.

46-J Neurosci. 2002 May 15;22(10):4057-65. Zwick M, Davis BM, Woodbury CJ, Burkett JN, Koerber HR, Simpson JF, Albers KM. Glial cell line-derived neurotrophic factor is a survival factor for isolectin B4-positive, but not vanilloid receptor 1-positive, neurons in the mouse.

47-Pain. 2005 May;115(1-2):37-49. Breese NM, George AC, Pauers LE, Stucky CL. Peripheral inflammation selectively increases TRPV1 function in IB4-positive sensory neurons from adult mouse.

48-J Neurosci. 2007 Mar 7;27(10):2435-43. Hjerling-Leffler J, Alqatari M, Ernfors P, Koltzenburg M. Emergence of functional sensory subtypes as defined by transient receptor potential channel expression.

49-EMBO J. 2011 Feb 2;30(3):582-93. doi: 10.1038/emboj.2010.325. Mishra SK, Tisel SM, Orestes P, Bhangoo SK, Hoon MA.TRPV1-lineage neurons are required for thermal sensation.

50-Neurosci Lett. 1998 Jul 10;250(3):177-80. Helliwell RJ, McLatchie LM, Clarke M, Winter J, Bevan S, McIntyre P. Capsaicin sensitivity is associated with the expression of the vanilloid (capsaicin) receptor (VR1) mRNA in adult rat sensory ganglia.

51-Cell Tissue Res. 2006 Jan;323(1):27-41. Funakoshi K, Nakano M, Atobe Y, Goris RC, Kadota T, Yazama F. Differential development of TRPV1-expressing sensory nerves in peripheral organs.

52-Brain Res. 2006 Apr 26;1085(1):87-94. Murata Y, Masuko S. Peripheral and central distribution of TRPV1, substance P and CGRP of rat corneal neurons.

53-Proc Natl Acad Sci U S A. 2000 Mar 28;97(7):3655-60. Mezey E, Tóth ZE, Cortright DN, Arzubi MK, Krause JE, Elde R, Guo A, Blumberg PM, Szallasi A. Distribution of mRNA for vanilloid receptor subtype 1 (VR1), and VR1-like immunoreactivity, in the central nervous system of the rat and human.

54-BrainRes. 2004 Jan9;995(2):176-83.RobertsJC, DavisJB, BenhamCD.
[3H]Resiniferatoxin autoradiography in the CNS of wild-type and TRPV1 null mice defines TRPV1 (VR-1) protein distribution.

55-Neuron. 2012 May 24;74(4):640-7. doi: 10.1016/j.neuron.2012.02.039. Kim YH, Back SK, Davies AJ, Jeong H, Jo HJ, Chung G, Na HS, Bae YC, Kim SJ, Kim JS, Jung SJ, Oh SB. TRPV1 in GABAergic interneurons mediates neuropathic mechanical allodynia and disinhibition of the nociceptive circuitry in the spinal cord.

56-Neural Plast. 2016;2016:5954890.10.1155/2016/5954890. Choi SI, Lim JY, Yoo S, Kim H, Hwang SW. Emerging Role of Spinal Cord TRPV1 in Pain Exacerbation.

57-J Neurosci. 2002 Aug 1;22(15):6724-31. Moore KA, Kohno T, Karchewski LA, Scholz J, Baba H, Woolf CJ. Partial peripheral nerve injury promotes a selective loss of GABAergic inhibition in the superficial dorsal horn of the spinal cord.

58-Pain. 2007 May;129(1-2):195-209. Epub 2007 Feb 20. Ferrini F[1], Salio C, Vergnano AM, Merighi AVanilloid receptor-1 (TRPV1)-dependent activation of inhibitory neurotransmission in spinal substantia gelatinosa neurons of mouse.

59-Pain. 2010 Jul;150(1):128-40. doi: 10.1016/j.pain.2010.04.016. Ferrini F, Salio C, Lossi L, Gambino G, Merighi A. Modulation of inhibitory neurotransmission by the vanilloid receptor type 1 (TRPV1) in organotypically cultured mouse substantia gelatinosa neurons.

60-JNeurosci. 2011 Mar30;31(13):5067-77.doi:10.1523/JNEUROSCI.6451-10.2011.
Cavanaugh DJ, Chesler AT, Jackson AC, Sigal YM, Yamanaka H, Grant R, O'Donnell D, Nicoll

RA, Shah NM, Julius D, Basbaum AI. Trpv1 reporter mice reveal highly restricted brain distribution and functional expression in arteriolar smooth muscle cells.

61-Proc Natl Acad Sci U S A. 2000 Mar 28;97(7):3655-60. Mezey E, Tóth ZE, Cortright DN, Arzubi MK, Krause JE, Elde R, Guo A, Blumberg PM, Szallasi A. Distribution of mRNA for vanilloid receptor subtype 1 (VR1), and VR1-like immunoreactivity, in the central nervous system of the rat and human.

62-Neuroscience. 2006;139(4):1405-15. Cristino L, de Petrocellis L, Pryce G, Baker D, Guglielmotti V, Di Marzo V. Immunohistochemical localization of cannabinoid type 1 and vanilloid transient receptor potential vanilloid type 1 receptors in the mouse brain.

63-Brain Res Mol Brain Res 135, 162-168 (2005). Tóth A, Boczán J, Kedei N, Lizanecz E, Bagi Z, Papp Z, Edes I, Csiba L, Blumberg PM. Expression and distribution of vanilloid receptor 1 (TRPV1) in the adult rat brain

64-Neuroscience. 2001;107(3):373-81.The distribution and regulation of vanilloid receptor VR1 and VR1 5' splice variant RNA expression in rat. Sanchez JF, Krause JE, Cortright DN.

65- Brain Res Mol Brain Res. 2002 Jan 31;98(1-2):51-7.Pharmacological characterization of vanilloid receptor located in the brain. Szabo T, Biro T, Gonzalez AF, Palkovits M, Blumberg PM.

66-Life Sci. 1996;59(22):1899-908. Acs G, Palkovits M, Blumberg PM. Specific binding of [3H]resiniferatoxin by human and rat preoptic area, locus ceruleus, medial hypothalamus, reticular formation and ventral thalamus membrane preparations.

67- Biochem Biophys Res Commun. 2001 Mar;281(5):1183-9.The tissue distribution and functional characterization of human VR1. Cortright DN, Crandall M, Sanchez JF, Zou T, Krause JE, White G.

68- J Mol Neurosci. 2013 May;50(1):23-32. doi: 10.1007/s12031-012-9849-7. Han P, Korepanova AV, Vos MH, Moreland RB, Chiu ML, Faltynek CR. Quantification of TRPV1 protein levels in rat tissues to understand its physiological roles.

69- Pain. 2000 Nov;88(2):205-15. Hayes P, Meadows HJ, Gunthorpe MJ, Harries MH, Duckworth DM, Cairns W, Harrison DC, Clarke CE, Ellington K, Prinjha RK, Barton AJ, Medhurst AD, Smith GD, Topp S, Murdock P, Sanger GJ, Terrett J, Jenkins O, Benham CD, Randall AD, Gloger IS, Davis JB. Cloning and functional expression of a human orthologue of rat vanilloid receptor-1.

70-Neuron. 2008 Apr 24;58(2):179-85. doi: 10.1016/j.neuron.2008.02.013. Sharif-Naeini R, Ciura S, Bourque CW. TRPV1 gene required for thermosensory transduction and anticipatory secretion from vasopressin neurons during hyperthermia.

71- Wood J N, editor. San Diego: Academic; 1993. pp. 105–138. Ritter S, Dinh T T. In: Capsaicin in the Study of Pain.

72- Neuroreport. 1992 Oct; 3(10):849-52. Honkaniemi J, Kainu T, Ceccatelli S, Rechardt L, Hökfelt T, Pelto-Huikko M. Fos and jun in rat central amygdaloid nucleus and paraventricular nucleus after stress.

73-J Neurosci. 2015 Jul 8;35(27):10039-57. doi: 10.1523/JNEUROSCI.4112-14.2015. Lee SH, Ledri M, Tóth B, Marchionni I, Henstridge CM, Dudok B, Kenesei K, Barna L, Szabó SI, Renkecz T, Oberoi M, Watanabe M, Limoli CL, Horvai G, Soltesz I, Katona I. Multiple Forms of Endocannabinoid and Endovanilloid Signaling Regulate the Tonic Control of GABA Release.

74-Brain Struct Funct. 2015 Mar;220(2):1187-94. doi: 10.1007/s00429-014-0711-2. Puente N, Reguero L, Elezgarai I, Canduela MJ, Mendizabal-Zubiaga J, Ramos-Uriarte A, Fernández-Espejo E, Grandes P. The transient receptor potential vanilloid-1 is localized at excitatory synapses in the mouse dentate gyrus.

75-Neuroreport. 2014 Apr 16;25(6):379-85. doi: 10.1097/WNR.0000000000000105. Huang WX, Min JW, Liu YQ, He XH, Peng BW.Expression of TRPV1 in the C57BL/6 mice brain hippocampus and cortex during development.

76-J Neurosci. 2003 Apr 15;23(8):3136-44. Marinelli S, Di Marzo V, Berretta N, Matias I, Maccarrone M, Bernardi G, Mercuri NB. Presynaptic facilitation of glutamatergic synapses to dopaminergic neurons of the rat substantia nigra by endogenous stimulation of vanilloid receptors.

77-Neuropsychopharmacology. 2007 Feb;32(2):298-308. Marinelli S, Di Marzo V, Florenzano F, Fezza F, Viscomi MT, van der Stelt M, Bernardi G, Molinari M, Maccarrone M, Mercuri NB. N-arachidonoyl-dopamine tunes synaptic transmission onto dopaminergic neurons by activating both cannabinoid and vanilloid receptors.

78-Neuropsychopharmacology. 2005 May;30(5):864-70. Marinelli S, Pascucci T, Bernardi G, Puglisi-Allegra S, Mercuri NB. Activation of TRPV1 in the VTA excites dopaminergic neurons and increases chemical- and noxious-induced dopamine release in the nucleus accumbens.

79-J Physiol. 2002 Sep 1;543(Pt 2):531-40.Capsaicin activation of glutamatergic synaptic transmission in the rat locus coeruleus in vitro. Marinelli S, Vaughan CW, Christie MJ, Connor M.

80- Neuroreport. 1998 Jun 22;9(9):2045-8. Sasamura T, Sasaki M, Tohda C, Kuraishi Y. Existence of capsaicin-sensitive glutamatergic terminals in rat hypothalamus.

81-Brain Res. 2005 May 10;1043(1-2):1-11. Karlsson U, Sundgren-Andersson AK, Johansson S, Krupp JJ. Capsaicin augments synaptic transmission in the rat medial preoptic nucleus.

82- Neuron. 2008 Mar 13;57(5):746-59. doi: 10.1016/j.neuron.2007.12.027. Gibson HE, Edwards JG, Page RS, Van Hook MJ, Kauer JA.TRPV1 channels mediate long-term depression at synapses on hippocampal interneurons.

83-Neuron. 2008 Apr 24;58(2):179-85. doi: 10.1016/j.neuron.2008.02.013. Sharif-Naeini R, Ciura S, Bourque CW. TRPV1 gene required for thermosensory transduction and anticipatory secretion from vasopressin neurons during hyperthermia.

84-J Neurosci. 2007 Jan 24;27(4):832-9. Marsch R, Foeller E, Rammes G, Bunck M, Kössl M, Holsboer F, Zieglgänsberger W, Landgraf R, Lutz B, Wotjak CT. Reduced anxiety, conditioned fear, and hippocampal long-term potentiation in transient receptor potential vanilloid type 1 receptor-deficient mice.

85-Nat Neurosci. 2010 Dec;13(12):1511-8. doi: 10.1038/nn.2684. Chávez AE, Chiu CQ, Castillo PE. TRPV1 activation by endogenous anandamide triggers postsynaptic long-term depression in dentate gyrus.

86-Nat Neurosci. 2010 Dec;13(12):1519-25. doi: 10.1038/nn.2685. Grueter BA, Brasnjo G, Malenka RC.Postsynaptic TRPV1 triggers cell type-specific long-term depression in the nucleus accumbens.

87-Nat Neurosci. 2011 Nov 6;14(12):1542-7. doi: 10.1038/nn.2974. Puente N, Cui Y, Lassalle O, Lafourcade M, Georges F, Venance L, Grandes P, Manzoni OJ. Polymodal activation of the endocannabinoid system in the extended amygdala.

88-Prog Drug Res. 2014;68:77-104. Review. Edwards JG.TRPV1 in the central nervous system: synaptic plasticity, function, and pharmacological implications.

89-J Neurosci Res. 2005 Aug 1;81(3):302-13. Kim SU, de Vellis J. Microglia in health and disease.

90-Cereb Cortex. 2005 Jul;15(7):938-49. Rezaie P, Dean A, Male D, Ulfig N. Microglia in the cerebral wall of the human telencephalon at second trimester.

91-Neuroscience. 1992;48(2):405-15. Lawson LJ, Perry VH, Gordon S. Turnover of resident microglia in the normal adult mouse brain.

92-Glia. 2007 Aug 15;55(11):1189-98.Xu H, Chen M, Mayer EJ, Forrester JV, Dick AD. Turnover of resident retinal microglia in the normal adult mouse.

93-Brain. 2006 Sep;129(Pt 9):2394-403. Djukic M, Mildner A, Schmidt H, Czesnik D, Brück W, Priller J, Nau R, Prinz M. Circulating monocytes engraft in the brain, differentiate into microglia and contribute to the pathology following meningitis in mice.

94-J Neurosci. 2006 Nov 8;26(45):11753-62. Priller J, Prinz M, Heikenwalder M, Zeller N, Schwarz P, Heppner FL, Aguzzi A. Early and rapid engraftment of bone marrow-derived microglia in scrapie.

95- Glia. 1994 Dec;12(4):245-58. Sievers J, Parwaresch R, Wottge HU. Blood monocytes and spleen macrophages differentiate into microglia-like cells on monolayers of astrocytes: morphology.

96-Eur J Neurosci. 2001 Aug;14(3):463-73. Schilling T, Nitsch R, Heinemann U, Haas D, Eder C. Astrocyte-released cytokines induce ramification and outward K+ channel expression in microglia via distinct signalling pathways.

97- Nat Immunol. 2006 Mar;7(3):284-92. Binstadt BA, Patel PR, Alencar H, Nigrovic PA, Lee DM, Mahmood U, Weissleder R, Mathis D, Benoist C. Particularities of the vasculature can promote the organ specificity of autoimmune attack.

98-Trends Immunol. 2007 Jan;28(1):12-8. Galea I, Bechmann I, Perry VH. What is immune privilege (not)?

99-Nat Neurosci. 2007 Nov;10(11):1387-94. Review. Hanisch UK, Kettenmann H. Microglia: active sensor and versatile effector cells in the normal and pathologic brain.

100-Science. 2005 May 27;308(5726):1314-8. Nimmerjahn A, Kirchhoff F, Helmchen F. Resting microglial cells are highly dynamic surveillants of brain parenchyma in vivo.

101-Exp Neurol. 2016 Jan;275 Pt 3:316-27. doi: 10.1016/j.expneurol.2015.08.018. Loane DJ, Kumar A. Microglia in the TBI brain: The good, the bad, and the dysregulated.

102-Biochem Pharmacol. 2016 Mar 1;103:1-16. doi: 10.1016/j.bcp.2015.11.003. Jha MK, Lee WH, Suk K. Functional polarization of neuroglia: Implications in neuroinflammation and neurological disorders.

103-Eur.J.Neurosci. 2000 Jun;12(6):2049-58.BoucseinC, KettenmannH, NolteC. Electrophysiological properties of microglial cells in normal and pathologic rat brain slices.

104-JNeurosci. 2008 Sep10;28(37):9133-44.doi:10.1523/JNEUROSCI.1820-08.2008.Avignone E, Ulmann L, Levavasseur F, Rassendren F, Audinat E. Status epilepticus induces a particular microglial activation state characterized by enhanced purinergic signaling.

105-JNeurosci. 2016 Jun8;36(23):6165-74.doi:10.1523/JNEUROSCI.4498-15.2016.WendtS, Wogram E, Korvers L, Kettenmann H. Experimental Cortical Spreading Depression Induces NMDA Receptor Dependent Potassium Currents in Microglia.

106-PhysiolRev. 2011 Apr;91(2):461-553.doi:10.1152/physrev.00011.2010. Review. Kettenmann H, Hanisch UK, Noda M, Verkhratsky A. Physiology of microglia.

107-Eur J Neurosci. 2016 Jun;43(11):1523-34. doi: 10.1111/ejn.13256. Epub 2016 May 21. Wogram E, Wendt S, Matyash M, Pivneva T, Draguhn A, Kettenmann H. Satellite microglia show spontaneous electrical activity that is uncorrelated with activity of the attached neuron.

108-J Neurosci. 2009 Apr 1;29(13):3974-80. doi: 10.1523/JNEUROSCI.4363-08.2009. Wake H, Moorhouse AJ, Jinno S, Kohsaka S, Nabekura J. Resting microglia directly monitor the functional state of synapses in vivo and determine the fate of ischemic terminals.

109-Sci Rep. 2016 Sep 8;6:32422. doi: 10.1038/srep32422. Pfeiffer T, Avignone E, Nägerl UV. Induction of hippocampal long-term potentiation increases the morphological dynamics of microglial processes and prolongs their contacts with dendritic spines.

110-Science. 2011 Sep 9;333(6048):1456-8. doi: 10.1126/science.1202529. Paolicelli RC, Bolasco G, Pagani F, Maggi L, Scianni M, Panzanelli P, Giustetto M, Ferreira TA, Guiducci E, Dumas L, Ragozzino D, Gross CT. Synaptic pruning by microglia is necessary for normal brain development.

111-Open Biol. 2013 Dec 18;3(12):130181. doi: 10.1098/rsob.130181. Sheridan GK, Murphy KJ. Neuron-glia crosstalk in health and disease: fractalkine and CX3CR1 take centre stage.

112-Proc Natl Acad Sci U S A. 1998 Sep 1;95(18):10896-901. Harrison JK, Jiang Y, Chen S, Xia Y, Maciejewski D, McNamara RK, Streit WJ, Salafranca MN, Adhikari S, Thompson DA, Botti P, Bacon KB, Feng L. Role for neuronally derived fractalkine in mediating interactions between neurons and CX3CR1-expressing microglia.

113-Mol.Cell.Biol. 2000 Jun;20(11):4106-14.Jung S, AlibertiJ, Graemmel P, Sunshine MJ, Kreutzberg GW, Sher A, Littman DR. Analysis of fractalkine receptor CX(3)CR1 function by targeted deletion and green fluorescent protein reporter gene insertion.

114-Nat Neurosci. 2014 Mar;17(3):400-6. doi: 10.1038/nn.3641. Zhan Y, Paolicelli RC, Sforazzini F, Weinhard L, Bolasco G, Pagani F, Vyssotski AL, Bifone A, Gozzi A, Ragozzino D, Gross CT. Deficient neuron-microglia signaling results in impaired functional brain connectivity and social behavior.

115- Glia. 2013 Jul;61(7):1003-17. doi: 10.1002/glia.22497. Prada I[1], Furlan R, Matteoli M, Verderio C. Classical and unconventional pathways of vesicular release in microglia.

116- Proc Natl Acad Sci U S A. 2012 Jan 24;109(4):E197-205. doi: 10.1073/pnas.1111098109. Pascual O, Ben Achour S, Rostaing P, Triller A, Bessis A. Microglia activation triggers astrocyte-mediated modulation of excitatory neurotransmission.

117- Neuron. 2014 Apr 2;82(1):195-207. doi: 10.1016/j.neuron.2014.01.043. Zhang J, Malik A, Choi HB, Ko RW, Dissing-Olesen L, MacVicar BA. Microglial CR3 activation triggers long-term synaptic depression in the hippocampus via NADPH oxidase.

118-EMBOJ. 2009Apr22;28(8):1043-54.doi:10.1038/emboj.2009.45. Bianco F, Perrotta C, Novellino L, Francolini M, Riganti L, Menna E, Saglietti L, Schuchman EH, Furlan R, Clementi E, Matteoli M, Verderio C. Acid sphingomyelinase activity triggers microparticle release from glial cells.

119-EMBO J. 2012 Mar 7;31(5):1231-40. doi: 10.1038/emboj.2011.489. Antonucci F, Turola E, Riganti L, Caleo M, Gabrielli M, Perrotta C, Novellino L, Clementi E, Giussani P, Viani P, Matteoli M, Verderio C. Microvesicles released from microglia stimulate synaptic activity via enhanced sphingolipid metabolism.

120-EMBORep. 2015Feb;16(2):213-20.doi:10.15252/embr.201439668.GabrielliM, Battista N, Riganti L, Prada I, Antonucci F, Cantone L, Matteoli M, Maccarrone M, Verderio C. Active endocannabinoids are secreted on extracellular membrane vesicles.

121-J.Neurosci. 2016 Apr 20;36(16):4624-34. doi: 10.1523/JNEUROSCI.3588-15.2016. Riganti L, Antonucci F, Gabrielli M, Prada I, Giussani P, Viani P, Valtorta F, Menna E, Matteoli M, Verderio C. Sphingosine-1-Phosphate (S1P) Impacts Presynaptic Functions by Regulating Synapsin I Localization in the Presynaptic Compartment.

122-J.Immunol. 2006 Oct 1;177(7):4322-9. Kim SR, Kim SU, Oh U, Jin BK. Transient receptor potential vanilloid subtype 1 mediates microglial cell death in vivo and in vitro via Ca2+-mediated mitochondrial damage and cytochrome c release.

123-Br.J.Pharmacol. 2014 May;171(9):2426-39. doi: 10.1111/bph.12615. Hassan S, Eldeeb K, Millns PJ, Bennett AJ, Alexander SP, Kendall DA. Cannabidiol enhances microglial phagocytosis via transient receptor potential (TRP) channel activation.

124-J.Neuroimmunol. 2009 Nov30;216(1-2):118-21.doi:10.1016/j.jneuroim.2009.07.008. Schilling T, Eder C.Importance of the non-selective cation channel TRPV1 for microglial reactive oxygen species generation.

125-Invest Ophthalmol Vis Sci. 2008 Jul;49(7):3004-17. doi: 10.1167/iovs.07-1355. Sappington RM, Calkins DJ. Contribution of TRPV1 to microglia-derived IL-6 and NFkappaB translocation with elevated hydrostatic pressure.

126-Principles of Neuroscience. New York: Appleton and Lange; 2000, In: Kandel ER, Schwartz J, Jessell T, editors. . pp. 472–491.Basbaum AI, Jessell T. The Perception of Pain.

127-In: McMahon SB, Koltzenburg M, editors. Wall and Melzack's textbook of Pain. Elsevier; 2008. pp. 49–72. McMahon SB, Bennett DLH, Bevan S. Inflammatory mediators and modulators of pain.

128-Cell. 2009Oct16;139(2):267-84.doi:10.1016/j.cell.2009.09.028.Basbaum AI, Bautista DM, Scherrer G, Julius D. Cellular and molecular mechanisms of pain.

129-Nat Rev Neurosci. 2007 Jan; 8(1):71-80. Perl ER. Ideas about pain, a historical view.

130-J.Neurosci.1995Jan;15(1 Pt 1):333-41.Schmidt R,Schmelz M, Forster C, Ringkamp M, Torebjörk E, Handwerker H. Novel classes of responsive and unresponsive C nociceptors in human skin.

131- Nat Rev Neurosci. 2010 Dec;11(12):823-36. doi: 10.1038/nrn2947. Todd AJ. Neuronal circuitry for pain processing in the dorsal horn.

132- Eur J Pain. 2005 Aug;9(4):463-84.Apkarian AV, Bushnell MC, Treede RD, Zubieta JK. Human brain mechanisms of pain perception and regulation in health and disease.

133- E. Pain. 2010 Mar; 148(3):359-60. Tracey I, Johns E. The pain matrix: reloaded or reborn as we image tonic pain using arterial spin labelling.

134-Textbook of Pain .5th ed. Philadelphia, Pennsylvania, USA: Elsevier Churchill Livingstone; 2005:107–124. Bushnell MC, Apkarian AV. Representation of pain in the brain. In: McMahon SB, Koltzenburg M,

135-Neuron 32, 927–946 (2001).Becerra, L., Breiter, H. C., Wise, R., Gonzalez, R. G. & Borsook, D. Reward circuitry activation by noxious thermal stimuli.

136-Neuron. 2010 Apr 15;66(1):149-60. doi: 10.1016/j.neuron.2010.03.002. Baliki MN, Geha PY, Fields HL, Apkarian AV. Predicting value of pain and analgesia: nucleus accumbens response to noxious stimuli changes in the presence of chronic pain.

137-J.Neurosci. 25, 7333–7341 (2005).Dunckley, P. et al. A comparison of visceral and somatic pain processing in the human brainstem using functional magnetic resonance imaging.

138-Annu Rev Neurosci. 1984;7:309-38. Basbaum AI, Fields HL. Endogenous pain control systems: brainstem spinal pathways and endorphin circuitry.

139-J.Neurophysiol. 50, 1479–1496 (1983).Kenshalo, D. R. Jr & Isensee, O. Responses of primate SI cortical neurons to noxious stimuli.

140-Pain 81, 273–282 (1999).Greenspan, J. D., Lee, R. R. & Lenz, F. A. Pain sensitivity alterations as a function of lesion location in the parasylvian cortex.

141-Science 277, 968–971 (1997).Rainville, P., Duncan, G. H., Price, D. D., Carrier, B. & Bushnell, M. C. Pain affect encoded in human anterior cingulate but not somatosensory cortex.

142-Cereb.Cortex 12, 376–385 (2002).Ostrowsky, K. et al. Representation of pain and somatic sensation in the human insula: a study of responses to direct electrical cortical stimulation.

143-Proc Natl Acad Sci U S A. 2001 Jul 3;98(14):8077-82. Johansen JP, Fields HL, Manning BH. The affective component of pain in rodents: direct evidence for a contribution of the anterior cingulate cortex.

144-JClinInvest. 2010Nov;120(11):3779-87.doi:10.1172/JCI43766.Ossipov MH, Dussor GO, Porreca F. Central modulation of pain.

145-Lancet, 354 (9186) (1999), pp. 1248–1252A.M. Elliott, B.H. Smith, K.I. Penny, W.C. Smith, W.A. Chambers. The epidemiology of chronic pain in the community

146-Pain, 136 (3) (2008), pp. 380–387 D. Bouhassira, M. Lantéri-Minet, N. Attal, B. Laurent, C. Touboul. Prevalence of chronic pain with neuropathic characteristics in the general population

147-Lancet Neurol, 8 (9) (2009), pp. 857–868H. Klit, N.B. Finnerup, T.S. Jensen Central post-stroke pain: clinical characteristics, pathophysiology, and management

148-Curr Pain Headache Rep, 16 (3) (2012), pp. 207–21. N.B. Finnerup, C. BaastrupSpinal cord injury pain: mechanisms and management

149- Pain, 154 (5) (2013), pp. 632–642 P.L. Foley, H.M. Vesterinen, B.J. Laird, E.S. Sena, L.A. Colvin, S. Chandran, M.R. MacLeod, M.T. Fallon Prevalence and natural history of pain in adults with multiple sclerosis: systematic review and meta-analysis

150-Lancet Neurol, 9 (8) (2010), pp. 807–819 R. Baron, A. Binder, G. Wasner. Neuropathic pain: diagnosis, pathophysiological mechanisms, and treatment

151-Neuroscience. 2005;25:7896–7904. Andre J, Zeau B, Pohl M, Cesselin F, Benoliel JJ, Becker C. Involvement of cholecystokininergic systems in anxiety-induced hyperalgesia in male rats: Behavioral and biochemical studies.

152- Pain. 2005;116:79–86. Khasar SG, Green PG, Levine JD. Repeated sound stress enhances inflammatory pain in the rat.

153-Behavioral Brain Research. 2008;189:159–169. Suarez-Roca H, Leal L, Silva JA, Pinerua-Shuhaibar L, Quintero L. Reduced GABA neurotransmission underlies hyperalgesia induced by repeated forced swimming stress.

154-Schmerz. 2014 Apr;28(2):141-6. doi: 10.1007/s00482-014-1394-6. Karmann AJ, Kundermann B, Lautenbacher S. Sleep deprivation and pain: a review of the newest literature.

155-Mol Pain. 2009; 5: 51.10.1186/1744-8069-5-51. Bai-Chuang Shyu and Brent A Vogt. Short-term synaptic plasticity in the nociceptive thalamic-anterior cingulate pathway

156-Mol.Cells.2007Jun 30;23(3):259-71.Zhuo M. A synaptic model for pain: long-term potentiation in the anterior cingulate cortex.

157-Nat Rev Neurosci. 2016 Aug;17(8):485-96. doi: 10.1038/nrn.2016.68. Bliss TV, Collingridge GL, Kaang BK, Zhuo M.Synaptic plasticity in the anterior cingulate cortex in acute and chronic pain.

158-J Neurosci. 2009 Mar 11;29(10):3307-21. doi: 10.1523/JNEUROSCI.4300-08.2009. Cao H, Gao YJ, Ren WH, Li TT, Duan KZ, Cui YH, Cao XH, Zhao ZQ, Ji RR, Zhang YQ. Activation of extracellular signal-regulated kinase in the anterior cingulate cortex contributes to the induction and expression of affective pain.

159-Trends Neurosci. 2008 Apr;31(4):199-207. doi: 10.1016/j.tins.2008.01.003.Zhuo M. Cortical excitation and chronic pain.

160-Nat Rev Neurosci. 2005 Jul;6(7):533-44. Vogt BA. Pain and emotion interactions in subregions of the cingulate gyrus.

161-Nat Neurosci. 2004 Apr;7(4):398-403. Johansen JP, Fields HL. Glutamatergic activation of anterior cingulate cortex produces an aversive teaching signal.

162-Neuron. 2015 Jan 21;85(2):377-89. doi: 10.1016/j.neuron.2014.12.021. Koga K, Descalzi G, Chen T, Ko HG, Lu J, Li S, Son J, Kim T, Kwak C, Huganir RL, Zhao MG, Kaang BK, Collingridge GL, Zhuo M. Coexistence of two forms of LTP in ACC provides a synaptic mechanism for the interactions between anxiety and chronic pain.

163-Science. 2000 Apr 14;288(5464):306-13. Caterina MJ, Leffler A, Malmberg AB, Martin WJ, Trafton J, Petersen-Zeitz KR, Koltzenburg M, Basbaum AI, Julius D. Impaired nociception and pain sensation in mice lacking the capsaicin receptor.

164-Davis JB, Gray J, Gunthorpe MJ, Hatcher JP, Davey PT, Overend P, Harries MH, Latcham J, Clapham C, Atkinson K, Hughes SA, Rance K, Grau E, Harper AJ, Pugh PL, Rogers DC, Bingham S, Randall A, Sheardown SA.Vanilloid receptor-1 is essential for inflammatory thermal hyperalgesia.Nature. 2000 May 11;405(6783):183-7

165-Eur J Pharmacol. 2002 Mar 29;439(1-3):69-75. Palazzo E, de Novellis V, Marabese I, Cuomo D, Rossi F, Berrino L, Rossi F, Maione S. Interaction between vanilloid and glutamate receptors in the central modulation of nociception.

166-Br J Pharmacol. 2007 Mar;150(6):766-81. Maione S, De Petrocellis L, de Novellis V, Moriello AS, Petrosino S, Palazzo E, Rossi FS, Woodward DF, Di Marzo V. Analgesic actions of N-arachidonoyl-serotonin,
a fatty acid amide hydrolase inhibitor with antagonisticactivity at vanilloid TRPV1 receptors.

167-J Neurophysiol. 2003 Oct;90(4):2702-10.McGaraughty S, Chu KL, Bitner RS, Martino B, El Kouhen R, Han P, Nikkel AL, Burgard EC, Faltynek CR, Jarvis MF. Capsaicin infused into the PAG affects rat tail flick responses to noxious heat and alters neuronal firing in the RVM.

168-PLoS.One. 2010Sep17;5(9). pii: e12748. doi: 10.1371/journal.pone.0012748. Mallet C, Barrière DA, Ermund A, Jönsson BA, Eschalier A, Zygmunt PM, Högestätt ED. TRPV1 in brain is involved in acetaminophen-induced antinociception.

169-PLoS.One. 2013 Aug 5;8(8):e70690. doi: 10.1371/journal.pone.0070690. Barrière DA, Mallet C, Blomgren A, Simonsen C, Daulhac L, Libert F, Chapuy E, Etienne M, Högestätt ED, Zygmunt PM, EschalierA.Fatty acid amide hydrolasedependent generation of antinociceptive drug metaboli tes acting on TRPV1 in the brain.

170-Mol Pain. 2006 Nov 8;2:34. Steenland HW, Ko SW, Wu LJ, Zhuo M. Hot receptors in the brain.

171-EurJPain. 2000;4(1):83-96.Calejesan AA, Kim SJ, Zhuo M. Descending facilitatory modulation of a behavioral nociceptive response by stimulation in the adult ratanterior cingulate cortex.

172-Mol Pain. 2011 Jan 17;7:7. doi: 10.1186/1744-8069-7-7. de Novellis V, Vita D, Gatta L, Luongo L, Bellini G, De Chiaro M, Marabese I, Siniscalco D, Boccella S, Piscitelli F, Di Marzo V, Palazzo E, RossiF, MaioneSThe blockade ofthe transient receptor potential vanilloid type 1 and fatty acid a mide hydrolasedecreases symptoms and central sequelae inthe medial prefrontal cortex of neuro pathic rats.

173-Riazi, K. et al. Microglia-dependent alteration of glutamatergic synaptic transmission and plasticity in the hippocampus during peripheral inflammation. *J Neurosci* **35**, 4942-4952 (2015).

174-J.Neurosci. 2004 Jan 21;24(3):722-32. Fiacco TA, McCarthy KD Intracellular astrocyte calcium waves in situ increase the frequency of spontaneous AMPA receptor currents in CA1 pyramidal neurons.

175-Ann.Neurol72,610-624(2012).Verderio,C.et al.Myeloid microvesicles are a marker and therapeutic target for neuroinflammation.

176-J.Immunol174,7268-7277(2005).Bianco,F.etal.Astrocyte-derived ATP induces vesicle shedding and IL-1 beta release from microglia

177-J.Neurochem. 2007Aug;102(3):977-90.Amantini C, MoscaM, NabissiM, Lucciarini R, Caprodossi S, Arcella A, Giangaspero F, Santoni G. Capsaicin-induced apoptosis of glioma cells is mediated by TRPV1 vanilloid receptor and requires p38 MAPK activation.

178-Cell. 2008 Oct 31;135(3):422-35.doi:10.1016/j.cell.2008.10.008. Turrigiano GG.The self-tuning neuron: synaptic scaling of excitatory synapses.

179-Proc Natl Acad Sci U S A. 2004 Mar 2;101(9):3214-9. Witting A, Walter L, Wacker J, Möller T, Stella N. P2X7 receptors control 2-arachidonoylglycerol production by microglial cells.

180-Front Cell Neurosci. 2014 Aug 1;8:195. doi: 10.3389/fncel.2014.00195. Raboune S, Stuart JM, Leishman E, Takacs SM, Rhodes B, Basnet A, Jameyfield E, McHugh D, Widlanski T, Bradshaw HB. Novel endogenous N-acyl amides activate TRPV1-4 receptors, BV-2 microglia, and are regulated in brain in an acute model of inflammation.

181-Eur J Neurosci. 2004 Mar;19(6):1469-74. Schilling T, Stock C, Schwab A, Eder C. Functional importance of Ca2+-activated K+ channels for lysophosphatidic acid-induced microglial migration.

182-Brain.Behav.Immun. 2012 Jul;26(5):797-802.doi:10.1016/j.bbi.2011.12.008.Kremsky I, Morgan TE, Hou X, Li L, Finch CE. Age-changes in gene expression in primary mixed glia cultures from young vs. old rat cerebral cortex are modified by interactions with neurons.

183-Neural.Plast.2013;2013:627325.doi:10.1155/2013/627325.Ji K, Miyauchi J, Tsirka SE. Microglia: an active player in the regulation of synaptic activity.

184-Neuroreport. 2004 Mar 22;15(4):655-8. Luo H, Cheng J, Han JS, Wan Y. Change of vanilloid receptor 1 expression in dorsal root ganglion and spinal dorsal horn during inflammatory nociception induced by complete Freund's adjuvant in rats.

185-J.Neurosci. 2015 Jan14;35(2):457-66.doi:10.1523/JNEUROSCI.2315-14.2015.
McKelvey R, Berta T, Old E, Ji RR, Fitzgerald M. Neuropathic pain is constitutively suppressed in early life by anti-inflammatory neuroimmune regulation.

186-J.Pain. 2009Sep;10(9):895-926.doi:10.1016/j.jpain.2009.06.012.Latremoliere A, Woolf CJ.
Central sensitization: a generator of pain hypersensitivity by central neural plasticity.

187-Mol.Brain. 2014 Oct31;7:76.doi:10.1186/s13041-014-0076-8.Chen T, Wang W, Dong YL, Zhang MM, Wang J, Koga K, Liao YH, Li JL, Budisantoso T, Shigemoto R, Itakura M, Huganir RL, Li YQ, Zhuo M. Postsynaptic insertion of AMPA receptor onto cortical pyramidal neurons in the anterior cingulate cortex after peripheral nerve injury.

188- Biochem Soc Trans. 2015 Aug;43(4):586-92. doi: 10.1042/BST20150058. Turkheimer FE, Rizzo G, Bloomfield PS, Howes O, Zanotti-Fregonara P, Bertoldo A, Veronese M.The methodology of TSPO imaging with positron emission tomography.

189-Neuron. 2015 Feb 18;85(4):669-82. doi: 10.1016/j.neuron.2015.01.009. Yung YC, Stoddard NC, Mirendil H, Chun J. Lysophosphatidic Acid signaling in the nervous system.

.

.

.